PROPERTY DISTRIBUTIONS AND CIRCULATION IN THE ANGOLA BASIN

by

Kevin G. Speer

B.S. Math, B.S. Physics
University of California at Santa Barbara
(1982)

SUBMITTED TO THE DEPARTMENT OF EARTH, ATMOSPHERIC AND
PLANETARY SCIENCES IN PARTIAL FULFILLMENT OF
THE REQUIREMENTS FOR THE DEGREE OF

MASTERS OF SCIENCE IN PHYSICAL OCEANOGRAPHY

at the

August 1985

Signature of author _____
MIT/WHOI Joint Program in Oceanography

_____
Bruce Warren - Woods Hole Oceanographic Institution
Thesis Supervisor

_____
Paola Rizzoli - Massachusetts Institute of Technology

_____
T.R. Madden - Chairman, Departmental Graduate Committee

PROPERTY DISTRIBUTIONS AND CIRCULATION IN THE ANGOLA BASIN

by

Kevin G. Speer

SUBMITTED TO THE DEPARTMENT OF EARTH, ATMOSPHERIC AND
PLANETARY SCIENCES IN PARTIAL FULFILLMENT OF
THE REQUIREMENTS FOR THE DEGREE OF

MASTERS OF SCIENCE IN PHYSICAL OCEANOGRAPHY

Abstract

In 1983 a section was occupied at 11°S in the South Atlantic by the R.V. Oceanus. This study deals with the eastern half of this section, in the Angola Basin. Four major results described in this thesis are the following: 1) Bottom water enters the Angola Basin from the north. The southern source found by Connary and Ewing (1974) is apparently prevented from entering the basin by a system of ridges near 30°S. 2) A new deep western boundary current has been identified in the Angola Basin. This current flows southward above the eastern flank of the Mid-Atlantic Ridge, with an estimated transport of 1.4×10^6 $m^3 s^{-1}$. 3) A model for a tracer distribution in the bottom layer of the basin is developed, based on the Stommel and Arons model for the circulation. The tracer model predicts a distribution of temperature and salinity in agreement with the observations at 11°S and 24°S. 4) A model for the deep oxygen minimum is presented, which includes boundary flux. It is suggested that the boundary flux must be included for agreement with observations in the eastern South Atlantic.

Thesis Supervisor: Dr. Bruce Warren
Title: Senior Scientist

Acknowledgments

I would like to thank my advisor, Bruce Warren, for giving me the opportunity to work on unique, high quality data which he collected. Our discussions were interesting and informative for me, and his criticisms on the interpretation of data were always constructive. His patience was appreciated. This work was supported in part by NSF grant number OCE-8213967.

Also I would like to thank Bob Weller for his support through his ONR grant number ONR N-000-14-84-C-0134. In addition, sincere thanks go to members of my thesis committee for their help: Paola Rizzoli, Nelson Hogg, and especially Mike McCartney for many lengthy discussions and the use of data collected by him at 24°S. Fred Sayles gave me helpful comment and references on decomposition in the sediments. Joe Reid kindly provided me with the data along 1°E, and the Bennekom and Berger (1984) reference.

TABLE OF CONTENTS

Chapter 1

Introduction

The Stommel and Arons model (SA, 1960a,b) is the foundation for our understanding of the general circulation of deep water. In this model, the assumption of an upward movement of deep water (presumed uniform) implies poleward interior flow. The model also requires one or more boundary currents to supply and feed the interior flow, and to recieve water from a source. In a closed region, which can be bounded by topography or the equator (since the interior flow is zero at the equator), a source is necessary to balance the loss of water from the upwelling in the region as a whole. The boundary currents are necessary to balance mass in any particular subregion. These boundary currents are allowed on any boundary whose normal vector has an eastward component. This restriction comes from traditional bottom and lateral friction models of boundary currents.

Deep western boundary currents (DWBCs) have been observed in most of the world's oceans at their western boundary with the continents (an exception is in the North Pacific, where the obsevation is not clear). Within the oceans, ridges form basins. These ridges are the western boundary for water below their level and indeed DWBCs have been observed above the eastern flanks of mid-ocean ridges. However, in the Angola Basin of the South Atlantic, where the Mid-Atlantic Ridge forms a western boundary for water below 3600 m, a DWBC has not previously been found, although sources of bottom water have been reported. The prediction of a

DWBC there by the SA model depends only on the assumption of vertical motion, necessary to close the interior flow. It does not depend on the location or strength of the source. If a DWBC does not exist with known upwelling, then the SA model fails to apply as a consistent model. On the other hand, if a DWBC does exist, one still wants to compare the predicted interior flow with observations.

This aspect of the SA model, the interior flow, has received less attention than the DWBC. A comparison of the interior flow pattern and resulting property distributions calculated from the model with observations is required to test its validity. This comparison is as significant because more elaborate extensions of the SA model, e.g. including topography or vertical structure, will not necessarily have the same interior flow as the simplest one-layer, flat bottom model. The SA model provides a straightforward, consistent framework for interpreting property distributions and inferring flow. The purpose of this thesis is to test the validity of the SA model in the Angola Basin, using a new oceanographic data set.

The need for a new data set was based on the high accuracy required of measurements in the eastern trough of the South Atlantic. High accuracy is required to be confident that apparent small variations in deep water properties of this region are connected with circulation, not measurement error. Previous studies of the circulation in the Angola Basin were based on pre-CTD accuracy measurements. However, horizontal changes in the properties of the deep water within the basin are generally the same as or smaller than the accuracy of the older

measurements. There is no indication of a DWBC in the temperature or salinity sections of either the Meteor (Wüst and Defant, 1936) or the International Geophysical Year (I.G.Y.; Fuglister, 1960) data. Below 3000m horizontal variations of temperature and salinity are unresolved and ragged in these data sets. There is a hint of a DWBC in the Meteor oxygen measurements (Wattenberg, 1939). The measurements show high oxygen concentrations above the Mid-Atlantic Ridge at 8°S, 16°S, 22°S, and 29°S in the Angola Basin below 3000m, with the highest values at 16°S. While the high values are consistent with the presence of a DWBC along the Ridge (since high oxygen might indicate water which has recently entered the basin), the sparse sampling and accuracy ($\pm$0.1-0.2 ml l^{-1}) make it impossible to infer even the direction of possible flow. Owing to the accuracy of these older measurements, our understanding of the deep circulation of the South Atlantic is based mostly on the strong spatial property variations in the western trough, which are well illustrated in the older data sets. This bias for the western trough has brought about a real need for the comparison of theoretically predicted interior circulation with observations in the eastern South Atlantic. The realization that modern measurements of higher accuracy might allow one to see the structure of the deep property fields of the Angola Basin and allow a test of the SA model motivated new field work in this region.

What previous work did address was sources of bottom water to the Angola Basin. The major source of bottom water to the Angola Basin is the Guinea Basin (Wüst, 1933). The Guinea Basin in turn receives its bottom

water from the western trough through the Romanche Fracture Zone (figure 1). In addition, a minor inflow is thought to occur in the southwest corner (Connary and Ewing, 1974) through the Walvis Passage. This source water from the south is believed to originate in the Cape Basin (as opposed to the Argentine Basin). None of the previous investigations was able to estimate the transport of the sources, which is needed to assess the strength of the general circulation there and to compare to other regions. Furthermore, without being certain about the sources and their relative magnitude, the SA model is of limited use: the magnitude and direction of the DWBC, as well as the predicted horizontal property distributions would be ambiguous. Again, more accurate data were needed better to determine the sources.

Indirect methods have traditionally been used to infer the intensity and direction of deep flow. An important example of this is the information that the distribution of oxygen and nutrients can give. The distribution of these properties has helped to form some of our basic ideas about the general circulation. For instance, the oxygen distribution sometimes gives clues about the age or ventilation time of deep water in a region. Also, the distribution of oxygen can be modeled and compared or fitted to observations. Two examples of oxygen distribution models which have tested our general circulation ideas are Wyrtki's (1962) model for the vertical structure, and the Kuo and Veronis (1973) model for the horizontal structure. Together they test both the vertical and horizontal components of the velocity field using oxygen as a tracer. In both of these models the process of decomposition, which uses up

oxygen and releases nutrients, is crucial for agreement with observations. Because of this consumption of oxygen, low oxygen layers form in Wyrtki's model, and low oxygen regions form in Kuo and Veronis' model. In addition, the consumption has been assumed to be independent of position (uniform) in deep water. Fair agreement with observations has been found with this assumption. Neither of these models, however, is able to explain the deep oxygen minimum in the Angola Basin. In this thesis it is suggested that a boundary flux is necessary to explain the distribution of oxygen in the deep water of the Angola Basin.

Geographical Setting and Data

In 1983 a transatlantic section at 11°S was occupied by the R.V. Oceanus. The eastern half of the section at 11°S cuts across the northern portion of the Angola Basin, from south of Ascension Island to south of Luanda on the west coast of Africa, in the Republic of Angola.

The Angola Basin extends north to near 5°S, where the Guinea Ridge separates it from the Guinea Basin. To the south the Walvis Ridge separates it from the Cape Basin. The bathymetry map of Uchupi (1981) for this region indicates that the Mid-Atlantic Ridge is regularly broken by fracture zones at depths between 3000m and 4000m. The Mid-Atlantic Ridge forms a gently sloping western boundary for water generally below 3600m. The Angola abyssal plain has its deepest depression near 11°S to depths greater than 5600m, although there are smaller-scale canyons and fractures to similar depths elsewhere in the basin. The abyssal plain slopes upward to the south to about 5200 m near 20°S. It remains at this

depth to about 25°S, where the bathymetry becomes complex in the region of the intersection of the Walvis and Mid-Atlantic Ridges.

At 11°S, 79 hydrographic stations were occupied. Measurements of temperature, salinity and oxygen were made with a CTD, along with water samples from a 24-bottle rosette to determine silica, phosphate, and nitrate concentrations. Oxygen and salinity measurements from water samples were used for calibrating the CTD data. Station spacing was designed to resolve possible smaller-scale features near the eastern and western boundaries and Mid-Atlantic Ridge. Near these features the spacing was about 50 km, with a minimum separation of 25 km, and away from them the spacing averaged about 90 km.

Specifically, stations 131 through 170 in the Angola Basin of R. V. Oceanus cruise number 133 provide the basic data for this study. Sections illustrating the distributions of potential temperature, salinity, oxygen, phosphate, nitrate, silica, potential density referred to 4000 decibars*, and specific volume anomaly have been prepared specifically for the deep water of the Angola Basin (figures 2-9). Thus isopleths marking changes in property value are closely spaced, and in some cases approach the limits of accuracy of measurement. A measure of the high quality of the observations discussed here is the ability to do this without producing noisy looking results. The vertical distortion in the plots is 500:1.

---

*In 1980 a new equation of state for seawater was adopted by the Joint Panel on Oceanographic Tables and Standards. This is the equation of state used here and it will be denoted EOS80.

Measurements at each station were made with a Neil Brown CTD with twenty-four 1.2 l, PVC Niskin bottles on a General Oceanic rosette. Records of pressure, temperature, salinity and oxygen every 2 db were constructed according to standard W.H.O.I. CTD group practices (Millard, 1982). Pre- and post-cruise calibrations of the CTD pressure, temperature and conductivity sensors were done at W.H.O.I.. Post-cruise calibrations of pressure and temperature were used as they were more stable. The expected accuracy of the temperature measurements is ± .002°C. The expected accuracy of the pressure measurements is ± 1db.

Salinity measurements were made with a Guideline Model 8400A Autosal salinometer. The measurements were standardized before and after an analysis of a group of three stations with I.A.P.S.O. standard sea water. The accuracy of the calibrated CTD measurements of salinity is expected to be ± .002 °/₀₀. Dissolved oxygen measurements were made with the modified Winkler method. Laboratory prepared solutions of potassium iodate were used to standardize the measurements every five stations on average. The oxygen sensor was changed before station 161 and then again before station 162. The accuracy of the thus calibrated CTD oxygen-sensor records is thought to be ± .05 ml l^{-1}. Nutrient measurements were made by L. Gordon's group at Oregon State University and are thought to be accurate to 1 percent.

Also used in this thesis are data from Oceanus cruise 133 leg 4, stations 85 through 112, at 24°S in the Angola Basin. The same measurements were made on this section, but the data were not processed

completely at the time of writing. In addition, a computer printout of the hydrographic data from a recently completed section along 1°E (the AJAX expedition) was made available to me by J. Reid (Scripps Inst. of Ocean.).

Chapter 2

Property Distributions

This chapter is a brief descriptive introduction to some of the property distributions in the deep water of the Angola Basin, as illustrated in the sections (figures 2-9). The purpose is to describe some peculiar and some well known features of deep water property distributions which are significant for the deep circulation.

The conception of deep water circulation in the South Atlantic has evolved during the past 100 years (Warren, 1981b). Before 1900 deep water was thought to move equatorward, except perhaps in regions of strong upper layer flow. In 1911 Brennecke presented a clear description of the southward flow of water in the depth interval 1500 m to 3000 m in the western South Atlantic. This flow contradicted the earlier direct convection cell pattern, in which water was thought to sink at high latitudes and rise near the equator uniformly across the basin. Merz and Wüst in 1922 contrasted the western and eastern troughs by the northward flow of bottom water in the west and southward flow of bottom water in the east. Later, Wüst (1935) described the layering of deep water. He stated that the influence of the deep water (called "spreading" everywhere) had the character of a current only near the western boundary. In the eastern trough, the influence of deep water is suggested to be due to eddy fluxes. His and other observations in higher latitudes of both the North and South Atlantic have demonstrated that the description of deep water layering is not mere naming, but reflects the origins of deep water.

2.1 Silica Minimum

At 1600 m depth and at a potential temperature of 3.5°C there is a silica minimum (Figure 7). This minimum exists throughout most of the Atlantic in a range of potential temperatures from 2.4°C at 35°S to 4°C in the northern parts of the western trough (Mann, Coote, and Garner, 1973). Low silica in the Atlantic is characteristic of water of northern North Atlantic origin and at this potential temperature represents the influence of Labrador Sea Water. At 11°S the average minimum values increase from 28 μmol l^{-1} in the east to 29 μmol l^{-1} near station 153, decreasing to 25 μmol l^{-1} near station 170. Values at the minimum decrease to less than 20 μmol l^{-1} near the western boundary with Brazil at 11°S.

At 24°S a silica minimum exists near 3.1°C (figure 12). Values at the minimum are higher than at 11°S, typically between 35μmol l^{-1} and 40μmol l^{-1}, increasing from the Walvis Ridge to the Mid-Atlantic Ridge. The maximum value at the silica minimum is about 43μmol l^{-1} at 10°W. They decrease again to the west to about 20μmol l^{-1} at the western boundary with Brazil at 24°S (McCartney, data pers. comm.). In general, silica increases to the south and southwest away from 11°S.

To the north and west, silica decreases (figure 12, GS 109 and 110). Thus at this depth, the source of water influencing property distributions in the Angola Basin is to the north and west. North of 11°S in the Guinea Basin, water is supplied by eastward flow along the equator at these depths, as indicated by the high salinity, high oxygen and low nutrient extrema there (Bainbridge, 1980).

2.2 Salinity

Close to 2000 m depth there is a salinity maximum across the basin (figure 3). The potential temperature at this level is close to 3.1°C. The maximum is most intense at station 170, the westernmost station in figure 3, where the salinity is 34.94°/oo. Salinity increases west of station 170 to a maximum of 34.96°/oo near the western boundary with Brazil. The salinity decreases eastward to less than 34.925°/oo at station 154, then increases to a maximum value of 34.935°/oo at the eastern boundary. This pattern of salty-fresh-salty appears in sections at 8°S, 16°S, and 24°S (Fuglister, 1960), and in the more recent CTD section at 24°S. It can be visualized as a core of high salinity water within the salinity maximum extending along the eastern boundary into the Cape Basin.

To the south, salinity decreases gradually to about 25°S, where the salinity maximum near 2000m ends somewhat abrubtly throughout the interior of the Angola Basin (that is, west of the Walvis Ridge; J. Reid, data pers. comm., Bennekom and Berger, 1984). In the South Atlantic outside the Angola Basin, in contrast, the salinity maximum does not end: between the Walvis Ridge and the African continent, and also west of the Mid-Atlantic Ridge, the salinity maximum exists as a continuous feature, deepening to 2600m south of 30°S (Bainbridge, 1980). At 24°S, the salinity maximum is still apparent near 2.7°C (figure 10, OC 107), with a salinity of about 34.88°/oo.

North and west of the section at 11°S in the Angola Basin, salinity increases slightly (figure 10, GS 110; Bainbridge, 1980). Therefore the

high salinity, as with the low silica, must be due to an influence from the north and west.

The general pattern of the salinity distribution below the maximum is of isohalines sloping downwards toward the eastern boundary. For instance, near 3000m, where isopycnals are fairly flat (figure 8), salinity increases from about 34.90°/∘∘ to about 34.91°/∘∘ from 10°W to 10°E. This variation of salinity of about 0.01°/∘∘ on isopycnals appears at the salinity maximum as a fresh region centered near 5°W, as mentioned above. Thus an alternative way to visualize the salinity distribution on an isopycnal near 3000m, say, is as a tongue of low salinity extending northwards above the eastern flank of the Mid-Atlantic Ridge. This latter picture is evident in the atlas of Levitus (1982).

To maintain the fresh region there must be a source of low salinity. However, the general southward movement of deep water inferred from the silica and salinity distributions in the Angola Basin and adjacent basins is supported by geostrophic calculations (section 3.4) in the station range 145 to 164 and below 2000m. Because salinity increases to the north above about 3600m, this motion tends to increase salinity at 11°S in this range (figure 10; J. Reid, data pers. comm.; Bainbridge, 1980; Fuglister, 1960). Evidently the southward movement of water below 3600m (about 2.1°C) above the eastern flank of the Mid-Atlantic Ridge, which brings fresher water to the Angola Basin from the Guinea Basin (section 3.4) is the source of low salinity. Presumably in the process of moving over the rough topography of the Ridge it mixes vertically along its path. Similar remarks seem to apply to the silica

distribution between 2000m and 3000m. A faint increase in silica concentration appears at the position of the silica minimum, vertically aligned with the fresh part of the salinity maximum near 5°W. Such a small increase, only about 1μmol l^{-1}, is too small to show up as a large-scale slope of isopleths of silica in the section at 11°S.

An additional, purely speculative mechanism may act to enhance mixing above the Ridge. Visible in figures 2 and 3 are about 100 km scale pertubations which are anomalous with respect to an average θ-S relation. That is, they are not the result of purely vertical motion. These pertubations have a greater strength and frequency above the Ridge than in the interior. Temperature and salinity do not entirely offset one another, so that density is perturbed, and hence velocity. This is evidence for an enhanced lateral mixing, with warmer, saltier water to the north mixing with cooler, fresher water to the south, owing to a net displacement of parcels of water by the motion. Perhaps this is accompanied by greater vertical mixing, too. The generation of topographic waves over the bumpy, sloping Ridge by small-scale currents penetrating from shallower levels could be responsible for these pertubations.

The Angola Basin south of about 20°S has an additional feature in the salinity distribution at mid-depth. That is the existence of a salinity minimum above the bottom in the approximate latitude range of 20°S to 25°S (figure 16b and c; Bennekom and Berger, 1984). The potential temperature of the minimum is about 2.3°C at 24°S. The salinity at the minimum ranges from 34.87°/°° to 34.878°°°, and

appears to have a very weak east-west trend, with fresher values in the east near the Walvis Ridge at 24°. The lower part of this minimum is within the density range 45.82 to 45.84 sigma-4. In the same density range farther south across the Walvis Ridge in to the Cape Basin, there is a salinity maximum (Bennekom and Berger, 1984; J. Reid, data pers. comm.). North of 28°S this density range is blocked to the east by the Walvis Ridge, except for a saddle near 22°S. Values in the saddle (GS 104, not shown) are higher than 34.88°/∘∘, so that low salinity does not appear to be advected in from the east. To the west at 24°S, across the Mid-Atlantic Ridge, salinity near 2.3°C increases. The source of low salinity must be to the south. Horizontal mixing on isopycnals would seem to be necessary to produc the salinity maximum south of the Walvis Ridge and salinity minimum north of the Walvis Ridge in the same density range. The corresponding depth range is about 2500m to 3500m. Additional support for this mechanism is the virtual coincidence of the oxygen maximum and salinity minimum at 24°S (figures 10 and 12). The source of low salinity is to the south while the source of high oxygen is to the north (Bainbridge, 1980; J. Reid data pers. comm.; see also section 2.4)

Temperature-salinity pertubations, mentioned above in the context of mixing at 11°S, are stronger at 24°S throughout the section (some hint in figure 15 and 16 with preliminary salinity data, above 3000m not shown). Why they should be stonger at 24°S is not clear.

It may be speculated that eastward flow across the Mid-Atlantic Ridge to the north near 21°S (Bainbridge, 1980; J. Reid, data personally

communicated) might help to maintain a stronger eddy field at 24°S. Evidence in the density field for such a flow near 20°S is on the map of steric height given by Reid (1981). Such a flow could generate stationary Rossby waves near the sill of the Ridge and in the Angola Basin. Although the waves are vertically trapped for eastward flow greater than β/K_H^2=0.25cm/s, where K_H is the wavenumber of the pertubations (100km, say), the trapping scale is about 3km. Hence the waves should be able to penetrate much of the mid-depth range of the basin. For these reasons, perhaps, horizontal mixing could be greater at mid-depth at 24°S.

2.3 Phosphate and Nitrate Minima

The layer of low phosphate and nitrate in the Angola Basin, defined approximately by nitrate less than 24μmol/l (minimum value 22.5) and phosphate less than 1.6μmol/l (minimum value 1.5μmol/l) , is quite thick, about 1000 m, and centered near 2400 m. In a density range corresponding to this layer, about 45.7 to 45.8g/cm^3, these properties have lower concentrations in adjacent basins to the north and west (Bainbridge, 1980). To the south they increase slightly and then decrease to a minimum near 21°S. From there southwards they increase (figure 12b; J. Reid, data pers. comm.). As with silica, phosphate and nitrate owe their low values to the influence of water from the north and west. The reduced nutrients at 21°S are accompanied by high oxygen and high salinity values and indicate eastward flow, with property extrema centered near 2200m (about 2.8°C; Bainbridge, 1980).

In the western trough of the South Atlantic the influence of water of low nutrient concentrations from the North Atlantic is stronger than in the

eastern trough. A minimum layer defined by the same limits is more than 2000 m thick, even though much higher nutrient values lie below in the AABW. In the eastern trough the generation of nutrients in shallower and deeper layers has reduced the vertical extent of the minimum.

2.4 Oxygen

Roughly centered at 2800 m east of 0° there is an oxygen maximum with a value of 5.3 ml l^{-1} (figure 4). The potential temperature range is between 2.4°C and 2.6°C. This uneven layer is made noisy by the pattern of low oxygen concentration above and below it. To the north, in the Guinea Basin, the oxygen values are between about 5.6ml/l and 5.7ml/l below 3.5°C (2000m), with maxima centered near 3.3°C (2000m) and 2.0°C (4000m; figure 12). Eastward flow induces isolated oxygen maxima on the equator at these depths in a north-south section farther east at 1°E (J. Reid, data pers. comm.; note that the GEOSECS section in Bainbridge (1980) is not north-south). Near 2°W at 11°S, the oxygen maximum merges with higher oxygen concentrations above the Mid-Atlantic Ridge. Oxygen concentrations above the eastern flank of the Mid-Atlantic Ridge are fairly uniform, and of intermediate value, near 5.5 ml l^{-1}. Below 3000m oxygen increases to about 5.6 ml l^{-1} at the bottom. Between 2000m and 3000m oxygen concentrations range from 5.4 ml l^{-1} to 5.6 ml l^{-1}, increasing from east to west. Oxygen concentration at 11°S increases west of the Mid-Atlantic Ridge to values of about 5.9ml/l near the western boundary with Brazil (not shown).

Congruent with the phosphate and nitrate distributions oxygen decreases and then increases southward to a maximum near 21°S on an isopcynal (Bainbridge, 1980; J. Reid, data pers. comm.). It then decreases again southward. At 24°S the oxygen maximum is near 2.2°C (about 3000m depth; figure 12, OC 107). Values at the maximum at 24°S decrease from 5.6ml/l above the Mid-Atlantic Ridge to 5.5ml/l near the Walvis Ridge. Thus in the temperature range of 2.05°C to 2.7°C spanning the oxygen maximum at 24°S, concentrations are higher than at 11°S. The eastward flow near 21°S has an oxygen maximum core centered at 2.8°C, with values greater than 5.55ml/l at 1°E (J. Reid, data pers. comm.). This raises oxygen concentrations at 24°S relative to 11°S.

In figure 12 the oxygen profile at 11°S (OC 148) between 3.0°C and 2.0°C, which includes the interior maximum and minimum, has a different shape from that in the Guinea Basin near the equator (GS 110). Isotherms slope downward slightly in the depth range 2000m to 3000m between 11°S and the equator. On isopycnals in this range, potential temperature increases by about 0.05°C. This change is small on the temperature scale of figure 12. In the temperature range below 2.5°C, where oxygen at 11°S is decreasing by about 0.1ml/l to its minimum value, oxygen at GS 110 is increasing by about the same amount. Although this depends on basically

*An estimate of the decrease in oxygen concentration due to aging is the product of the advective time and the interior consumption HQ/w, where H is the vertical scale, Q is the consumption, and w is the vertical velocity scale. For $w=10^{-5}$cm/s, $H=10^{5}$cm, and $Q=10^{-10}$ml $l^{-1}s^{-1}$, this is 1 ml/l. This is plenty to account for the decrease in oxygen to the east at this latitude, but the details of the distribution will be seen in chapter 4 to require horizontal mixing and boundary consumption to be important, too.

one measurement in the figure, the same pattern occurs on profiles farther east up to 5°S in the Guinea Basin (J. Reid, data pers. comm.). Although interior consumption can account for a general decrease in oxygen concentration in southward flow*, it cannot change the vertical profile unless the flow itself varies. Apparently water near the density of the oxygen minimum at 11°S either takes longer to reach 11°S than water above or below, or is influenced by nonuniform consumption, or both.

At 11°S there is large scale shear below the isopycnal 45.85g/cm^3 relative to mid-depth, indicating an increasing southward component of flow toward the bottom (figure 8, see also section 3.4). There is not an obvious meridional mean velocity extremum at 11°S near the level of the oxygen minimum, as would be indicated by a reversal in isopycnal slope. Yet transport calculations in section 3.4 indicate a southward transport above and below a 3600m zero velocity reference level in the station range 145 to 164. Some hint of a reversal in isopycnal slope is indicated by the lower specific volume anomaly in the west near 2800m (figure 9). The transport calculations and specific volume field together do, then, support the presence of a mean velocity extremum near 3600m in the above station range. Owing to this and the previous discussion of property distributions in which a general southward flow was inferred, the circulation is thought to be one of fairly uniform southward flow east of about 4°E (station 145), and southward flow west of this longitude, zero near 3600m.

Details of the oxygen minimum at 11°S are discussed in chapter 4. Details of the flow above the Mid-Atlantic Ridge are given in the next chapter. Also, the meridional variations in properties are considered in the context of a SA circulation scheme.

Chapter 3

Bottom Water Circulation

3.1 Introduction and Abstract

The densest water in the South Atlantic is Antarctic Bottom Water (AABW), which has spread northwards from its formation region near Antarctica. It has been known for over one hundred years that the Walvis Ridge is a substantial barrier to AABW in the eastern trough of the South Atlantic (see appendix). Thus the bottom circulation there is very different from that in the western trough, where the AABW flows northwards as a western boundary current. The AABW surrounds the eastern trough at the sill depths of the Mid-Atlantic and Walvis Ridges and finally crosses the Mid-Atlantic Ridge through the Romanche Fracture Zone near the equator. It moves eastward through the Romanche Fracture Zone into the Guinea Basin, where it can enter the Angola Basin from the north. Evidence for a minor inflow across the Walvis Ridge has been presented by Connary and Ewing (1973). With either or both of these two sources a model to be developed based on the Stommel and Arons (1960a,b) theory predicts a DWBC and an interior circulation pattern. The purpose of this chapter is to clarify sources of bottom water to the Angola Basin, and compare the circulation pattern of the model with observed property distributions. For the purpose of discussion bottom water is denoted roughly by a potential temperature less than 2.1°C, a salinity less than 34.895°/₀₀, and therefore depth greater than about 3600 m. This definition is meant to correspond approximately with a marked decrease in

vertical gradient of potential temperature and salinity profiles which occurs near 3500 m across the basin (figures 2 and 3). The bottom water includes a mixture of NADW and AABW, with roughly 15°/∘ AABW, assuming salinities of 34.67°/∘∘ and 34.92°/∘∘ as AABW and NADW mixing endpoints.

In section 3.2 the characteristics of the two bottom water sources are described. The properties in the bottom water are only consistently explained as a mixture of Guinea Basin source water and overlying water. It is suggested that the southern source is prevented from supplying the Angola Basin by a system of ridges near 30°S.

In section 3.3 a model for bottom circulation based on SA theory is presented in order to predict flow and property distributions. In sections 3.4 and 3.5 the model is compared with observations. First, evidence is given for the existence of a DWBC in the Angola Basin. Next, the model is tested by developing an equation for the change in temperature and salinity along a horizontal streamline in the bottom layer. The data at 11°S are used to predict the distribution of these properties at 24°S. The pattern and value of temperature and value of salinity predicted agree with observations at 24°S when vertical diffusion is included.

3.2 Bottom Water Sources

To facilitate a discussion of bottom water properties and possible sources, plots of salinity, oxygen, silica, and phosphate versus potential temperature have been prepared. Several observations and arguments will be presented to show that the only source of bottom water to the

Angola Basin is from the north, in the Guinea Basin. The discussion is designed to illustrate two things. First, that there is a fairly tight relation between potential temperature and salinity in the bottom water of the Angola and Guinea Basins, and that moving south from the equator there is a clear progression to lighter density within this relation. That is, as one moves south on the bottom, the most extreme water type (cold, fresh, dense) progressively disappears. Second, that the bottom water properties in the Angola Basin are not the result of mixing between Guinea and Cape Basin and overlying water, but between Guinea Basin and overlying water only.

Figure 10 is plots of salinity versus potential temperature at GEOSECS station 110 (Bainbridge, 1980) on the equator in the Guinea Basin, Oceanus stations 148 at 11°S, and 107 at 24°S, GEOSECS station 102 at 32°S, and Atlantis stations 5829 and 5842, and the last two values at 5828 at 32°S. The station locations are illustrated in figure 1. The Oceanus stations chosen have the coldest, freshest and densest bottom values in their respective sections. Both Atlantis stations 5828 and 5829 are in the region of northward influence of Cape Basin water according to Connary and Ewing (1974). There are three things to note in this figure:

1) The water at the sill depth of the Walvis Passage (4200 m) is much colder (potential temperature = 1.0°C) and fresher than the bottom water in the Angola Basin at 11°S or 24°S.

2) The bottom water at the Atlantis stations in the southwest corner of the Angola Basin has a relatively high density.

3) The density of bottom water at 24°S is less than that at 11°S.

Figure 11 illustrates the progression of bottom water up the θ-S relation with latitude in the Guinea and Angola Basins. The extreme properties of Cape Basin water are reflected in the mixing solutions to be discussed next.

Mixing Solutions

Characteristics of bottom water at 11°S and 24°S, and of water at the sill depths of the Guinea Ridge (4300 m) and Walvis Ridge (4200 m) are given in the left box in table 1 (sources of data were Connary and Ewing, 1972; Bainbridge, 1980; the recent 11°S and 24°S sections; and Fuglister, 1960). Also given are the characteristics of overlying water at 11°S which will be used to represent vertical mixing. The overlying water characteristics are assumed to be average values of properties near the 3600m level. The definition of overlying water is somewhat arbitrary; it is simply meant to represent the influence of warmer, saltier, higher-nutrient, and lower-oxygen water above the bottom layer. The given conservative estimate of these characteristics and the neglect of consumption in these solutions provides the best case for the presence of a component of Cape Basin water.

In the next two boxes of table 2 the percent of each component is given first for mixing between all three water types, and second for mixing between Guinea Basin and overlying water alone. In the first case these percentages were computed for pairs of properties, with salinity always being one of the pair, by writing the 11°S bottom water characteristics as the sum of unknown percentages of each of the components. This results in three equations in three unknowns. In the second case each property gives two equations in two unknowns. The results for the three component mixing show an order of magnitude range of contributions of Cape water to the solution in addition to no solution for the pair potential temperature and salinity (since the sources lie almost on a straight line). The results for the two component mixing (except for phosphate) show a fairly consistent mixture of 4/5 Guinea Basin water and 1/5 overlying water. Phosphate requires a larger component of overlying water since Guinea Basin water is so low in phosphate, although 1.5μmol/l seems about right (figure 12; further discussion of phosphate in section 4.1). The silica and salinity mixture is sensitive to the choice of the overlying value and is easily chosen to be almost any combination of the two components. For these reasons the only acceptable composition for bottom water at 11°S is of overlying and Guinea Basin water. At 24°S potential temperature and salinity have increased owing to vertical fluxes as the water moves south (section 3-5). Oxygen and nutrients at 24°S are discussed in chapter 4.

Figure 12 illustrates oxygen, silica, and phosphate in water below 4°C in the Guinea, Angola, and Cape Basins. Visible in figure 12 is the

tendency of bottom water at 11°S (OC 148), and 24°S (OC 107) toward high oxygen and low silica. Only the influence of northern source water can raise oxygen and decrease silica concentrations. The low silica from the north helps to maintain an above bottom silica maximum above the abyssal plain of the Angola Basin, by reducing the concentration near the bottom. A southern bottom water source would have the opposite effect (table 1, figure 13, and see below). Furthermore the bottom water at 24°S is not dense enough, and is too low in oxygen to be the source for 11°S bottom water.

As a further illustration of the high-oxygen-low-silica tendency, in figure 13 the relation between oxygen and silica for water of potential temperature less than 2.5°C is shown for the deepest stations at 11°S (OC 148) and 24°S (OC 107). Also shown are stations in the Guinea and Cape Basins (110 and 102 respectively, 102 is representative of values south of the Walvis Ridge). The dashed line represents an estimate of silica released by dissolution of the hard parts associated with organic matter which remains in the water column. It depends on the silica to carbon ratio in the particular piece of matter, which is assumed to be 0.2 (estimates in the region range from 0.1 to 0.4). It has a slope of about 8 μmol l^{-1} per ml l^{-1}. The position of the line is arbitrary, but in this figure it has been placed to intercept the bottom values at 11°S (circles). This line then intercepts the Guinea Basin curve (diamonds) at a potential temperature near the sill depth. Both of the Oceanus station profiles hook first through an oxygen minimum, and then through a silica maximum. The near bottom values at OC

148 are found progressively closer to the northern source. All bottom water lies near (within 2μmol/l) or above the dashed line, which implies that all the silica and oxygen values in the bottom water can be explained by decomposition and vertical mixing alone, from a source located in the Guinea Basin at the sill depth of the Guinea Ridge.

Conclusion

In summary, the only source of bottom water in the Angola Basin is to the north, in the Guinea Basin. The water in the southwest corner of the Angola Basin is shallower and more dense than the water farther north, and does not influence properties farther north. It therefore is likely that this water is prevented from entering the Angola Basin by a ridge or system of ridges near 30°S, between the Walvis Ridge and Mid-Atlantic Ridge, and which forms the true seperation between the Angola and Cape Basins. Some hint of such a ridge is on the bathymetry chart of Uchupi (1981). Isobaths indicate a ridge extending from the Walvis Ridge at 29°S and almost meeting a ridge from the Mid-Atlantic Ridge in the region 0° to 2°W and 29.5°S to 30.5°S. It is this ridge system which seems to form the true division between the Cape Basin bottom water and the Angola Basin bottom water, as indicated by the following measurements of temperature and salinity.

Measurements by Bennekom and Berger (1984) show bottom water near 2°C potential temperature just to the northwest of this region (their station 80-24 at 30°S,3.5°W). Measurements by Connary and Ewing (1974) show anamolously low bottom water temperatures at two stations just to the south of this region (their stations 259 and 260 at 31°S). At 33.5°S and 5.5°W, south of this region, but on the Angola Basin side of the

Walvis Ridge, Bennekom and Berger's station 80-25 shows a bottom water potential temperature and salinity of about 1.7°C and 34.83°/oo. This data point lies on the Cape Basin θ-S curve (figure 10, At 5842 and GS 102, and figure 11). Isobaths indicate a sill depth between 4000m and 4400m. From the data of Connary and Ewing (1974), 4400m is too deep to prevent northward movement of the relatively fresh water below 2°C in the southwest corner, but 4100m or 4200m may be enough to do so. Further bathymetric and hydrographic measurements in this region are necessary to determine the nature of bottom water circulation there.

3.3 Circulation Model

With the knowledge of the location of the source of bottom water to the Angola Basin it is possible to construct a unique interior and boundary current circulation model based on Stommel and Arons (1960a,b) theory. The model is for the flow in the bottom layer of the Angola Basin, that is, below 3600m. The western boundary is the Mid-Atlantic Ridge, the eastern boundary is the African continent north of about 20°S and the Walvis Ridge south of this point. The northern boundary is the Guinea Ridge. They are assumed to be vertical, and the bottom is assumed to be flat at the basin's average depth of 5000m. The boundary condition is no normal flow on the eastern boundary. The only difference between this model and the original model of Stommel and Arons is a representation of the Walvis Ridge for the southern-eastern boundary (see figures 1 and 14). This diagonal boundary induces mean vorticity in the interior flow in the southern half of the basin because the eastern boundary condition makes the zonal velocity a function of y. The

presence of a southern boundary also allows the possibility of a recirculation region (see below). The presence of a northern boundary south of the equator means that v is not zero on the boundary and a source there will be distributed along this boundary in a current which feeds the interior flow. The exact location of the source is not critical, and is chosen here to be at the middle of the Guinea Ridge, where there is some hint of a passage (Uchupi, 1981).

The momentum equation for steady, large scale, small amplitude motion is the geostrophic balance

$$\begin{aligned} -fv &= -P_x \\ fu &= -P_y \end{aligned} \qquad 3\text{-}1$$

where $f=\beta y$ (equatorial β-plane) is the coriolis parameter, u and v are the horizontal velocities, P is the pressure divided by the (constant) density, and x and y are zonal and meridional coordinates. The vertical component of momentum is just the hydrostatic balance. The mass conservation equation is

$$u_x + v_y + w_z = 0 \qquad 3\text{-}2$$

The bottom layer is assumed to be homogenous. Taking the curl of the x and y components and using continuity gives the linear vorticity balance

$$\beta v = f w_z \qquad 3\text{-}3$$

The horizontal velocity is assumed to be independent of z in this layer, so from the mass equation w is linear in z. The velocity at the top of the layer is w_o, assumed to be independent of x and y. The source, S, to the layer must equal the mass leaving so that $w_o A=S$, where A is the area of the basin. At the bottom of the layer an Ekman exists to bring the horizontal velocities to zero at the bottom boundary. Although in the northern half of the basin the solution will have no interior vorticity, the interior velocity is divergent, and hence a vertical flow out of the Ekman layer exists. In the southern half of the basin the solution will have in addition interior vorticity. However, the vertical velocity out of Ekman layer is smaller than w_o by the factor $E^{1/2}$, where $E=K_v/fH^2$ is the Ekman number, K_v is the vertical turbulent diffusion coefficient, and H is the depth scale. For $K_v=1cm^2/s$, H=1km, and $f=10^{-4}s^{-1}$, $E^{1/2}$ is 10^{-3}, and hence this flow will be neglected.

Therefore integrating from the basin's average depth of 5000m to 3600m gives

$$\beta V = f w_o .$$

Now capital letters denote the integrated flow, or transport. Using the mass equation and $f=\beta y$ gives

$$V = y\, w_o$$

$$U_x = -2\, w_o$$

The eastern boundary condition is U=VdX/dy, where X is the position of the eastern boundary. In the northern half of the Angola basin, -L<y<0.2, the eastern boundary is at X=L, so U=0 there. In the southern half, -2L<y<-L, X=y+2L, so U=V. Therefore

$$V = y\, w_0$$

$$U = \begin{cases} 2\, w_0(L-x) & -L < y < 0.2 \\ w_0(3y-2x+4L) & -2L < y < -L \end{cases} \qquad 3\text{-}4$$

Note that at y=-L, the discontinuous slope of the eastern boundary induces a discontinuity in U. A discontinuity in velocity indicates that friction becomes important. Going back to the original integrated vorticity equation and retaining bottom vertical velocity one can show that a frictional boundary layer at y=-L will connect the zonal velocity smoothly. This additional structure will not be discussed since it does not modify the interior trajectories noticeably.

Figure 14 is the pattern of the circulation obtained from equations 3-4. The approximate positions of 11°S, 24°S, and the Greenwich Meridian are indicated. A northern boundary near 5°S representing the Guinea ridge is included in the scheme. The open circles are placed at equal intervals of time following a fluid column, to illustrate the different lengths of time it takes on different paths to reach the southern half of the basin. It is assumed that the boundary current (discussed in the next sections) distributes the source instantaneously around the northern boundary and part way down the western boundary. The Walvis Ridge

modifies the flow by causing streamlines to intersect the western boundary south of $y=-4L/3$.

This additional streamline curvature means that the velocity field in the southern half of the basin has vorticity, that is, mean shear, whereas there is no interior vorticity for a meridional eastern boundary. The magnitude of the shear is small, about $10^{-4}f$ (the shear scale is the inverse of the advective time scale, which is large compared to f). Perhaps mixing within the layer could be increased by this shear in the southern half of the basin.

It has been assumed that the bottom is flat and the walls are vertical. This is obviously not realistic, but the model is greatly simplified by this assumption while still retaining substantial dynamics. A bottom slope of 10^{-3} is typical of the Mid-Atlantic Ridge and continental rise, and implies a topographic β of the same magnitude as planetary β. Thus topography could modify the interior and DWBC in the model. However, for a single homogenous layer, topography which varies only in x, and if the the layer depth is not allowed to be small compared with the scale depth (1 km), the interior flow changes orientation only slightly. The main effect of a sloping western boundary on the flow pattern of the SA model is to spread the DWBC throughout the region of the slope. This happens because the topography tilts f/H contours, giving their tangent a component parallel to the boundary which can carry some of the flow. This effect is apparent in a study by Kuo (1974), but his calculations are probably not directly relevant to the Angola Basin since the bottom friction parameter E was taken to be much

larger than the above estimate. In his study $E^{1/2}=0.08$. The more realistic case of stratified mean flow over a large-scale slope is not well understood.

The flat bottom SA model gives an accurate representation of the basic flow pattern for weak topography and friction and will be used to discuss property distributions. By weak I mean that the depth changes are small compared to the scale depth H, and that friction is small as measured by E, so that $E^{1/2}<<1$ where E is the Ekman number.

Western Boundary Current

The interior circulation scheme presented above requires a western boundary current to feed the interior north of y=-4/3L. It also must receive a mass flux from the interior south of this point, and satisfy the no flux boundary condition in the west. The transport in this boundary current can be calculated by requiring the conservation of mass in any region that includes the western boundary and the source. The transport so calculated is also illustrated in figure 14 on the left. This western boundary current is a basic element of the model. The magnitude of the transport is scaled by the source strength, negative values are northward, positive southward. Note that although in the figure the DWBC seems to occupy only a small part of the basin in the west, it is assumed that this region is the entire area above the sloping western boundary, i.e., almost half of the basin.

The importance of the transport calculation is that it shows how far along the western boundary water with strong source-like

characteristics penetrates. At y=-3L/4 on the the western boundary, the transport of the boundary current is zero. Thus trajectories which emanate from points north of the zero transport position will carry source-like water properties into the interior. South of this point there is a northward transport. This part of the DWBC is recieving water from the interior south of a point y=-4L/3 where U=0. Between this point and the zero transport point to the north, it feeds water into the recirculating region in the western portion of the figure. This is the basis for the distribution of properties to be discussed below. The distribution strongly depends on the location of the source.

The source of bottom water to the Angola Basin has been shown to be in the north. The model predicts that about 20°/∘ of the source enters the interior directly, from a northern boundary current, the other 80°/∘ moves southward in the western boundary current. The question of whether or not the source water enters the basin as a DWBC will be discussed next.

3.4 A Deep Western Boundary Current in the Angola Basin

In the bottom water of the Angola Basin at 11°S, neither temperature nor salinity is uniform. The lowest potential temperatures were found at the bottom at station 148, which is within the broad central depression of the abyssal plain near its intersection with the ridge (figure 2). The potential temperature at this location was about 1.91°C. Near the continental rise (about 5°E) at a comparable depth the potential temperature was close to 1.92°C. Along with this increase in temperature to the east was an increase in salinity (figure 3). Thus the

bottom water is characterized by relatively cold, fresh water in the west. Potential temperature is not vertically uniform in the water below the sill depth of the Guinea Ridge, about 4400m, indicating that the flow over the Guinea Ridge is not restricted to a narrow depth range.

In the station range 145 to 160 and below 2.1°C, isopycnals slope downward to the west indicating an increasing southward component of the flow towards the bottom (figure 8). Specific volume anomaly shows a consistent opposite slope in this range (figure 9). In the same station range and between 1.92°C and 2.1°C, isotherms and isohalines are not parallel. That is, moving westward along an isopycnal in this region, potential temperature and salinity decrease. This must be the result of the movement of water from a source with a different potential temperature-salinity relation because isotherms and isohalines are parallel in the same density range east of station 145, and below 2.1°C. Oxygen in the bottom water is higher in the west than in the east. It is high enough so that a mixture of southern source water (figure 12, At 5829, GS 102) with the relatively high oxygen overlying water at 24°S (OC 107) does not produce water of such concentration. The zonal trend at 11°S is not an artifact of the low oxygen near the eastern boundary since below 1.95°C oxygen isopleths parallel isopycnals. Silica is lower in the west but nitrate and phosphate do not change consistently below their deep maximum across the basin. The lower salinity, lower temperature, higher oxygen, and lower silica water could only have a source in the Guinea Basin. Properties near the sill depth of the Guinea Ridge have

all these characteristics to a somewhat greater degree (table 1). This feature at 11°S is therefore identified as a DWBC, carrying water southward from the Guinea Basin along the eastern flank of the Mid-Atlantic Ridge.

An estimate can be made of the transport in this southward flow, consistent geostrophically with the slope of the isopycnals and an upper zero reference level in the station group 145 to 164. A choice of reference level shallower than about 3500m results in a net northward transport below the reference level above the Mid-Atlantic Ridge. The previous discussion indicated that water below 2.1°C was moving southward above the Ridge. For net southward transport, a choice of reference level near 3500m is necessary. Following the previous discussion, the reference level is chosen to be the 2.1°C isotherm, very nearly 3600m depth. With this zero reference level choice, the transport in the DWBC between this level and the bottom in the above station group is $1.4 \times 10^6 m^3 s^{-1}$ southward. The average velocity in this flow is 0.1cm s^{-1}. The net transport above the reference level to 2000m is $3.3 \times 10^6 m^3 s^{-1}$ southward, consistent with the observed high oxygen and low nutrients in this layer. The average velocity in this flow is also about 0.1cm/s.

The model predicted that at 11°S the transport in the DWBC would be about 60°/∘ of the source strength. The estimate of the source strength is thus $2.5 \times 10^6 m^3 s^{-1}$. Given this net source of water to the Angola Basin, an estimate can be made of the upwelling. The area of the basin bounded by the 3600m isobath is about $5 \times 10^{16} cm^2$. Assuming the water

leaves the basin uniformly across the upper surface of the layer the estimated vertical velocity there is thus 5×10^{-5} cm/s.

The SA model also predicts a northward flowing DWBC at 24°S, because of the Walvis Ridge. The density field at 24°S was calculated using preliminary salinity data (not shown). It is expected to be an accurate representation of the pattern because the discrepancy between salinometer and CTD salinity results is small above 4000m, and below 4000m the density pattern essentially follows temperature. The large-scale pattern for water below 2000m in the Angola Basin at 24°S is of density decreasing from the Mid-Atlantic Ridge to near the Walvis Ridge above 3000m, and increasing in the same range below 3000m. Above the Mid-Atlantic Ridge at 24°S there is a hint of isopycnal slope indicating an increasing northward component of flow toward the bottom (essentially the same pattern as for temperature in figure 15, stations 93 to 98). There is a decrease in salinity to the west in the station range 88 to 95 and depth range 3200m to 4200m (figure 16; also supported by salinometer measurements, figures 16b,c). This is also a hint of northward flow since salinity decreases to the south along the Ridge. If such flow exists and if it acquired its low salinity from mixing in more southerly portions of the basin, it should have a correspondingly high silica signal. If anything, silica decreases slightly to the west in the same depth or density range (not shown). Farther south, there is no oxygen maximum above the bottom, oxygen is generally lower (figure 12). Therefore northward flow should have a low oxygen signal. However oxygen increases on isopycnals towards the west in the same range as above (not

shown). In short, property trends are conflicting for meridional mean flow above the eastern flank of the Mid-Atlantic Ridge at 24°S. This discussion is tentative, though, and more detailed calculations of the flow need to be considered along with properties. Estimates of flow and transport must await the fully processed data.

3.5 Distribution of Temperature and Salinity

The purpose of this section is to compare the observed distributions of properties in the interior of the Angola Basin with some predictions of the SA model. The streamlines of horizontal interior flow, or isobars, are illustrated in figure 14. These are also the trajectories of columns of water in the bottom layer. With these streamlines, the transport in the DWBC, and the property distribution at 11°S, zonal variations in the properties further south can be deduced. Data from a section at 24°S will be used to make this comparison.

Unfortunately, there is not a large enough zonal variation of oxygen and nutrients at 24°S to make such a comparison for these properties. Sections of these properties at 24°S are not displayed here but a summary is given for reference. Figure 12 illustrates these properties at 24°S at station 107. In the bottom layer at 24°S, the concentration of oxygen is quite uniform at 5.4 ml l^{-1} throughout the minimum layer between 3500m and 4500m, and between 5°W and the Walvis Ridge. West of 5°W the oxygen increases to 5.45ml/l at the Mid-Atlantic Ridge. Below the minimum, oxygen increases to 5.45ml/l at the bottom. The concentration of phosphate is close to 1.67 μmol l^{-1}. The silica

concentration increases from 52μmol l^{-1} to about 54 μmol l^{-1} from 3500m to the bottom. Over the abyssal plain there is a maximum near 2°C. The slight decrease in silica (and salinity) below the maximum indicates the waters origin in the northern part of the Angola Basin. It decreases to the west on isotherms by about 1μmol l^{-1} from the interior to the Mid-Atlantic Ridge. These values are all close to their average values in the bottom layer at 11°S. So the distribution of these properties at 24°S can be characterized as the result of horizontal and vertical mixing within the bottom layer as the water moves southward. Some mixing is expected owing to eddies, shear and strain in the velocity field.

The potential temperature in the bottom layer at 24°S does show a significant horizontal variation in the interior, to be discussed below, and so it will be used for the comparison. The average values of both potential temperature and salinity in the bottom layer are different at 11°S and 24°S. A simple model for the expected change in these properties consistent with the SA flow will be given.

A Model for Advection and Vertical Diffusion

The time independent equation for a tracer, C, is

$$u\,C_x + v\,C_y + w\,C_z = K_H(C_{xx} + C_{yy}) + K_v C_{zz} \qquad 3\text{-}5$$

when there are no internal sources. Here K_H and K_v are horizontal and vertical turbulent diffusion coefficients, assumed uniform. Except

for the northern boundary and northern part of the western boundary, which are upstream for the interior flow, there are no horizontal sources of temperature or salinity. Hence the main effect of horizontal mixing would be to smooth the tracer fields across trajectories. It could not produce a net increase in tracer concentration in the basin. Therefore for simplicity, horizontal diffusion is neglected. Vertically averaging (defined as the integral divided by the thickness) 3-5 through the bottom layer gives

$$u\,\overline{C}_x + v\,\overline{C}_y + \frac{w_o}{H}\,(C_o - \overline{C}) = K_v\,C_z^o$$

where the overbar denotes a layer average, and the zero sub- or superscript denotes a value at the top of the layer. The velocity is independent of z, so u=U/H, v=V/H. The flux K_vC_z is zero at the bottom. The coordinates x and y are nondimensionalized by L, z by H, and u and v by w_oL/H. For $w_o=5\times10^{-5}$cm/s, L=1500km, $H=10^5$cm, the velocity scale $w_oL/H = 7.5\times10^{-2}$cm/s. Writing the equation following the trajectory of a fluid column in the bottom layer (the characteristics of the equation) gives

$$\frac{d\overline{C}}{dT} = \overline{C} - C_o + Pe^{-1}\,C_z^o \qquad 3\text{-}6$$

where T, the advective time scaled by H/w_o, is the coordinate along a trajectory. The parameter $Pe=w_oH/K_v$ is the Peclet number representing the relative importance of advection and diffusion. For the

above values of w_o and H, and for K_v=1cm^2/s, H/w_o is about 67 years and Pe=5.

Equation 3-6, together with equations 3-4 for the streamlines are a system of first order equations, and can be solved by the method of characteristics. In equation 3-6, the horizontal convergence in the layer ($U_x+V_y<0$) is a source of tracer and gives rise to the C term on the RHS via the mass equation. The difference between this and the net advective plus diffusive flux changes the average concentration of the tracer following a fluid column. To solve this equation, the mean tracer concentration must be given initially, and one must know the value of the concentration and its vertical derivative at the top of the layer all along a trajectory.

As mentioned in chapter 1, the θ-S profile is characterized by strong gradients near 3500m, compared to those below. Therefore first assume that $dC/dT = Pe^{-1}C_z^o$. Then the mean value of the tracer changes along a trajectory by an amount proportional to the advective time T. This simplest case results in a distribution of tracer in the southern half of the basin which is more source-like in the east, because water columns following eastern trajectories were more recently on the northern and western boundary, where source-like properties are strongest (figure 14). In this figure, young and east refer to an average age of all the trajectories in the east which are not part of the recirculation. The trajectories run into the western boundary and enter the recirculation boundary current in the southern part of the basin. Water then moves north with some average value of tracer. It reenters

the interior, and is again subject to equation 3-6. Since bottom temperature tends to increase with time, the lowest temperatures should be transposed to the eastern side at 24°S.

For salinity the situation is complicated by the fact that it has a different vertical structure in different regions of the Angola Basin. South of about 20°S there is a salinity minimum above the bottom near 2.6°C (figures 10 and 16). Therefore vertical mixing would lower salinity in bottom water. For this reason salinity, if anything should be higher in the east at 24°S.

For comparison the situation for a southern source will be briefly outlined. The interior pattern is the same. The transport is changed since it is required to be northward in the southwest corner. The addition of a southern source essentially shifts the solid line representing the transport calculation in figure 14 to the left, increasing the northward component along the Mid-Atlantic Ridge. The location of the zero transport point changes, and if the southern source is any stronger than about 1/2 the northern source strength, the transport is northward at 11°S. Of course if the northern source strength is zero, the transport is northward at 11°S, decreasing to zero at the northern boundary. Property distributions would be correspondingly different, with property values nearer those of the Cape Basin values in table 1 strongest in the southwest, and weakest in the southeast. This is not what is observed.

The potential temperature and salinity pattern at 24°S (figures 15 and 16) reveals lower temperatures in the east as predicted. For

instance, at 4500m temperature decreases from above 2.0°C to below 1.99°C near the Walvis Ridge. There is a slight hint of fresher water in the east in the uncalibrated CTD salinity data (figure 16). However this is not confirmed by salinometer data (figures 16b and c). Salinity does not appear to have a significant trend in the bottom layer, and it seems unlikely that the calibrated CTD data will have one, given the salinometer results. Any salinity trend is apparently too weak to persist with horizontal mixing, which has reduced horizontal salinity variations to within measurement error. Salinity does decrease to the bottom below a maximum near 4000m, a sign of its origins in the northern part of the basin. Both the average temperature and average salinity have increased in the bottom layer from 11°S to 24°S. Isotherms below about 1.99°C and isohalines below about 34.884°/∞ do not appear at 24°S. However water fresher and cooler than this enters the interior farther north. Since water is assumed to be upwelling throughout the bottom layer in the interior, as it moves south, it crosses isotherms and isohalines. Neither property is conserved on streamlines, and the terms on the right hand side (RHS) of equation 3-6 will have to be estimated.

Since there are only data at 11°S and 24°S, the evolution equation for the tracer cannot be solved continuously from the beginning of a trajectory to its end. What can be done instead is to use the data at 11°S to estimate the RHS of the equation as a function of longitude and calculate the value of the tracer farther south. Trajectories which reach 24°S but originate from the southward moving part of the DWBC south of 11°S are included, since θ-S values close to those at 11°S should

continue that far. An estimate of the RHS of equation 3-6 from plots of potential temperature and salinity versus depth for stations 140 to 150 at 11°S was made by graphically measuring slopes and averaging at each station. This estimate gives an increasing tracer concentration following trajectories for some values of the Peclet number. The RHS is assumed to be constant along a trajectory, except that the downward flux of salinity is set to zero at 21°S, where the minimum layer above begins. The RHS is not necessarily the same on each trajectory; it generally increases to the east.

In table 2 an average of dS/dT and dθ/dT for stations 140 to 150 for different Peclet numbers and two depths is given. The numbers for 4000m are shown for comparison, but they are generally too small to account for the increase of salinity and temperature to the south. This is because 4000m is still within the bottom layer, below the level of stronger vertical gradients. At any rate, to be consistent with the SA model the fluxes should be calculated at the top of the layer, which is near 3600m (assumed to be the same as at 3750m in table 2).

To get the value of the tracer at 24°S, the RHS must be multiplied by the time it takes for a parcel of fluid to reach 24°S. This time is different for the different trajectories, and so the system of equations was solved numerically for different values of Pe. The best agreement is for a Peclet number of about 2.0 with the top of the layer at 3750 m. This value of Pe gives average temperature and salinity closest to that observed at 24°S (figures 15 and 16b,c). In figure 17 the solution is illustrated for trajectories which begin at 11°S and in the DWBC as far

south as y=-0.75, where it changes sign. In this figure y=-1.5 corresponds approximately to 24°S. The initial condition for potential temperature is 1.95°C, and for salinity, 34.885°/oo. The Peclet number is 2.0. This value is smaller than the value of 5 estimated earlier, but it is not unreasonable given the weak mean circulation in the Angola Basin. In this figure one must visually average the property values shown in the east in a direction perpendicular to the boundary, since some horizontal mixing does exist, and this is the direction of maximum gradients.

The first two terms of the RHS , $\bar{C}-C_0$, are needed in the model for a consistent, reasonable Peclet number for the two properties. Without these two terms, Pe>4 for θ, while Pe>8 for salt.

The results for salinity are in good agreement with the data at 24°S, where the mean values are between 34.88°/oo and 34.89°/oo (figure 16b). The results for potential temperature are somewhat high, with observed mean values at 24°S between 2.0°C and 2.05°C, rather than between 2.04°C to 2.06°C. The error in the flux estimate could account for this difference (see below). In any case, the model with vertical diffusion and a Peclet number of 2.0 can account for the increase in salinity and temperature from 11°S to 24°S, based on vertical fluxes estimated at 11°S. The Peclet number could not be greater than 2.5 or less than 1.5 for a reasonable agreement. For $w_0=5\times10^{-5}$ and H=1km, K_v is then constrained to be between about $2.5cm^2/s$ and $3.3cm^2/s$. This value is in agreement with vertical mixing coefficients inferred in the studies of Hogg et al. (1982) and Whitehead and Worthington (1982) at similar depths.

The estimated error for the calculated changes is about 20°/∘, but the more important variation comes from different choices of layer depths. The top of the layer is in a region where the vertical variation of temperature is different from the vertical variation of salinity. So the flux term will have a different relative importance for the two properties at different depths. An average of the flux values near 3750m was used to compute the flux at 3750m, and similarly for 4000m, since the model should not depend critically on a particular choice of layer depth.

Thus both the pattern and the average value of temperature and the average value of salinity in the bottom layer at 24°S can be fitted by an advection-vertical diffusion model following trajectories of the SA flow. An additional observation relevant to the pattern of source-like properties illustrated in figure 17 comes from a section at 1°E (J. Reid, data personally communicated). An isolated high-oxygen-low-salinity area appears on the bottom near 19°S, reminiscent of the source-like property tongue entering the interior from the west in the figure (e.g. near y=-1.0 and x=0.5). In overview, observations gave us the transport of the DWBC and vertical fluxes at 11°S in the Angola Basin. This model is a simple and dynamically consistent way of interpreting these observations allowing one to infer average property values elsewhere in the basin. To the extent that the model agrees with observations at 24°S for reasonable values of the Peclet number, it probably represents the magnitude of southward transport accurately.

The Density Field

The changing temperature and salinity cause the density to change along the trajectories, too (see, e.g., figure 11). A mean temperature increase of about 0.04°C and mean salinity increase of about 0.005°/∘∘ implies a 0.005g/cm^3 decrease in sigma-4 between 11°S and 24°S. The net zonal thermal wind induced across a layer 1km thick is about 0.005cm/s. This is smaller than an estimate of the horizontal velocity from equation 3-4, which would be Lw_0/H =0.05cm/s. The induced thermal wind may not be negligible near the eastern boundary, though, and a brief discussion of how this component of flow can be seen in the model follows.

The effect of an evolving density field on the flow is not included in the SA model. In this model, the assumption of uniform density allows u and v to be independent of z. If density is not uniform, the SA model still gives the vertically averaged flow in the layer from the vorticity and mass equations alone. However, because of the possibility of vertical shear, a simple vertical average of the density equation equivalent to the above passive tracer equation (3-6) does not obtain. To get the same equation the advection of density by the baroclinic velocity, or thermal wind, must be neglected.

Some idea of the sense of the induced thermal wind can be seen in the northern half of figure 17. The meridional mean density gradient implies a net velocity difference between the top and bottom of the layer. Since isotherms are very nearly isopycnals, this velocity difference is parallel to the isotherms in figure 17. The sign of the shear is such that the thermal wind is eastward at the bottom of the

layer, and westward at the top. In the southern half, the younger water in the east is also denser. Hence associated with this zonal gradient is an increasing southward component of flow with depth (figure 15). However an estimate of the velocity increment across a 1km layer near 2°E at 24°S is about 0.01cm/s. As with the zonal thermal wind, this estimate is small compared to an estimate from equation 3-4: $v=w_0 y/H=0.095$cm/s for $w_0=5\times10^{-5}$cm/s, y=2664km, and $H=1.4\times10^{5}$cm.

Note that the baroclinic zonal velocity does not satisfy the no-normal-flow boundary condition at the eastern wall. One way to do so is in a narrow boundary layer of width on the order of the deformation radius (O(10km)), in which a vertical velocity can arise and close the flow (Pedlosky, 1979). The presence of the continental rise will probably modify the solution, but there does not appear to be a solution of this problem for scales appropriate for deep circulation.

Although a hint of vertical structure was inferred above, it is not clear that stratification can be consistently incorporated into the SA model. One could iterate the advection-vertical diffusion model with new velocity fields, corrected by a new thermal wind at each step. However, the mean density field only gives the net velocity difference across the layer, the structure within the layer must be assumed from the initial conditions. In the Angola Basin, at least, this correction is small, and probably not fruitful. In any case, the interaction of the thermal wind, which depends on the temperature and salinity characteristics of the source of water to a basin, with the vertically averaged flow, which depends only on the existence of the source, deserves further study.

This discussion is meant to introduce a method for beginning such a study, namely the advection-vertical diffusion model. The motivation is to understand how the basic temperature-salinity stratification is established by the different sources in different ocean basins, and how it might adjust to changing sources. One could, for instance, extend the model to the western trough and high latitudes, and represent different buoyancy forcing by different initial conditions. The resulting change in baroclinic flow might be estimated.

Discussion

With the tracer model I have tried to answer the question: how do the properties of bottom water change as the water moves away from its source in the Angola Basin, with a velocity given by the SA model. This model illustrates the evolution of temperature and salinity in the bottom layer. There is a net flux of density out of the bottom layer, which is approximately $-0.01 g/cm^3/70 yrs$. The importance of vertical diffusion suggests that future models of the bottom circulation in the Angola Basin and probably the eastern trough in general must have a more realistic density equation, i.e., including dissapation. Nevertheless, in spite of the idealizations of the SA model, the results of this section show that it provides an accurate and dynamically consistent description of the distribution of temperature and salinity in the interior of the Angola Basin.

Summary of the Tracer Model

Neglecting horizontal diffusion allows the advection-diffusion equation for a tracer to be written in characteristic coordinates, where the characteristics are the horizontal trajectories of fluid columns in the bottom layer. The trajectories come from a SA model of the flow. Vertical diffusion is necessary to account for the increase in mean temperature and salinity moving south on a trajectory in the basin. An estimate of the average increase in concentration of these two properties based on the data at 11°S gives fair agreement with measurements at 24°S.

Chapter 4

The Deep Oxygen Minimum.

4.1 Introduction

At 3500 m depth throughout the interior of the Angola Basin at 11°S there is an oxygen minimum layer (figure 4). It is not horizontally uniform, and all its characteristic properties are most extreme at the eastern boundary, which it intersects at 4000 m. In figure 18, profiles of silica and oxygen concentration at three stations across the basin are shown, illustrating the changing structure of the minimum and its relation to a silica maximum. Phosphate and nitrate maxima are coincident with the oxygen minimum, but a silica maximum is only coincident near the boundary (figures 5, 6, 7). The most extreme values are at the bottom at station 136 and oxygen increases both westward and vertically. The lowest oxygen value is about 5.0 ml l^{-1} (calibrated CTD value) increasing uniformly to 5.4 ml l^{-1} near 2°W where the minimum layer ends. Phosphate decreases from 1.7 μmol l^{-1} to 1.6 μmoll^{-1}, and nitrate decreases from 25 μmol l^{-1} to 24 μmol l^{-1} at the same position. Silica is a maximum of 62 μmol l^{-1} at the eastern boundary, and then follows the oxygen minimum decreasing to a value of 55 μmol l^{-1} at station 141, at which point the position of the silica maximum shifts downward reappearing at 4800 m, west of station 144. Along a level surface near 4000 m from the interior to the eastern boundary, the potential temperature is constant, while salinity increases very slightly.

At 24°S there is an oxygen minimum near 2°C (figure 12). Values at the minimum in the interior are quite uniform (not shown) at about 5.4ml/l, with no apparent tendency to be lower near the Walvis Ridge. The depth of the minimum is near 4000m. There is a silica maximum at 24°S, also at 2°C (figure 12). The core of the maximum tracks the 2°C isotherm in figure 15, with values close to 54μmol l^{-1}. It too, is not enhanced near the eastern boundary with the Walvis Ridge (not shown).

The oxygen minimum and phosphate and nitrate maxima are not independent features. As a first step in understanding the distribution of oxygen and nutrients I will consider just the amplitude of their variation. In a later section the structure of the oxygen distribution will be considered in the context of several models.

The decomposition of organic matter by bacteria consumes oxygen and releases nutrients. The reduction in oxygen concentration by 1 ml l^{-1} produces 0.32 μmol l^{-1} phosphate, and 4.8 μmol l^{-1} nitrate (Redfield et al., 1963). To use this one must choose a base oxygen and nutrient value from which to compute deviations. A reasonable assumption is that the base value is determined by averaging between levels where horizontal advection determines the concentration. This would be just the average of the values at the oxygen maximum above and at an oxygen value of 5.5 ml l^{-1}, say, near the bottom, which for oxygen is 5.40 ml l^{-1}. For phosphate the value predicted for an oxygen deviation of .4 ml l^{-1} is about 1.73 μmol l^{-1}; for nitrate, 26 μmol l^{-1}. Therefore local oxygen consumption can account for the increase in phosphate and nitrate (although it overestimates nitrate).

A study of the silica distribution in the northeast Angola Basin has been made by Bennekom and Berger (1984). They account for a high silica feature on the upper continental rise at 6°S, similar to the one observed at 11°S (figure 7), by the dissolution of diatoms produced in the high productivity area in the region of the outflow of the Zaire River (the upper continental rise is near 4000m from 6°S to 18°S). The section at 11°S extends their map of silica anomaly relative to a base value of 53.3μmol l^{-1} (their figure 22b) southward along the upper continental rise. A station at 18°S (also Oceanus cruise 133, station 129, not shown) also has high silica, with a bottom silica value close to 59μmol l^{-1} at a potential temperature of 2.09°C, slightly above the temperature of the core of the feature at 11°S. This must be close to the maximum southward extent, since the feature (low oxygen in the east) does not appear at 24°S in the interior of the Angola Basin.

The absence of the feature at 24°S together with the apparent uniformity of silica and oxygen at 2°C (figure 12), might suggest no advection in the east, in contrast to figure 14. But it could just as well argue for mixing along the 2°C isotherm. Values of silica of about 54μmol l^{-1} at 24°S are intermediate between values along 2°C at 11°S, which range from 52μmol l^{-1} to 60μmol l^{-1} (figure 6). Oxygen ranges from 5.6ml/l to 5.1ml/l on the 2°C isotherm at 11°S (figure 3), which similarly bound the value of 5.4ml/l at 24°S. The uniformity of oxygen and silica extrema along 2°C at 24°S has been remarked on above. This latter view is thought to be the case, and two additional things add some support. First, isobaths on the continental rise diverge near 20°S to

surround a seamount several hundred kilometers north of the Walvis Ridge (at about 6°E). This could guide properties near the eastern boundary into the interior, helping to mix them. Second, the high values of phosphate in the interior at 11°S and 24°S are otherwise puzzling. Recall the mixing solutions in section 3.2 were unable to accomodate high phosphate in bottom water at 11°S, given a source concentration of 1.5μmol l^{-1} and overlying water concentration of 1.65μmol l^{-1} (figure 12 and table 1). A component of water from the region of the continental rise would help explain these high values*. At 11°S the highest phosphate concentration is 1.71μmol l^{-1} at the bottom at station 136. At 18°S two stations (stations 29 and 30) which reached about 3500m (about 2.1°C) showed phosphate concentrations of 1.76μmol l^{-1} and 1.87μmol l^{-1}.

The enhanced delivery of biological matter to the upper continental rise lowers oxygen concentrations there. Estimates of the consumption are examined in section 4.3. For completeness, potential source regions for this feature other than the Angola Basin are eliminated by considering various property-property plots in the next section .

4.2 Local Generation of the Continental Rise Feature

High nutrients in the Angola Basin could only have as their source water from the south, in the Cape Basin, where AABW raises the nutrient

*Note that a higher component of water from the region of the continental rise does not significantly alter the oxygen solution in section 3.2. For an overlying oxygen concentration of 5.0 ml/l instead of 5.25 ml/l, the Guinea Basin component is 85°/° instead of 78°/°.

concentrations in the deep layers (figure 12). However at the density of the rise feature only nitrate is higher in the Cape Basin than it is in the rise feature itself. Phosphate is lower and silica is the same. Therefore no entrainment of nearby water could produce the correct nutrient concentrations. In addition oxygen is too high (by 0.5 ml l^{-1}) in the Cape Basin at this density. Furthermore any southern source would have a low temperature, low salinity signal, while the rise feature has no temperature contrast and a very slight salinity increase (figures 2 and 3).

More generally we can ask if the values of various properties lie on a mixing line between the potential sources in the Guinea and Cape Basins. Salinity is a good property against which to plot nutrients since it is conservative and the two basins have a substantial contrast (figure 10). Figure 19 demonstrates the high silica within the oxygen minimum near the eastern boundary of the Angola Basin (open symbols). This value lies well off the trend connecting NADW to AABW in the western basins (the western basin trend is from Chan et al., 1977), requiring local generation. Figure 20 gives the relationship between oxygen and salinity in the deep water of the Angola Basin (open symbols) and surrounding basins (the western basin trend is from Broecker et al., 1980). Again, no mixture of deep water surrounding the Angola Basin could produce the characteristics of the rise feature. This feature must therefore be generated locally within the Angola Basin. In the next section the processes of consumption are reviewed. Following that, a mechanism for the maintenance of the rise feature is suggested.

4.3 Interior and Boundary Consumption

Indirect evidence has been presented demonstrating that the deep oxygen minimum in the Angola Basin must be formed locally, by the decomposition of organic matter. In this section a discussion of the consumption of oxygen in deep water is given. The purpose of this discussion is to determine the correct consumption term and boundary conditions for the oxygen equation. The method is as follows: The process of decomposition, which brings about the consumption of oxygen, depends on a supply of organic matter generated in the upper layers by biological activity. The two sources of organic matter to deep water are a downward flux in the water column, and a transport down the continental slope. Therefore variations in the supply of organic matter to deep water and the implications for the interior and boundary consumption are discussed. The significance of these variations to the oxygen equation will be explored in the next section on models. Although this discussion is for the oxygen distribution, the decomposition releases phosphate and nitrate in the Redfield ratios whether it occurs in the water or upper sediment column. Hence this discussion applies to their distribution, also.

The eastern boundary is notable because of the presence of regions of high biological productivity associated with the upwelling of nutrient rich water and river input. Upwelling occurs all along the eastern boundary of the South Atlantic; at 11°S the upweeling is predominantly seasonal (a recent reference is Picaut, 1983). This intense productivity results in a greater flux of organic material to the eastern continental margin. The material continues to be consumed by bacteria on the bottom and in the sediment column as new sediment accumulates.

Thus oxygen is consumed within the sediment column in addition to within the water column. The chemical reaction describing decomposition in the presence of oxygen is the same in either case, releasing nutrients approximately in the Redfield ratios. Studies of bottom decomposition have shown that one of the most important factors in oxygen consumption by the sediment is the supply of organic matter (Patamat, 1977). These studies also show that variations in oxygen concentration do not affect the rate of consumption down to extremely low values of oxygen (below any observed in the deep water of the Atlantic). So high organic carbon (a measure of organic matter) in the sediments is not the result of overlying low oxygen concentrations. Furthermore, the role of the rate of accumulation of organic matter on the chemistry and rate of decomposition occurring within the sediment column is emphasized. High accumulation rates imply higher rates of decomposition at the bottom and within the sediment column. The decomposition produces gradients in oxygen and nutrient concentrations at the sediment surface, and therefore oxygen fluxes into the sediment and nutrient fluxes out of the sediment. Thus these fluxes also depend on the amount and rate of accumulation of organic matter*.

Of particular importance for the models of the oxygen structure in deep water is the evidence for variation in oxygen flux across the continental margin off northwest Africa at 10°-25°N, owing to variations in organic carbon accumulation rates. The situation is schematically

*Even with a gross estimate of oxygen flux arrived at by assuming that the interior oxygen value decays to zero in the first centimeter of sediment, one can show it is enough to absorb the input of oxygen to the Angola Basin by deep water.

illustrated in figure 22. The oxygen and nutrient measurements in figure 22 are from Weichart (1974) and are at 20°N off northwest Africa. In the figure the larger nutrient gradients and high organic matter concentrations in the sediment column occur near the foot of the slope, where there is an oxygen minimum and high phosphate concentrations. He suggested that enhanced fluxes may explain the low oxygen and high nutrients near 2000 m, close to the eastern boundary.

Bennekom and Berger (1984) interpret the results of a number of stations in the Angola and Guinea Basins, occupied for hydrographic and geochemical purposes. They conclude that the Zaire River has a substantial effect on the distribution of oxygen and nutrients in the deep water of the northeast Angola Basin, both in terms of the productivity in the surface layers and the delivery of material to abyssal depths. In particular, they comment on the consumption of oxygen and build up of nutrients in the bottom water at the base of the Zaire Canyon at 6°S, at a depth of about 3500m, owing to the delivery of organic matter and the reduced mixing. Their extreme values for these properties are all comparable to the extreme values at 11°S. It appears that the delivery of organic material is greatest near the Zaire Canyon at 6°S, but occurs to a lesser extent all along the continental margin.

Chemists have made measurements of oxygen flux in a few locations. These measurements have been both in situ and laboratory analyses of samples. Smith (1984) compiled many results and reported magnitudes of in situ measured fluxes of oxygen across the sediment interface of about 10^{-7} ml $s^{-1}cm^{-2}$ at 4000 m, away from areas of active upwelling,

resulting from decomposition in the upper layers of the sediment column. This value will be compared to measurements in the eastern Atlantic, with the goal of arriving at a reasonable estimate for the upper continental rise of the Angola Basin.

Pfannkuche et al. (1983) published a laboratory analysis of the oxygen flux in bottom sediments at 35°N off Morocco, an area of weak upwelling. Unlike the region farther south, where material can pile up at the foot of a steep continental slope, the continental margin here is not characterized by a steep continental slope relative to the continental rise but rather a uniform slope from shelf to abyssal plain. Their measurements reveal an oxygen flux of about 2×10^{-7} ml $s^{-1}cm^{-2}$ below 400 m into the sediment, in reasonable accord with Smith's (1984) values away from an upwelling region. This is the closest area to the northwest African upwelling region with direct measurements of oxygen flux.

Unfortunately, there is no deep profile along the continental slope and rise in the Angola Basin of direct measurements of oxygen fluxes which could provide documentation of greater oxygen fluxes on the upper continental rise. However, an estimate of oxygen flux can be made based on the relative increase of the supply of organic carbon to the foot of the slope with a site in deeper water. The data off northwest Africa provide justification for this method of estimating flux, since low oxygen at the eastern boundary is correlated with high organic carbon and an increased supply of organic carbon. Measurements of oxygen flux to the sediment from Smith (1984) can be used as a conservative estimate of the average oxygen flux in the Angola Basin away from the upper

continental rise. To get the estimate for the flux at the upper continental rise, multiply the average figure by the relative increase in organic carbon flux there (Muller and Suess, 1979). The relative increase in accumulation rates and organic carbon content is estimated as follows. Accumulation rates of organic carbon from Hartmann et al. (1976) are about a factor of ten higher on the upper rise off northwest Africa than above or below. Data from Jansen, et al (1984) in the Angola Basin also show at least a factor of ten increase in accumulation rates on the rise near the Zaire fan at 6°S to 9°S. As a conservative estimate, then, a factor of five to ten increase in oxygen flux at the foot of the slope is chosen. Then the value for the flux becomes order 10^{-6}ml $cm^{-2}s^{-1}$. This estimate is meant to include consumption in material stirred up within a few meters of the bottom and the bottom itself, as well as the sediment column.

Now interior consumption values will be considered. Suess (1980) has put forward a tentative prediction of interior oxygen consumption arrived at by computing organic carbon flux divergence from a model based on measured organic carbon flux data from particle traps. Using a production rate of organic carbon of 250 $gCm^{-2}yr^{-1}$ characteristic of a high productivity region, his estimate is about 10^{-10}ml $l^{-1}s^{-1}$, approximately independent of depth below 2000 m. Therefore a depth independent consumption term of 10^{-10}ml $l^{-1}s^{-1}$ will be accepted as reasonable for the Angola Basin. If the above boundary oxygen sink were spread through a volume of unit cross-section stretching 500 km into the interior, it would be equivalent to an interior sink of

$2x10^{-11}$ml $l^{-1}s^{-1}$. This is to be compared with the value of interior consumption to see if it might be expected to have a large-scale influence. Apparently the eastern boundary sink has a net effect comparable to, but smaller than the interior consumption. The boundary sink will be seen in the next section to have an important effect on the distribution of oxygen.

There does not appear to be a specific property that would distinguish interior from boundary consumption. One additional property which might be expected to answer this question is carbon-14. If low carbon-14 values were found to correspond with low oxygen values, the argument could be made that the water is simply old. However, sediments have generally lower carbon 14 values than the sea-water above, and low carbon-14 values would not distinguish between old interior water and younger water affected by sediment fluxes. The deep oxygen minimum in the Angola Basin does have low carbon-14 values associated with it (figure 21). A method of distinguishing these sources would be helpful.

With values for the interior and boundary consumption, we can proceed to the oxygen equation. In the next section the Wyrtki and Kuo and Veronis models are discussed, and a model with boundary flux is given.

4.4 Models of the Deep Oxygen Minimum

Two models have been used in the past to explain the large-scale distribution of oxygen in deep water. They are Wyrtki's (1962) model, and Kuo and Veronis's (1973) model. Both include advection, diffusion and consumption as the basic physics. The Wyrtki model is purely

one-dimensional in the vertical direction, while the Kuo and Veronis model is two dimensional in the horizontal plane. These models and their predictions for the Angola Basin region will be described first, and then a model with the added process of boundary consumption will be presented.

The oxygen equation is

$$uO_x + vO_y + wO_z = K_H O_{xx} + K_H O_{yy} + K_v O_{zz} - Q \ , \qquad 4\text{-}1$$

where u,v,w are the velocity components, O is the concentration of oxygen in ml l^{-1}, K_H is the horizontal turbulent diffusion coefficient, and K_v is the vertical turbulent diffusion coefficient. Values for these coefficients will be discussed later. The interior consumption term is Q. To this equation boundary conditions are added, which are different for the different models and geometries.

Wyrtki's Model

Wyrtki developed his model to explain the vertical distribution of oxygen near minima. He assumed that within these low oxygen layers, horizontal advection and diffusion are negligible, and that the vertical velocity is constant. Thus the oxygen equation becomes

$$wO_z = K_v O_{zz} - Q \ . \qquad 4\text{-}2$$

Upper and lower boundary conditions on the oxygen concentration are prescribed at depths where horizontal advection dominates, and the equation breaks down. Oxygen minimum layers form because the presence of consumption allows the right-hand side of the equation to be zero. At this depth the curvature is positive, i.e., a minimum. In these layers a steady state balance exists between vertical advection, diffusion, and consumption. The vertical velocity and diffusion coefficient occur as a ratio in the solution. This ratio times the length scale is the vertical Peclet number (Pe). This parameter occurred in the model for the temperature and salinity distributions discussed previously, and will be compared to the best value for the oxygen distribution below.

The oxygen minimum in the Angola Basin between 3500 m and 4000 m intensifies toward the eastern boundary by about 0.1 ml l^{-1} every 200 to 300 km. Therefore Wyrtki's model must be examined to look for ways in which it could account for this horizontal variation. Rewriting equation 4-2 in nondimensional form,

$$O_z = Pe^{-1} O_{zz} - J \ , \qquad 4\text{-}3$$

$$Pe^{-1} = K_v / w_o H \ .$$

Here z is scaled by H, and Q is scaled by Hw_o^{-1}, where w_o is the vertical velocity, assumed constant. The scaled consumption term is J. The oxygen concentration is scaled by 1 ml l^{-1}. The model has two parameters, Pe and J. Variations in these parameters and the boundary

conditions are the only way horizontal differences can occur. The strength of this model has been its applicability without ad hoc variations in the parameters. Bennekom and Berger's (1984) summary of productivity estimates in the region west of about 8°E indicates generally high values as far west as 4°W. The generally higher productivity in this region has been taken into account by the choice of Q. In addition, vertical velocity might be expected to vary because of the continental rise. However, as long as f/H, where H is the thickness of the bottom layer, increases northward near the eastern boundary, u is positive (the SA model with topography is not developed here). Then a positive vertical velocity of order w_0 is induced at the bottom, for a bottom slope of about $2x10^{-3}$. W still must change linearly to w_0 at the top of the bottom layer, so the assumption of uniform w in the oxygen minimum layer near the top of the bottom layer is probably good, insofar as the assumption of w_0=constant in the SA model is good. Therefore there is no clear basis for varying these parameters horizontally in the interior. So the only alternative is a variation in the boundary conditions.

The upper boundary condition is chosen to be at the oxygen maximum, where horizontal advection dominates the oxygen equation. There the value is O=5.3 (figure 4). The lower boundary condition is also chosen to be in a layer which has higher oxygen values owing to horizontal advection. There the value is O=5.45 at 4800 m, which is approximately along the 45.875 isopycnal. The boundary conditions for the oxygen minimum do not vary, and so the Wyrtki model cannot account for the

distribution of oxygen in the Angola Basin. Instead, the Wyrtki model will be found to be one component of the solution.

The Kuo and Veronis Model

Models fashioned after Wyrtki's have been used to explain quantitatively the large-scale structure of oxygen in some regions of the deep ocean. For example, Warren (1973) applied the model to the South Pacific Ocean and Warren (1981a) similarly applied the model to the South Indian Ocean. However, in the eastern basin of the South Pacific Warren (1973) noted the low oxygen near the eastern boundary and added horizontal diffusion to the model, so that the oxygen structure determined near the eastern boundary by other physical balances became the eastern boundary condition. This structure subsequently dominated the interior solution.

The traditional explanation for the low-oxygen values near the eastern boundaries of the oceans relative to the western boundaries is contained in the Kuo and Veronis model, and is discussed below. In this model it is the horizontal advection, horizontal diffusion, and interior consumption which determine the oxygen distribution. They neglect the vertical terms in the oxygen equation. The horizontal velocity comes from the SA model. Thus the distribution depends on the horizontal Peclet number and consumption term. They found that their model gave good agreement with the global distribution of oxygen. However, because the model is vertically averaged, it cannot explain why the oxygen minimum is most intense on the upper rise. To emphasize the importance of eastern boundary consumption, a further discrepancy between the model and observations in the eastern tropical Atlantic is suggested below.

To derive the model, the oxygen equation is vertically integrated. The appropriate layer in the Angola Basin is from 3000 m to the bottom, which extends through the deep oxygen minimum. As by Kuo and Veronis, the bottom is assumed to be flat. The region is the area east of 10°W, bounded to the north and east by Africa. Since the model is flat bottom, there is no Mid-Atlantic Ridge, and the western boundary is open. The southern boundary near 20°S is also open without the Walvis Ridge. The SA model with a meridional eastern boundary will be used to represent the deep flow in the eastern tropical Atlantic, since this discussion is for water at low latitudes (5°N to 20°S). The region and flow are illustrated in figure 23. Observations show that oxygen is fairly uniform at 5.5 ml l^{-1} at the western boundary of this region near the Mid-Atlantic Ridge (Reid, 1981). Close to the equator values of oxygen concentration increase to near 5.7 ml l^{-1} at this longitude. This range is not large and the values are substantially higher than concentrations in the minimum. Therefore 5.5 ml l^{-1} will be taken as the western boundary condition. At the northern boundary at 5°N a boundary current is predicted by the SA model which would absorb the interior flow and leave the region. So the northern boundary is effectively open. At the eastern boundary there is a no-flux boundary condition.

Vertically averaging 4-1 gives, assuming the horizontal velocity to be independent of z,

$$u\bar{O}_x + v\bar{O}_y + \frac{w_o}{H}(O_o - \bar{O}) = K_H \nabla_H^2 \bar{O} + K_v O_z^o - Q \qquad 4\text{-}4$$

The overbar denotes a vertical average. From the assumption that u and v are independent of z, the continuity equation requires w to be linear in z. Let w_o be the velocity at the top of the layer. The third term represents the effect of this horizontal convergence on the distribution. O_o is the oxygen concentration at the top of the layer, and $K_v O_z^o$ is the diffusive flux there. Following Kuo and Veronis, the vertical terms are assumed to balance (they do not try to justify this assumption, and they acknowledge that it may be wrong), leaving

$$u\bar{O}_x + v\bar{O}_y = K_H \nabla_H^2 \bar{O} - Q$$

Scaling x and y by L, and u and v by Lw_o/H gives

$$u\bar{O}_x + v\bar{O}_y = Pe^{-1} \nabla_H^2 \bar{O} - J \qquad 4\text{-}5$$

$$Pe^{-1} = K_H / w_o H .$$

The scaled velocity field from the SA model (as by Kuo and Veronis) is

$$u = -2x$$
$$v = y$$

where the origin of the coordinate system is at the intersection of the eastern boundary and the equator. In terms of an initial value problem, the oxygen will be advected into the region from the west, decay, and diffusion will become important near the eastern boundary. By balancing

advection and diffusion one obtains the scale for which diffusion will become important (note that u goes as x). This is for the region east of $x=-Pe^{-1/2}$. Therefore the oxygen distribution will have the large length scales of the interior flow initially, and as a first approximation diffusion can be ignored. Then equation 4-5 becomes

$$-2xO_x + yO_y = -J \qquad 4\text{-}6$$

The characteristics (streamlines) of this equation are the curves

$$(-x)^{1/2}\, y = c.$$

Integrating along a characteristic from a point on the western boundary of the region gives

$$O(x,y) = 5.5 + J \ln[(-x^{1/2})] \qquad 4\text{-}7$$

So the interior distribution is independent of y. The oxygen decreases logarithmically towards the eastern boundary because of aging. This is the essential explanation for low oxygen values near the eastern boundaries in this model. Diffusion will become important in the region east of $x=-Pe^{-1/2}$, and will remove the unboundedness and satisfy the no flux condition.

Because the boundary conditions are independent of y and the interior flow with a meridional eastern boundary does not generate variations

in the y direction, the full solution is independent of y. It satisfies

$$-2xO_x = Pe^{-1}O_{xx} - J.$$

The solution is

$$O = 5.5 + J\pi/8\ [erf^2(\ Pe^{1/2}x) - erf^2(-Pe^{1/2})]. \qquad 4\text{-}8$$

where erf is the error function. This solution is plotted in figure 24, for J=4.3 and Pe=3.4, which Kuo and Veronis decided were optimum values in their numerical model (their model was for the entire globe). Thus the model predicts a low oxygen region given by the above solution all along the eastern boundary, with a value there of 4.7 ml l^{-1}.

However, the deep oxygen minimum in the Angola Basin does not extend northwards toward the equator, into the Guinea Basin (figure 25). In this figure, there is low oxygen in the Angola Basin at 8°S and 11°S near 2.0°C. On the equator and at 6°N there is no low oxygen layer. The data are from Crawford stations during the I.G.Y., in addition to GEOSECS and Oceanus stations. This simple prediction and disagreement indicates that while the model can explain a tendency for lower oxygen concentrations in the eastern Atlantic, it cannot explain the vertical or horizontal structure of the deep oxygen minimum in the Angola Basin. It suggests the need for a different mechanism or physical process.

There are several possibilities. One is that the SA flow field is wrong and that eastward flow along the equator greater than that in the

SA model wipes out the low oxygen near the eastern boundary. This is unlikely since the zonal flow is zero at the eastern boundary. Second, as with the Wyrtki model, the parameters should not be varied to produce a special region of low oxygen without physical justification. Finally, there is the possibility that some process is left out. Previous sections have presented evidence for a boundary-flux term in the oxygen equation for the Angola Basin. The effect of this term is discussed next.

A Model with Boundary Flux

Starting with the oxygen equation 4-1, the goal is to arrive at a simpler model relevant to the oxygen minimum layer in the Angola Basin. The upper boundary condition is at the oxygen maximum, where horizontal advection dominates the oxygen equation. There the value is O=5.3 (figure 4). The lower boundary condition is also in a layer which has higher oxygen values owing to horizontal advection. There the value is O=5.45 at 4800 m, which is approximately along the 45.875 isopycnal.

This model is for the region east of $x=-Pe^{-1/2}$, which turns out to be about 2°W for the range of Pe used here, and so zonal advection is neglected as discussed above. Owing to the flux at the eastern boundary, horizontal diffusion is necessary. Only zonal diffusion is allowed since the interior flow does not generate y-variations (equation 4-8). The western part of this region between about 2°W and 3°E is within the longitude range where the meridional velocity is thought to be zero near 3600m, the approximate level of the minimum there (section 3.4). Therefore the western boundary condition is the Wyrtki solution. The

eastern boundary condition is a flux of oxygen into the boundary representing consumption centered near 4000m (given below). Thus in the western part of the region, meridional advection is thought to be a small term in the equation for this layer. In the eastern part, the fairly uniform v (a high estimate is 0.1cm/s) and O_y (of order 10^{-9}ml/l/cm) act as a basically constant source term counteracting Q (J in the scaled equation). Since a fairly wide range of Q does not change the results significantly, meridional advection is neglected for simplicity. Thus 4-1 gives

$$wO_z = K_V O_{zz} + K_H O_{xx} - Q \ . \qquad 4\text{-}9$$

Nondimensionalizing as before and scaling x by $(H/L)(K_H/K_V)^{1/2}$ gives

$$O_z = Pe^{-1} (O_{zz} + O_{xx}) - J \ . \qquad 4\text{-}10$$

For simplicity let the flux boundary condition be $F_o \sin(\pi z) e^{Pez/2}$, where $F_o = H(K_H K_V)^{-1/2} F$, and F is chosen to be 10^{-6} ml $cm^{-2}s^{-1}$ at its maximum. This is the value for flux estimated in section 4.3. This form is supposed to represent enhanced flux on the upper continental rise, as discussed previously. Equation 4-10 is well known, but the inclusion of a boundary flux term is new.

Then the solution is

$$0 = A\,Pe^{-1}\,e^{Pez} - Jz + B + F_0/\alpha\; e^{\alpha x + Pez/2}\sin(\pi z) \qquad 4\text{-}11$$

$$A = \frac{Pe(0.15-J)}{e^{-Pe}-1} \qquad \alpha = (\pi^2 + Pe^2/4)^{1/2}$$

$$B = 5.3 - A/Pe\ .$$

With $H = 2 \times 10^5$ cm, $w = 5 \times 10^{-5}$ cm s^{-1} , and $K_V = 3$ $cm^2 s^{-1}$ (section 3.5), then J=0.4 , α=3.6, and Pe=3.3. Solutions for several values of Pe and J=1 are plotted in figure 26. Variations in J between 0.4 and 3 are not important. The solution for Pe=1.5 (26b) is in better agreement with the oxygen section (figure 4), judging by the value at the boundary and the penetration of the 5.15 and 5.2 isopleth. The horizontal scale for these parameters and $K_H = 10^5$ is about 500km. This value for K_H is within the range of K_H suggested by the model (see below) and seems low, but might be appropriate in the deep water of the Angola Basin, since it is a region away from intense upper layer flow. Note also the upward displacement of the core of the minimum in figure 26 and figure 4. This is due to the different decay scales at the boundary from those in the interior. That is, the western part of the solution has a minimum at a different level from the eastern boundary part, and they merge across isopycnals. It is much weaker than observed, but note that the displacement across isopycnals is somewhat less than the displacement across level surfaces. Perhaps a better representation of the vertical structure of the boundary flux (more confined vertically)

would help reproduce this feature.

One can use the model to put bounds on the physical processes parameterized in the model. This is important because if more elaborate models, for instance a model including zonal or meridional flow, also stay within these bounds, then one can be confident that the model's basic assumptions are reasonable. For this model to agree reasonably well with observations, horizontal diffusion should be in the range 10^5 to 10^6 cm^2s^{-1}. A higher K_H allows too much diffusion of oxygen towards the boundary, raising the values there unacceptably. The Peclet number should be in the range 1.5 to 2.5. Higher Pe numbers do not reproduce the tongue-like character of the pattern. Although one might argue about which values were best, the restriction to the above ranges is fairly strong.

A lower bound for the boundary flux was estimated in section 4.3, and used in this oxygen model. The model suggests that the notion that the boundary flux has an influence on the large-scale distribution of oxygen in the Angola Basin is quantitatively correct. Recall that for the salt and potential temperature distributions the best value of Pe in the model was 2. Together the models suggest a consistency between source strength, vertical velocity, and meridional velocity (related by SA physics), and temperature, salinity, and oxygen variations in and near the bottom layer in the Angola Basin. The relation is indirect because Pe is a free parameter, that is, because the real velocity field (at all scales) is not known. This makes their usefulness for determining the true velocity field practically nil. It is hoped that once an idea of

the mean flow is gotten from general considerations of the property distributions, the models can be useful for understanding the important physical balances in some limited region. The consistency between the two models is satisfying and suggests that the important component of the flow and the important physical balances are both represented.

Final Remarks

Summary

A summary of the basic features of the property distributions at 11°S and their interpretation as discussed in the text is given next.

1) A layering of properties influenced from the north and west, and eastward flow along the equator indicates a general southward component of flow at 11°S.

2) A large scale isopycnal slope above the Mid-Atlantic Ridge is identified with a deep western boundary current below a zero velocity reference level of 3600m.

3) Property values in the bottom water indicate a northern source alone. It is suggested that a ridge near 30°S forms the true seperation between the Angola and Cape Basins.

4) A low-oxygen-high-nutrient feature near 4000m on the eastern boundary is suggested to be maintained by boundary flux.

A preliminary summary of basic features at 24°S in the Angola Basin is given next.

1) Bottom water is cooler in the east, consistent with the Stommel-Arons circulation scheme.

2) An oxygen-maximum-salinity-minimum layer exists near 3000m. An oxygen-minimum-silica-maximum layer near 2°C is quite uniform (deviations less than measurement accuracy) in the interior. From this and consideration of surrounding property values it appears that horizontal mixing is important throughout the depth range 2500m to 4500m.

3) Both an increasing northward component of flow toward the bottom and low salinity above the Mid-Atlantic Ridge are consistent with northward flow there, as in the SA scheme, but the higher oxygen and lower silica there are not. The analysis is incomplete pending calibration of the data.

A simple model for the change in θ-S properties in the bottom layer from 11°S to 24°S, using the horizontal velocity from the SA model and an estimate of the vertical fluxes, suggests that K_v is about $3cm^2/s$ for the optimum Peclet number of about 2. An oxygen model suggests that boundary flux is important for maintaining the deep oxygen minimum in the Angola Basin. An optimum Peclet number near 1.5 together with an estimate of boundary flux resricts K_H to be between $10^5 cm^2/s$ and $10^6 cm^2/s$. The above vertical turbulent diffusion coefficient agrees with other studies. K_H and the Peclet number are somewhat less than typically quoted values (e.g. by Kuo and Veronis, 1973) and presumably reflect generally weaker velocities in the region.

Some suggestions for field work and some unanswered questions are offered next.

Further hydrographic and bathymetric measurements betwwen the Walvis Ridge and Mid-Atlantic Ridge are needed to determine the nature of the seperation between the Angola and Cape Basins. At the same time it would be possible to determine if flow actually exists in the Walvis Passage.

A zonal section of radiocarbon measurements in the Angola Basin is necessary to see if low values, which typically are used to infer old age, are due to a flux into deep water on the eastern boundary, as with oxygen. Note that Freon measurements taken approximately along 1°E in the Angola Basin, which could also be used to infer age, are probably at or below the noise level (R. Wiess, personal communication).

In general a method of distinguishing boundary fluxes from interior sources would be useful in tracing the influence of the fluxes. Eastern boundary fluxes also seem to occur from about 10°N to 20°N in the eastern North Atlantic, an area with relatively few modern deep observations, and perhaps have a large scale influence. Direct measurements of oxygen flux in profile across the continental margin in the eastern Atlantic at more locations are needed.

The assumption of no eastern boundary currents at any level is a basic assumption of the SA circulation scheme. Direct current and hydrographic measurements which resolve scales less than 10km perpendicular to the boundary (i.e. the deformation radius) along the eastern boundary of the tropical Atlantic are needed to test this assumption. This need is emphasized by the eastward flow at the equator and near 21°S, since the flow eventually reaches the eastern boundary and must turn.

Dynamical questions

Some deficiences in the SA model have been discussed previously, most importantly the assumption of uniform density. The connection between source T-S characteristics, T-S advection, and the thermal wind has been noted, but a consistent development of the dynamics with

nonuniform density has not been given. Similarly, for the deep boundary current the combined effect of stratification and topography is not well understood. Both need to be included since isopycnal and topographic slopes are of the same magnitude.

Another point is simply dissatisfaction with the limitations of the SA model. Once property distributions were used to infer a reference level and calculate transport, the SA model was then able to provide an estimate of the source strength. One should be able to determine the T-S distribution and velocity in the boundary current (including a reference level, if it exists) from the T-S structure upstream or in adjacent basins, with a knowledge of bathymetry and the dynamics. More simply the desire is to have a theory for velocity, not its vertical integral.

The last comment is about eastward flow along the equator. It is not known how deep flow is established and maintained along the equator, and how it satisfies the eastern boundary condition (e.g. with a narrow or broad flow off the equator).

These dynamical questions could be summarized in one sentence: a theory for large-scale mean flow in the tropics which includes stratification, and hence vertical structure, is lacking.

Appendix

There are no modern studies of the deep or bottom circulation in the Angola Basin. For this reason I have included this appendix which summarizes the significant oceanographic history of this region.

Historical Remarks

The modern oceanographic history of the eastern basin of the South Atlantic begins with the prediction by Thomson (1878) of the existence of a connection between the mid-Atlantic Ridge and the African continent "probably near 25°S" (pg. 249). He based his prediction on the evidence of bottom temperatures gathered by the Challenger, and presumably some other measurements as well since the track of the Challenger did not lie in the eastern South Atlantic at all. For instance, his bathymetry chart shows several soundings lying on a line between St. Helena and the Cape of Good Hope, away from the Challenger track, and he mentions the use of previously acquired data but not his source. According to Wüst (1933), a number of expeditions have provided reliable data from the Angola Basin (sometimes called the Congo Basin before Wüst, 1933). Wüst lists the following ships in his sources: the Gazelle, 1874-76; Waterwitch, 1894-95; Valdivia, 1898-99; Gauss, 1901-03; Planet, 1906-07; Mowe, 1914-15; Meteor, 1925-27. Only the first ship, the Gazelle, could have provided reliable data to Thomson, but there is no mention of this expedition as his source. This barrier was named the Walvis (Whale) Ridge by Supan in 1899, but the confirmation of its existence as a continuous ridge was not well established until 1907 after several expeditions had visited it.

Thomson believed that the deep water, approximately defined as being that water below the thermocline and above a potential temperature of 1.5°C, was part of the Antarctic water mass and was also moving northward. This water was apparently supplied evenly along the southern boundary of the South Atlantic, and flows northward unobstructed in the western trough. However in the eastern trough he postulated a ridge sufficiently shallow to block the northward passage of water at a temperature less than 1.9°C to 2.0°C. He made no mention of any southward flow above, and, on the contrary, thought that the flow of deep water was balanced by evaporation in the northern portions of the Atlantic, which was subsequently carried south as water vapor.

Somewhat later Buchanan (1888) postulated two sills surrounding the Guinea Basin, one connecting Ascension Island to northwest Africa, and one between the Guinea and Angola Basins connecting St. Helena to Annobon or Pagalu on the basis of bottom temperatures he measured during the Buccaneer Expedition to the Gulf of Guinea. As discussed by Wüst (1933) his measurements were made with thermometers that couldn't detect the temperature inversion in the northern Angola Basin, but they were helpful in shedding light on the problem of the passage of water from the western to eastern troughs. The northern sill he postulated doesn't exist to the extent that he suggested -- this topographic feature is now called the Ivory Coast Rise. The southern sill is now called the Guinea Ridge.

Measurements in the area of the eastern equatorial Atlantic were helping to establish the presence and propagation of Antarctic Bottom Water (AABW) in the eastern trough. It apparently was a matter of some

controversy whether or not a deep passage existed between the eastern and western troughs and where it was located. This is demonstrated by a chronology of opinion extracted from Wüst (1933): Murray, 1899 - yes; Drygalski, 1904 - yes; Krummel, 1907 - no; Groll, 1912 - yes; Schott and Schultz, 1914 - yes; Drygalski, 1926 - no; Schott, 1926 - no. Bohnecke (1927) showed, on the basis of Meteor observations, that a break in the Mid-Atlantic Ridge must occur at a depth of 4100 m to 4400 m in the region of the Romanche Fracture Zone. Thus, AABW from this depth enters the Guinea Basin from the west. Wüst (1933, 1935) in his studies traces AABW north and south in the eastern trough by its low potential temperature, extending its influence out of the Guinea Basin poleward. He was not able to determine, on the basis of temperature measurements and soundings then available, the depth and extent of the gaps in the Romanche Fracture Zone region, but he did believe that the sill depth ranged from 4500 m to 4800 m, which was deeper than Bohnecke's estimate. A more recent estimate is 3800 m (Metcalf, Heezen, and Stalcup, 1964).

Wüst (1933) traced AABW over the Guinea Ridge, of sill depth 4500 m, into the Angola Basin, on the basis of Meteor data, "...filling its depression where the depth exceeds 5000 m with a homogeneous water (θ = 1.86°-1.99°)". He also stated that the shape of the isotherms in his bottom potential temperature chart (Wüst, 1933, pg. 58) showed that the flow was deflected eastward by the Coriolis force, entering the Angola Basin in its northeastern corner.

Wüst (1933) defined the oxygen maximum "layer" (in quotes since it does not exist throughout the Angola Basin) as Middle NADW. This defini-

tion is based on Wattenberg's (1929) conclusion that the oxygen distribution indicates that the main mass of NADW is formed north of 40°N in the western trough of the Atlantic, and on Wüst's observation of two deep oxygen maxima at many of his stations. He called the lower oxygen maximum the core of Lower NADW. Upper NADW was denoted by the salinity maximum. This classification proved useful in characterizing water of distinct origin in the western trough. However the terms are meaningless in the eastern South Atlantic: For example, Middle and Upper NADW, which are distinct layers in the western trough, are coincident in the Guinea Basin, while only slightly farther south, in the Angola Basin, they again lie at different densities. Another unsatisfactory situation is that Lower NADW in the Angola Basin has the AABW-like characteristic of lower salinity. The confusion occurs simply because oxygen has strong horizontal and vertical structure near the eastern boundary. Wüst (1933) noted the lower oxygen content of Middle NADW in the eastern trough, but his data could not adequately resolve the deep oxygen minimum (see e.g. Wattenberg, 1939 and 1957). In the South Atlantic he attributed the difference to age. With turbulent diffusion and geographical variations in consumption, however, one cannot strictly equate age with decreased oxygen concentration (chapter 4).

In his discussion of vertical profiles Wüst mentioned that the curvature of the potential temperature profile with depth increases between 3000 m and 4500 m and that this was due to AABW influence. Wüst also commented on the salinity distribution in the Angola Basin, especially its "remarkable uniformity" (Wüst, 1933, pg. 72). Sixteen of twenty

measurements he uses to discuss salinity there were the two values 34.88°/oo and 34.89°/oo. He presents this as another hint of the presence of AABW, regarding S = 34.90°/oo as "the threshold value, in which the last traces of Antarctic water are noticeable..." Summing up his discussion of the thermohaline features of the water of the Angola Basin, Wüst states that

> "complete vertical homothermal and homohaline conditions exist in the actual bottom water between 4500 m and 6000 m of the Angola, Cape Verde, and Canary Basins. Here the water masses are in a weakly stable, at places even indifferent, equilibrium."

Wüst presented sections of various water properties along the middle of the eastern and western troughs of the Atlantic. His purpose was to emphasize the different thermohaline structure and the propagation of water masses. Commenting on the profiles he made a curious statement regarding the eastern trough: "A complete stagnation of the water masses is observed at the Walvis Ridge below the depth of 3000 m" (Wüst, 1933, pg. 109). He made a similar but less direct statement in The Stratosphere of the Atlantic Ocean (Wüst, 1935) when he said that the relation between salinity and oxygen "...becomes unsteady due to the build up (Stau) of water masses in the Angola Basin." These remarks are meaningful only if we note the way in which Wüst used the term water mass. In the last few sentences of The Stratosphere of the Atlantic Ocean, Wüst acknowledged

> "Our scheme is designed to demonstrate the meridional spreading of the stratospheric core masses. It was not possible to

> create with current lines or arrows a closed circulation for the entire water column. To do so would cross the boundaries set by the qualitative analysis of the thermohaline structure, since the spreading of water masses in the ocean is not identical with the water motions."

Thus Wüst's statements about the water masses in the Angola Basin refer to the distribution of properties only and are not a pronouncement of no motion. In fact Wüst (1933) did describe the sloping of isotherms in zonal sections as evidence of motion of the bottom water there, albeit weak. Finally, Wüst (1955) presented geostrophic velocity calculations in a section crossing the Angola Basin with nonzero deep velocities. It is impossible to be content with these calculations, however, because of the paucity of data and the required accuracy, and the arbitrary assumption of a 1000 m zero reference level, even though they may be satisfactory in other regions.

References

Bainbridge, A. E. (1980) GEOSECS Atlantic Expedition: Volume 2, Sections and profiles. National Science Foundation, Washington, D. C., 196 + xiv pp.

Bennekom, Van A.J., and G.W. Berger (1984) Hydrography and silica budget of the Angola Basin. Netherlands Journal of Sea Research, 17(2-4):149-200.

Bohnecke, G. (1927) Die Bodenwassertemperaturen bei der Romanche-Tiefe. Zietschrift der Gesellschaft fur Erdkunde zu Berlin, Jahrgang 1927:

Brennecke, W. (1911) Ozeanographischen Arbeiten der Deutschen Antarktischen Expedition (Pernambuco-Buenos Aires) 111. Bericht. Annalen der Hydrographie und Maritimen Meteorologie, 39:642-647.

Broecker, W. S., T. Takahashi, and M. Stuiver (1980) Hydrography of the Central Atlantic-II. Waters beneath the two-degree discontinuity. Deep-Sea Research, 27A:397-419.

Buchanan, J. Y. (1888) The Exploration of the Gulf of Guinea. Scottish Geographical Magazine, pp. 178-251.

Chan, L. H., D. Drummond, J. M. Edmond, and B. Grant (1977) On the barium data from the Atlantic GEOSECS Expedition. Deep-Sea Research, 24:613-649.

Connary, S. D., and M. Ewing (1974) Penetration of AABW from the Cape Basin into the Angola Basin. Journal of Geophysical Research, 79:463-469.

Craig, H. (1971) The deep metabolism: oxygen consumption in abyssal ocean water. Journal of Geophysical Research, 76:5078-5086.

Fuglister, F. C. (1960) Atlantic Ocean Atlas of Temperature and Salinity Profiles and Data from the International Geophysical Year of 1957- 1958. Woods Hole Oceanographic Institution Atlas Series 1, 209 pp.

Hartmann, M., P. J. Muller, E. Suess, and C. H. van der Weijden (1976) Chemistry of late quaternary sediments and their interstitial waters from the northwest African continental margin. "Meteor" Forschungsergebnisse C, 24:1-67.

Hogg, N., P. Biscaye, W. Gardner, and W.J. Schmitz, Jr. (1982) On the transport and modification of Antarctic Bottom Water in the Vema Channel. Journal of Marine Research, 40(Suppl.):231-263.

Jansen, J.H.F., T.C.E. Van Weering, R. Gieles, and J. Van Iperen (1984) Middle and late quaternary oceanography and climatology of the Zaire-Congo fan and the adjacent eastern Angola Basin. Netherlands Journal of Sea Research, 17(2-4):201-249.

Kuo, H.-H. (1974) The effect of bottom topography on the stationary planetary flow on a sphere. Deep Sea Research, 21:933-945.

Kuo, H.-H., and G. Veronis (1973) The use of oxygen as a test for an abyssal circulation model. Deep-Sea Research, 20:871-888.

Levitus, S. (1982) Climatological Atlas of the World Ocean. NOAA Professional Paper 13, U.S. Government printing office, Washington D.C., 173pp.

Mann, C. R., A. R. Coote, and D. M. Garner (1973) The meridional distribution of silicate in the western Atlantic Ocean. Deep Sea Research, 20:791-801.

Merz, A., and G. Wust (1922) Die Atlantische Vertikalzirculation. Zietschrift der Gesellschaft fur Erdkunde zu Berlin, Jahrgang 1922:1-35.

Metcalf, W. G., B. C. Heezen, and M. C. Stalcup (1964) The sill depth of the Mid-Atlantic Ridge in the Equatorial region. Deep-Sea Research, 11:1-10.

Millard, R.C., Jr. (1982) CTD Calibration and data processing techniques at WHOI using the 1978 practical salinity scale. Proceedings of the MTS conference, San Diego, California, February 1982. 7pp.

Muller, P.J., and E. Suess (1979) Productivity, sedimentation rate, and sedimentary organic matter in the oceans - I. Organic carbon preservation. Deep Sea Research, 26A:1347-1362

Murray, J. (1899) On the temperature of the floor of the ocean and of the surface waters of the ocean. Geographical Journal of London.

Patamat, M. M. (1977) Benthic community metabolism. A review and assessment of present status and outlook. In: Ecology of Marine Benthos. B. C. Coull (ed.), University of South Carolina Press, pp. 89-111.

Pedlosky, J. (1979) Geophysical Fluid Dynamics, Springer-Verlag, New York, 624pp.

Picaut, J. (1983) Propagation of the seasonal upwelling in the eastern equatorial Atlantic. Journal of Physical Oceanography, 13:18-37.

Pfannkuche, O., R. Theig, and H. Thiel (1983) Benthos activity, abundance, and biomass under an area of low upwelling off Morocco, N.W. Africa. "Meteor" Forschungsergebnisse E, 36:85-96.

Redfield, A. C., B. H. Ketchum, F. A. Richards (1963) The influence of organisms on the composition of seawater. In: The sea, ideas and observations on progress in the study of the seas, 2: The composition of seawater, comparative and descriptive oceanography. M. N. Hill, editor, Wiley Interscience, New York, pp. 26-77.

Reid, J. L. (1981) On the middepth circulation of the world ocean. In: Evolution of Physical Oceanography Scientific Surveys in Honor of Henry Stommel, B. A. Warren and C. Wunsch, editors; The MIT Press, Cambridge, Massachusetts; pp 70-111.

Smith, K. L. (1984) Measured fluxes across the sediment-water interface: a status report. In: Global Ocean Flux Study, Proceedings of a Workshop. National Academy Press, Washington, D.C, pp. 326-340.

Smith, K. L., and K. R. Hinga (1983) Sediment community respiration. In: The Sea, Vol. 8, Deep Sea Biology. G. T. Rowe (ed.) Wiley Interscience, New York, pp. 331-371.

Stommel, H., and A. B. Arons (1960a) On the abyssal circulation of the world ocean - I. Stationary planetary flow patterns on a sphere. Deep-Sea Research, 6:140-154.

Stommel, H., and A. B. Arons (1960b) On the abyssal circulation of the world ocean - II. An idealized model of the circulation pattern and amplitude in oceanic basins. Deep-Sea Research, 6(3):217-233.

Suess, E. (1974) Nutrients near the depositional interface. In: The Benthic Boundary Layer, I. N. McCave, ed. Plenum Press, New York and London, pp. 57-79.

Suess, E. (1980) Particulate organic carbon flux in the oceans-surface productivity and oxygen utilization. Nature, 288:260-263.

Supan, A. (1899) Die Bodenform des Weltmeeres. Peterson. Mitt.

Thomson, C. W. (1878) The voyage of the CHALLENGER: The Atlantic. Harper and Bros., New York, 340 pp.

Uchupi, E. (1981) Bathymetric Atlas of the Atlantic, Caribbean, and Gulf of Mexico. Woods Hole Oceanographic Institution Technical Report, WHOI Reference number 71-71, 10 pp., revised 1981.

Warren, B. A. (1973) Transpacific hydrographic sections at latitudes 43°S and 28°S: the Scorpio Expedition-II. Deep Water. Deep-Sea Research, 20:9-38.

Warren, B. A. (1981a) Transindian hydrographic section at latitude 18°S: property distributions and circulation in the South Indian Ocean. Deep-Sea Research, 28:759-788.

Warren, B. A. (1981b) Deep circulation of the world ocean. In: Evolution of Physical Oceanography, Scientific Surveys in Honor of Henry Stommel, B. A. Warren and C. Wunsch, editors; The MIT Press, Cambridge, Massachusetts; pp. 6-41.

Wattenberg, H. (1929) Durchluftung des Atlantischen Ozeans. (Vorlaufige Mitteilung aus der Ergebnissen der Deutschen Atlantischen Expedition.) Journal du Counseil, 4:68-79.

Wattenberg, H. (1938) Die Verteilung des Sauerstoff im Atlantischen Ozean. In: Wissenschaftliche Ergebnisse der Deutschen Atlantischen Expedition auf dem Forschungs- und Vermessungsschiff "Meteor" 1925-1927, 9, (1) und (2), pp. 1-179.

Wattenberg, H. (1939) Atlas zu: die Verteilung des Sauerstoff im Atlantischen Ozean. In: Wissenschaftliche Ergebnisse der Deutschen Atlantischen Expedition auf dem Forschungs- und Vermessungsschiff "Meteor" 1925-1927, 9, Atlas, 72 plates.

Wattenberg, H. (1957) Die Verteilung des Phosphats im Atlantischen Ozean. In: Wissenschaftliche Ergebnisse der Deutschen Atlantischen Expedition auf dem Forschungs- und Vermessungsschiff "Meteor" 1925-1927, 9: 2nd part, 2, 133-180.

Weichart, G. (1974) Meereschemische Untersuchungen im nordwestafrikanischen Auftriebsgebiet 1968: "Meteor" Forschungsergebnisse A, 14:33-70.

Whitehead, J.A.,Jr. and L.V. Worthington (1982) The flux and mixing rates of Antarctic Bottom Water within the North Atlantic. Journal of Geophysical Research, 87:7903-7924.

Wust, G. (1933) Schichtung und Zirkulation des Atlantischen Ozeans. Das Bodenwasser und die Gliederung der Atlantischen Tiefsee. In: Wissenschaftliche Ergebnisse der Deutschen Atlantischen Expedition auf dem Forschungs- und Vermessungsschiff "Meteor" 1925-1927, 6:1st part, 1, 106 pp. (Bottom Water and the Distribution of the Deep Water of the Atlantic. M. Slessers, translator, D. E. Olson, ed., 1967, U.S. Naval Oceanographic Office, Washington, D.C., 145 pp.

Wust, G. (1935) Schichtung und Zirkulation des Atlantischen Ozeans. Die Stratosphare. In: Wissenschaftliche Ergebnisse der Deutschen Atlantischen Expedition auf dem Forschungs- und Vermessungsschiff "Meteor" 1925-1927, 6:1st part, 2, 180 pp. (The stratosphere of the Atlantic Ocean, W. J. Emery, editor, 1978, Amerind, New Delhi, 112 pp).

Wust, G. (1955) Stromgeschwindigkeiten im Tiefen-und Bodenwasser des Atlantischen Ozeans auf Grund dynamisher Berechnung der "Meteor" - Profile der Deutschen Atlantischen Expedition 1925-1927. Papers in Marine Biology and Oceanography. Deep-Sea Research, 3(supp):373-397.

Wust, G., and A. Defant (1936) Atlas zur Schichtung und Zirculation des Atlantischen Ozeans. Schnitte and Karten von Temperatur, Salzgehalt, und Dichte. In: Wissenschaftliche Ergebnisse der Deutschen Atlantischen Expedition auf dem - Forschungs - und Vermessungsschiff "Meteor" 1925-1927, 6: Atlas, 103 plates.

Wyrtki, K. (1962) The oxygen minima in relation to ocean circulation. Deep-Sea Research, 9:11-23.

List of Figures

Figure 12: a) Oxygen, silica, and phosphate versus potential temperature for bottom water in the Guinea, Angola, and Cape Basins (CTD oxygen values at 11°S). The I.G.Y. oxygen values have been corrected by adding 5°/∘. b) Meridional variation within the Angola Basin. AJ 29 is at 21°S, 1°E, about 100km southwest of GS 105 in figure 1, which is closer to the property extrema in deep water near this latitude discussed in the text.

Figure 13: Oxygen-silica relation for potential temperature less than 2.5°C.

Figure 14: Pattern of circulation for bottom water. The transport of the western boundary current is indicated to the left. The open circles are placed at equal intervals of time since leaving the boundary current.

Figure 15: Section of potential temperature for bottom water at 24°S in the Angola Basin.

Figure 16: Same as figure 15 for salinity (uncalibrated).

Figure 16b,c: Salinometer data for the interior at 24°S.

Figure 17: Predicted pattern of potential temperature and salinity south of 11°S in the basin.

Figure 18: The character of the deep oxygen minimum across the basin at 11°S.

Figure 19: Silica-salinity relation for stations in and surrounding the Angola Basin.

Figure 20: Oxygen-salinity relation.

Figure 21: Total dissolved carbon dioxide concentration and carbon-14 at GEOSECS station 107 at 12°S (about 4°/∘ accuracy).

Figure 22: From Suess (1976). Schematic representation of the relationship among (A) oxygen, (B) phosphate, (C) the amount of organic matter at the sediment surface, and (D) the nutrient concentration gradients within the sediment column. The low-oxygen-high-phosphate concentrations, high surface organic carbon, and high nutrient fluxes in the sediment column are vertically aligned with the upper continental rise. A deep oxygen minimum exists near 2000m on the upper cont. rise, but does not penetrate the interior. Sections are from Weichart (1974), at 20°N.

Figure 23: Circulation pattern for the flat bottom SA model, extending, approximately from 5°N to 20°S.

Figure 24: Zonal variation of oxygen concentration.

Figure 25: Oxygen profiles at four stations along the eastern boundary of the tropical Atlantic. The scales are different and are offset to illustrate the vertical profiles. Station CF 446 is from Crawford cruise 22, station CF 92 is from Crawford cruise 10, both during the I.G.Y..

Figure 26: Predicted oxygen distribution for the model with boundary flux. The vertical scale is z, the horizontal is x, with x=0 at the eastern boundary. In figure 26a, Pe=1; 26b, Pe=1.5; 26c, Pe=2; 26d, Pe=3.

List of Tables

	11°S	24°S	Guinea	Over	Cape	Cape	Guinea	Over	Guinea	Over
θ	1.91	1.98	1.89	2.05	1.0	no solution			88	12
S	34.88	34.888	34.875	34.893	34.76	no solution			72	28
O	5.6	5.4	5.7	5.25	5.1	0.4	72	27.6	78	22
Si	55	54	53	56	100	1	65	34	sensitive	
Ph	1.6	1.65	1.51	1.65	2.0	4	48	48	38	62

Table 1

Pe	Stations 150 to 140	
	3750 m	4000 m
1	.008 .14	.002 .03
1.5	.004 .07	-.002 .01
2	.001 .02	-.002 -.02

Table 2

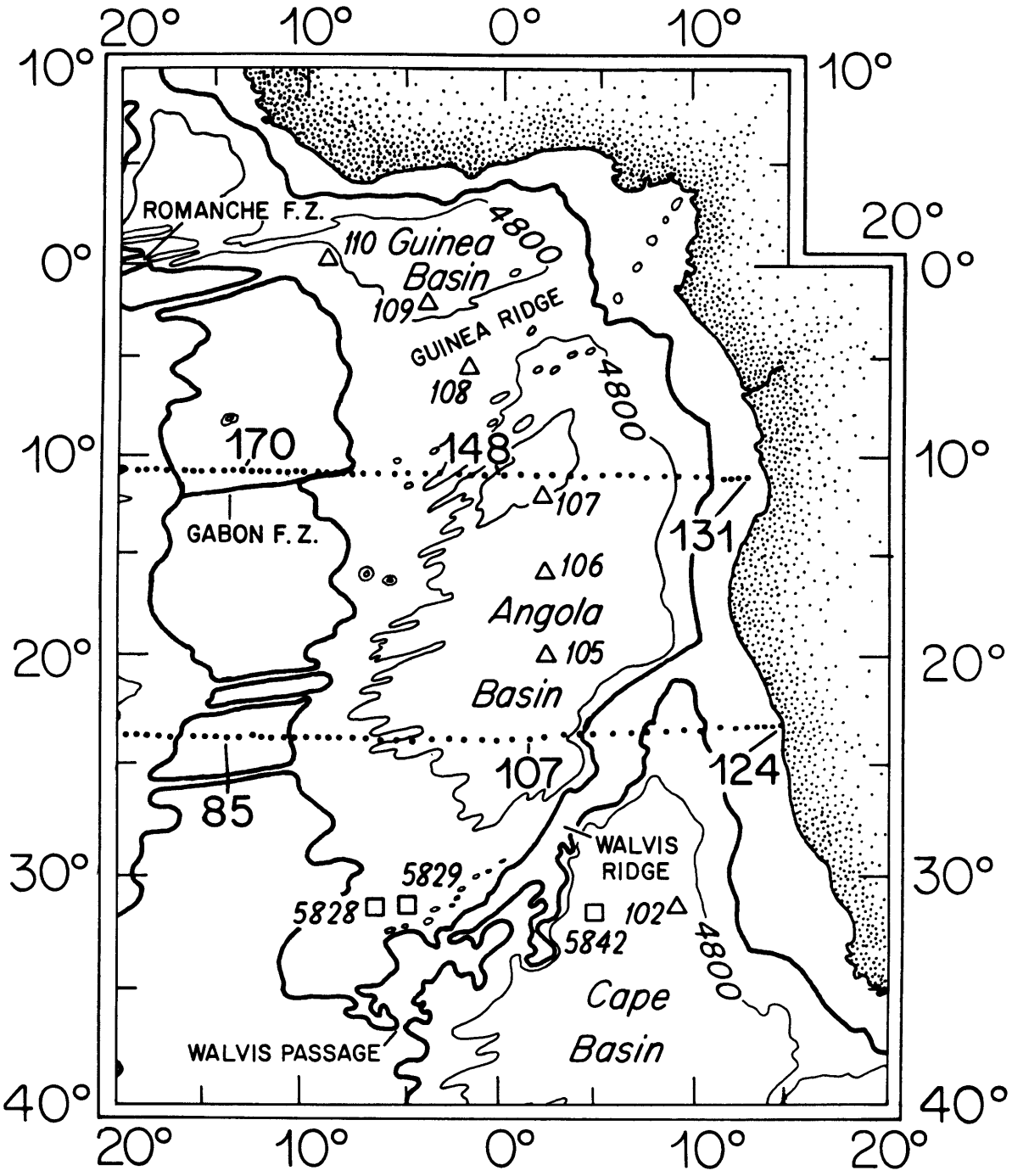
20°
10°
0°
10°
20°
10°
0°
10°
20°
30°
40°
ROMANCHE F.Z.
110
Guinea
Basin
4800
109
GUINEA RIDGE
108
4800
170
148
107
GABON F.Z.
131
106
Angola
105
Basin
107
124
85
WALVIS
RIDGE
5829
5828
102
5842
4800
Cape
Basin
WALVIS PASSAGE

Figure 1

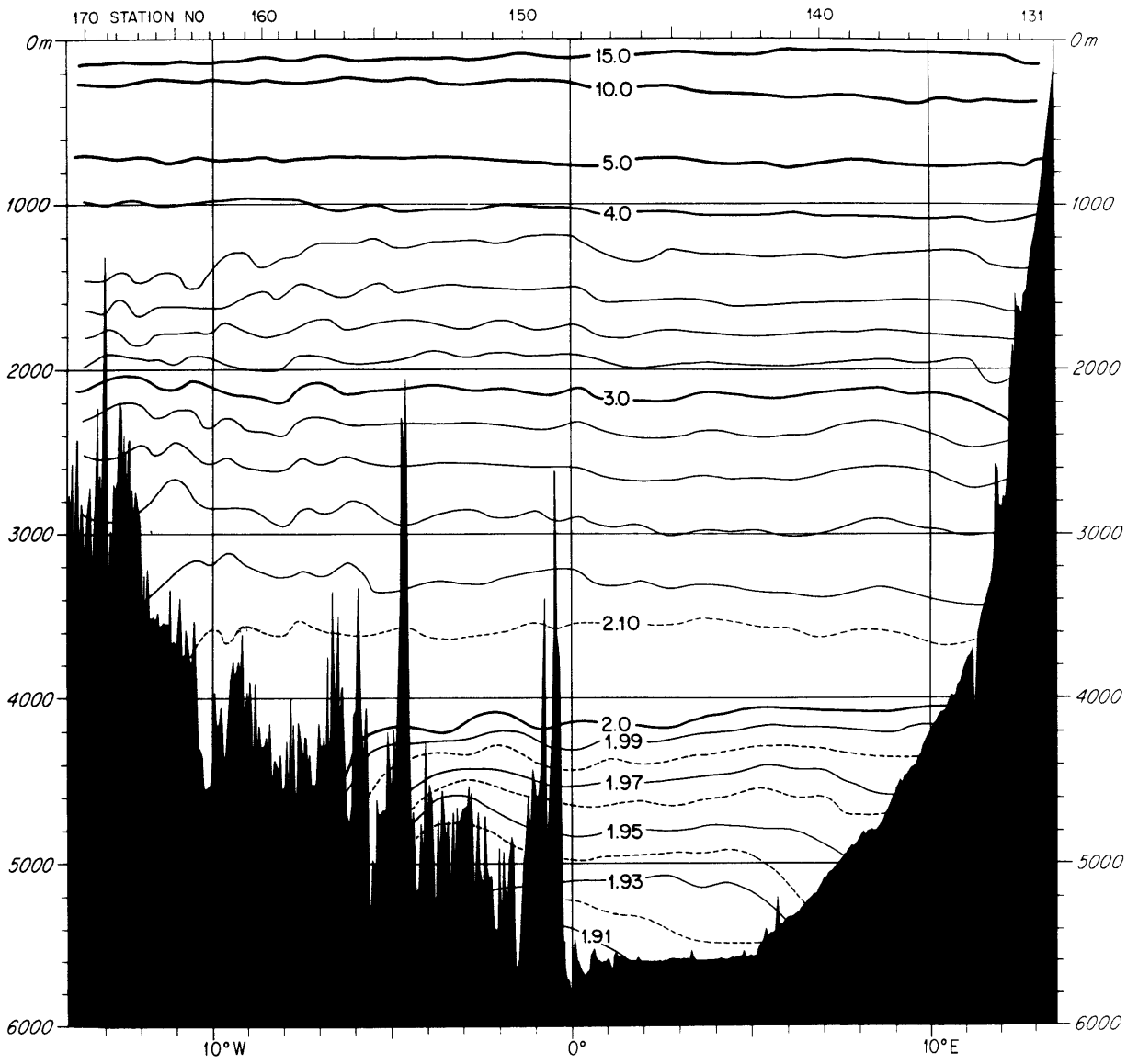
170 STATION NO
160
150
140
131
0m
1000
2000
3000
4000
5000
6000
15.0
10.0
5.0
4.0
3.0
2.10
2.0
1.99
1.97
1.95
1.93
1.91
10°W
0°
10°E

Figure 2

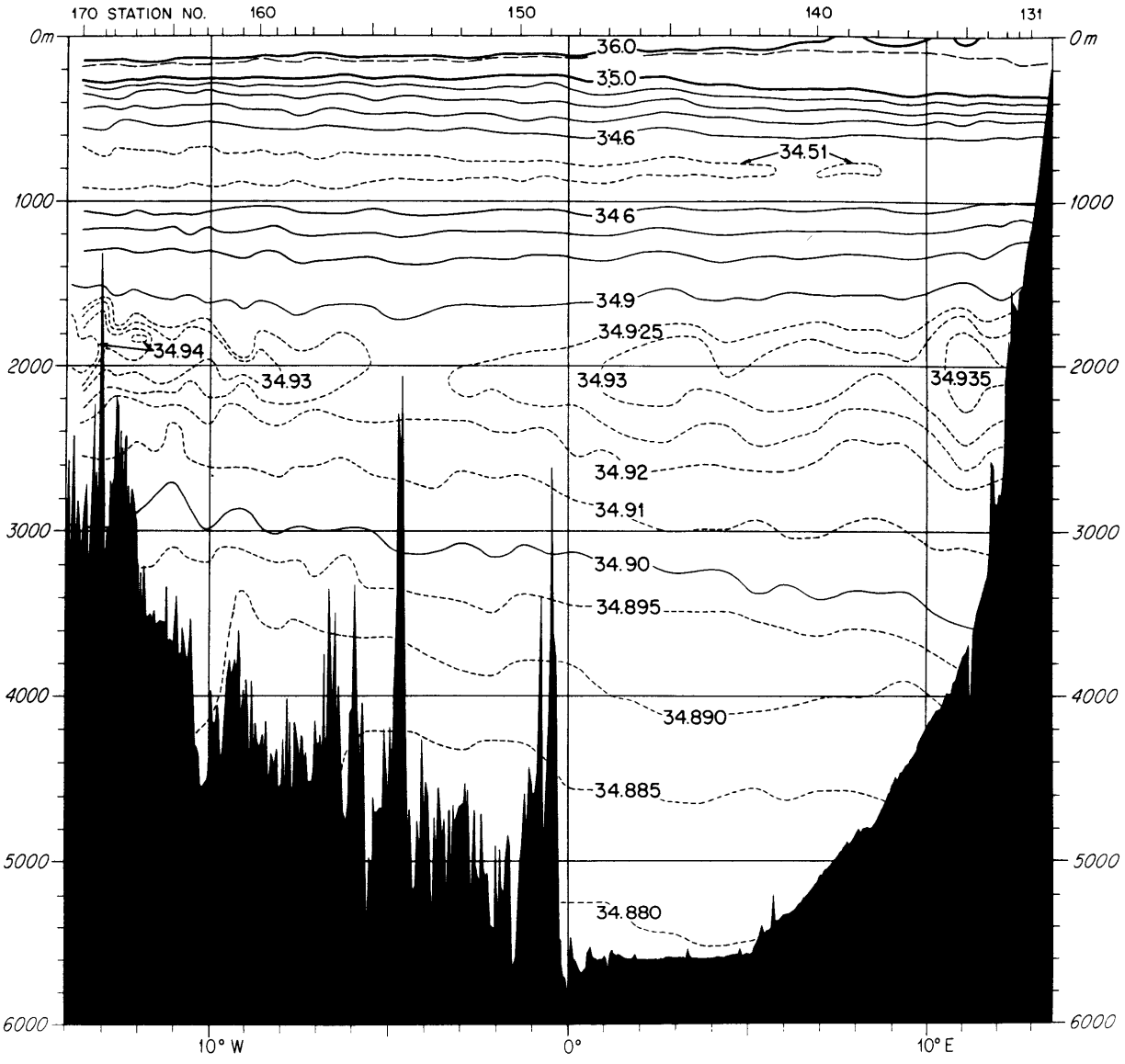
170 STATION NO.
160
150
140
131
0m
1000
2000
3000
4000
5000
6000
36.0
35.0
34.6
34.51
34.6
34.9
34.925
34.94
34.93
34.93
34.935
34.92
34.91
34.90
34.895
34.890
34.885
34.880
10° W
0°
10° E

Figure 3

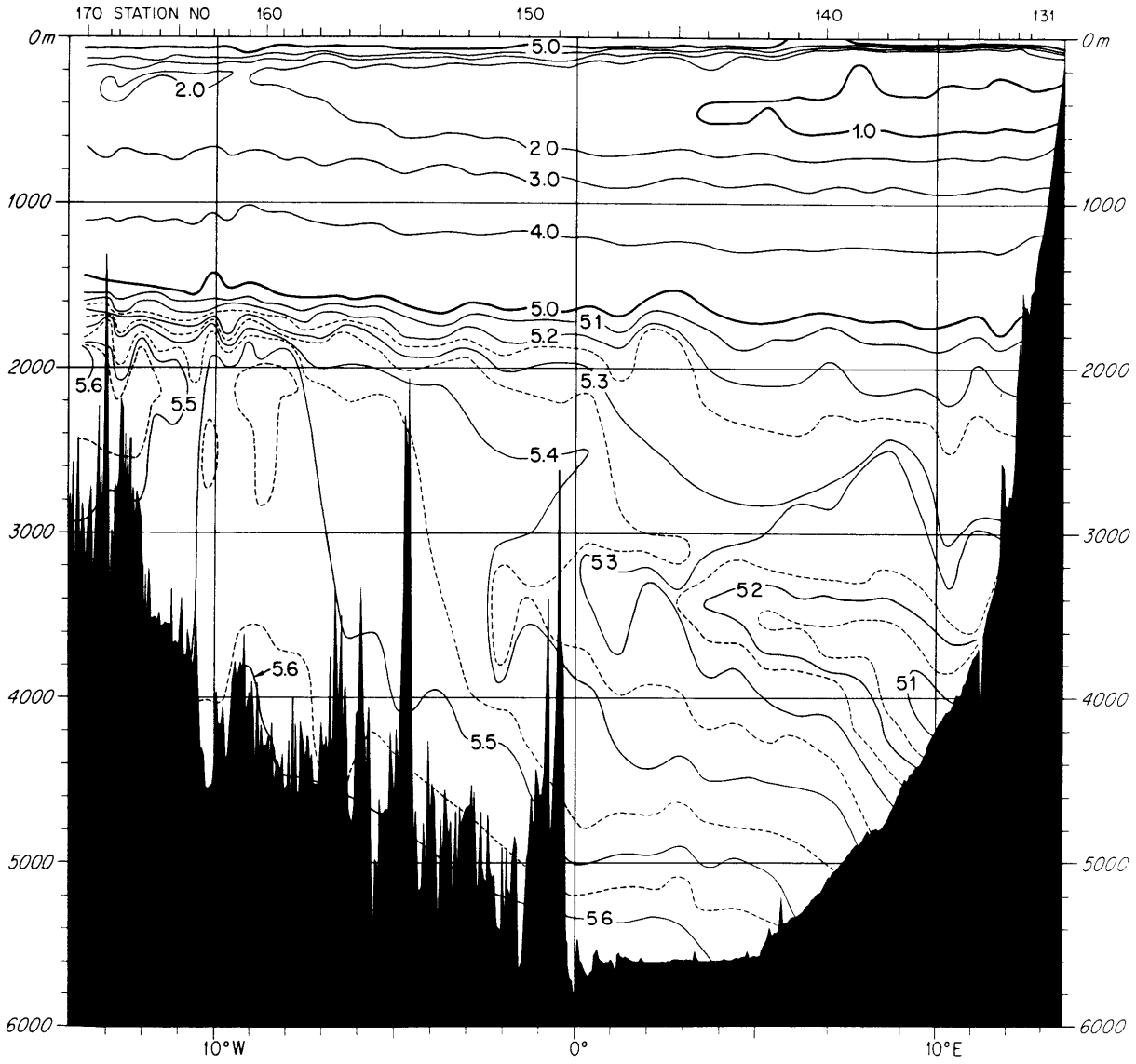
170 STATION NO
160
150
140
131
0m
1000
2000
3000
4000
5000
6000
10°W
0°
10°E
5.0
2.0
1.0
2 0
3.0
4.0
5.0
51
5.2
5.6
5.5
5.3
5.4
53
52
5.6
51
5.5
56

Figure 4

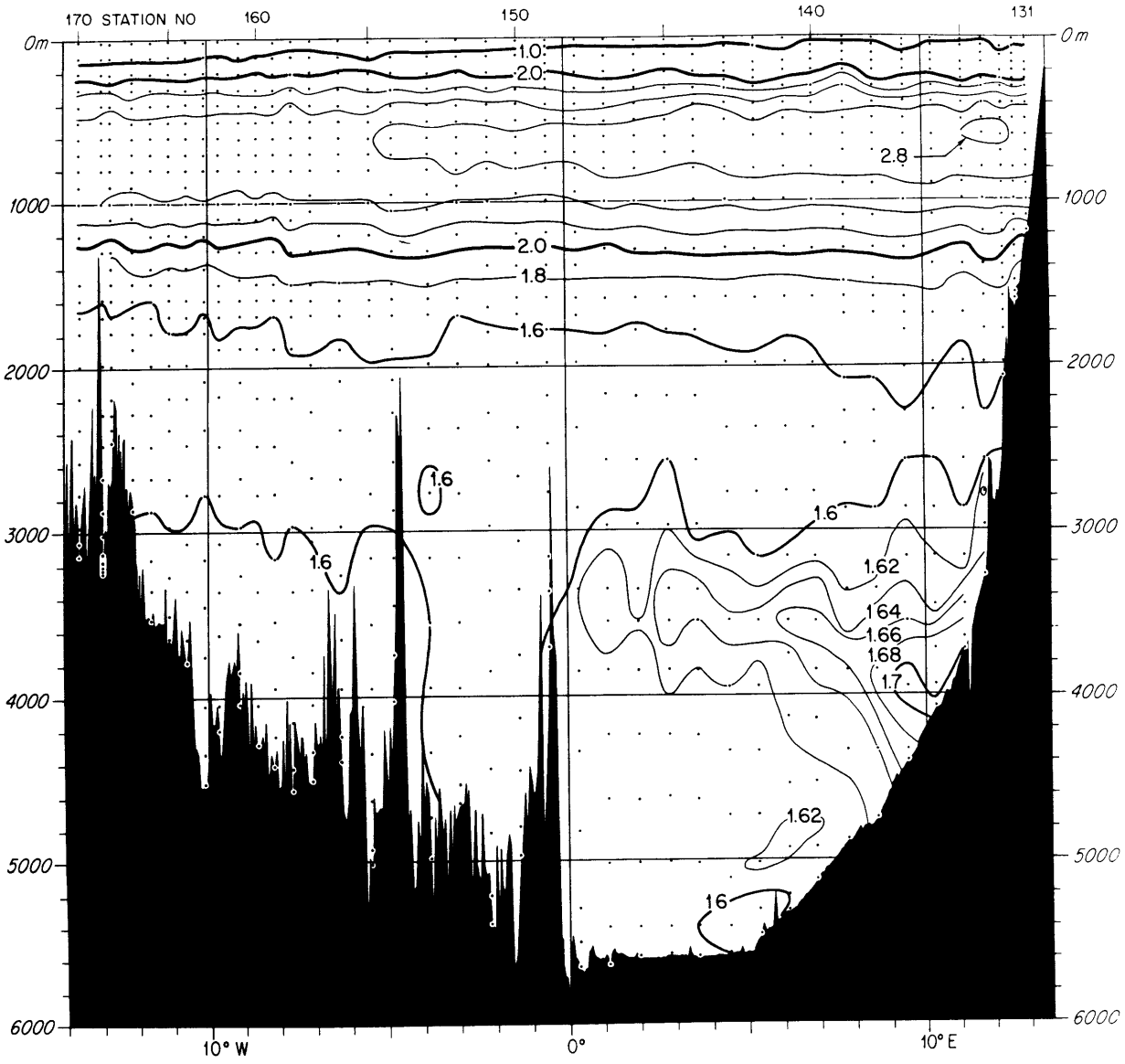
170 STATION NO
160
150
140
131
0m
1000
2000
3000
4000
5000
6000
1.0
2.0
2.8
1.8
1.6
1.62
1.64
1.66
1.68
1.7
16
10° W
0°
10° E

Figure 5

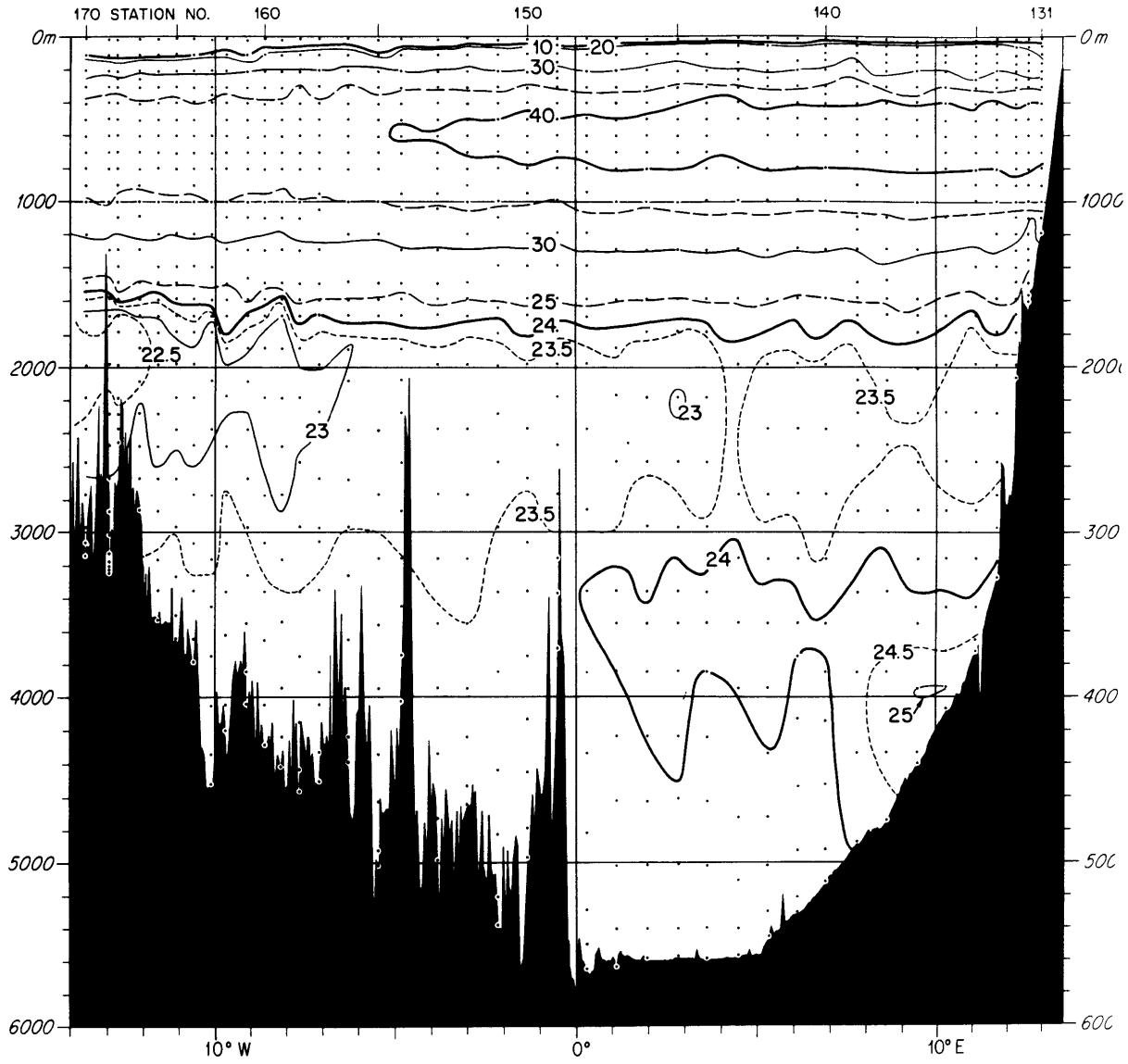
170 STATION NO.
160
150
140
131
0m
1000
2000
3000
4000
5000
6000
10
20
30
40
30
25
24
23.5
22.5
23
23
23.5
23.5
24
24.5
25
10° W
0°
10° E

Figure 6

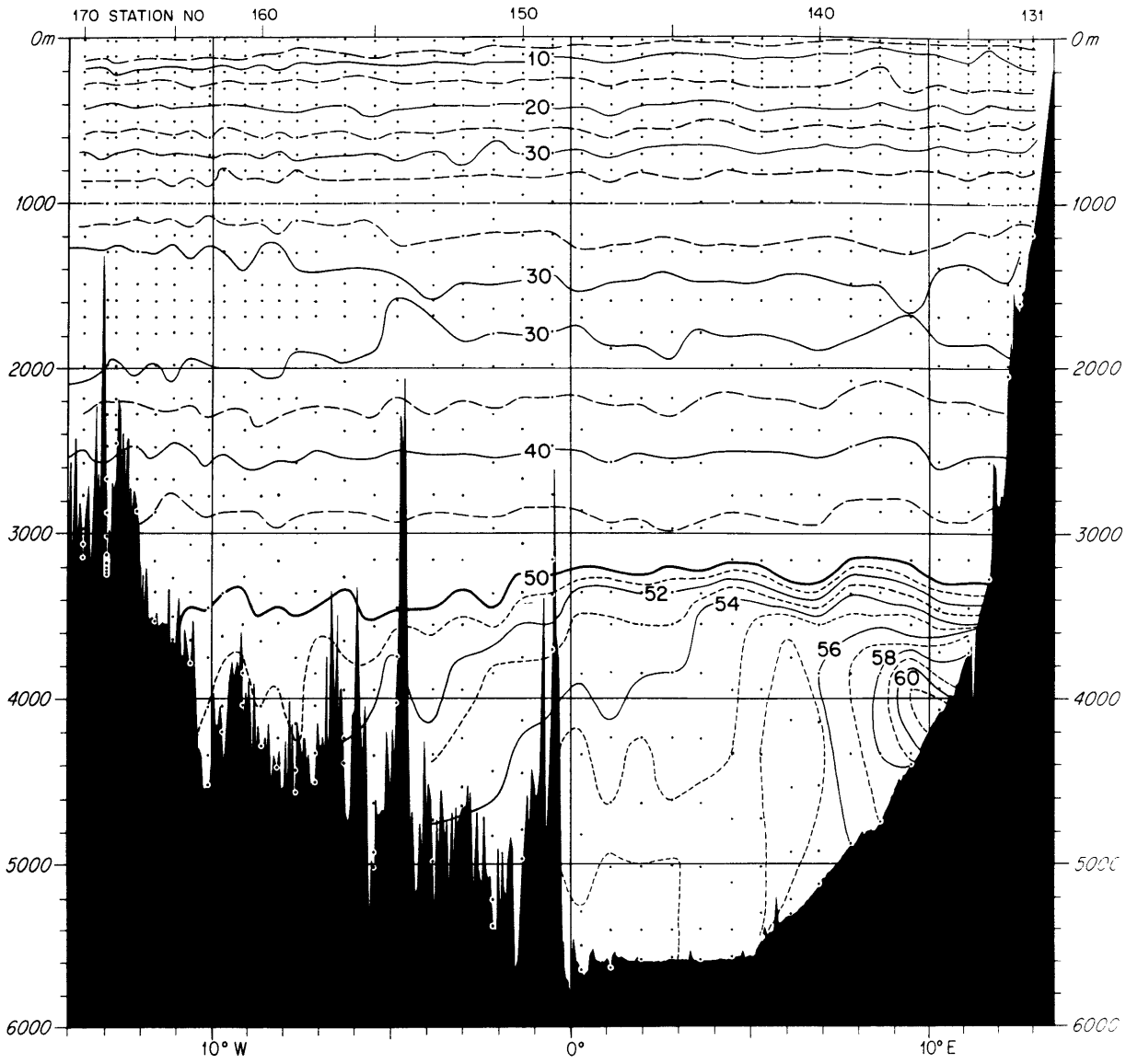
170 STATION NO
160
150
140
131
0m
1000
2000
3000
4000
5000
6000
10
20
30
30
30
40
50
52
54
56
58
60
10° W
0°
10° E

Figure 7

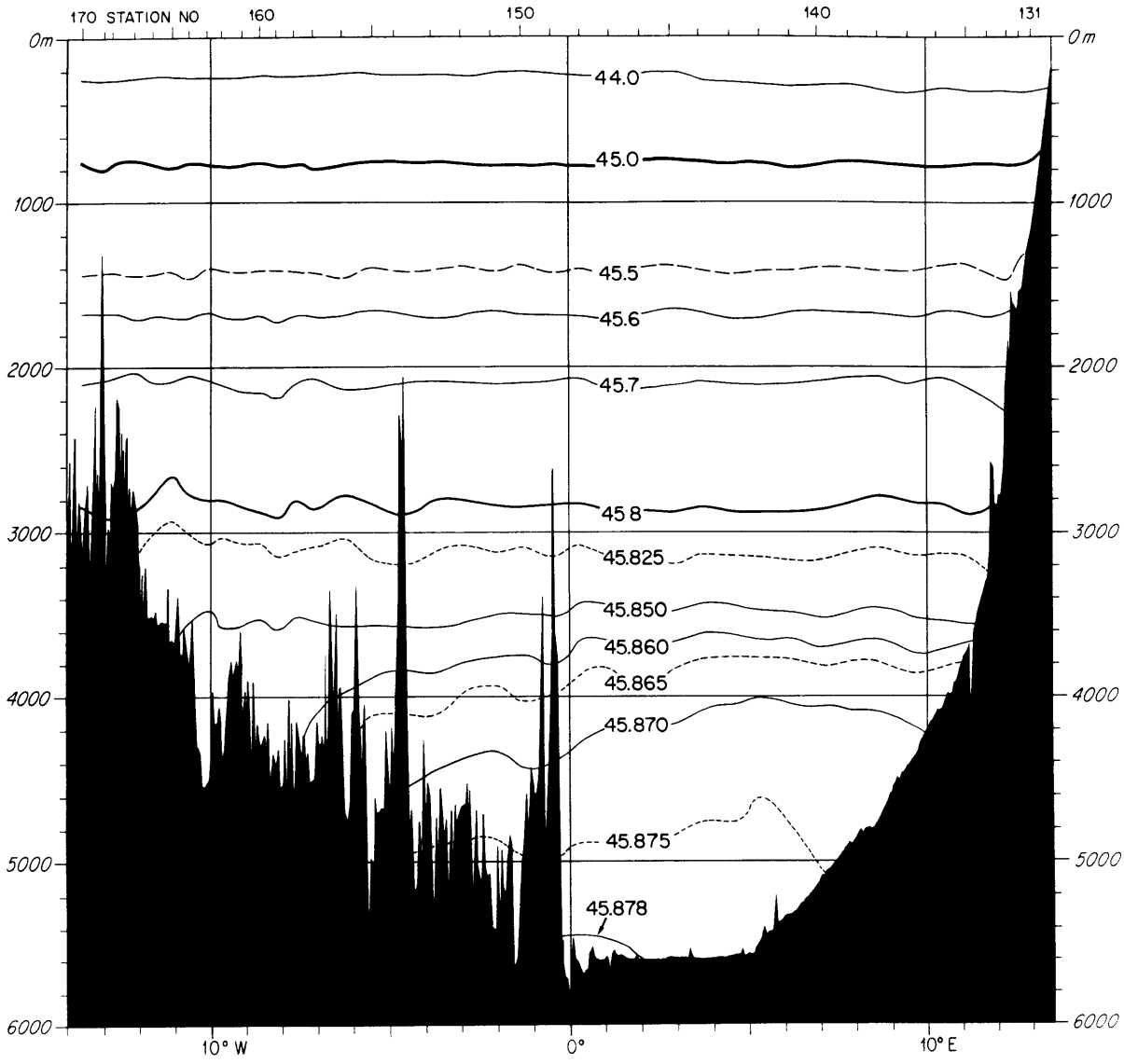
170 STATION NO
160
150
140
131
0m
1000
2000
3000
4000
5000
6000
44.0
45.0
45.5
45.6
45.7
45.8
45.825
45.850
45.860
45.865
45.870
45.875
45.878
10° W
0°
10° E

Figure 8

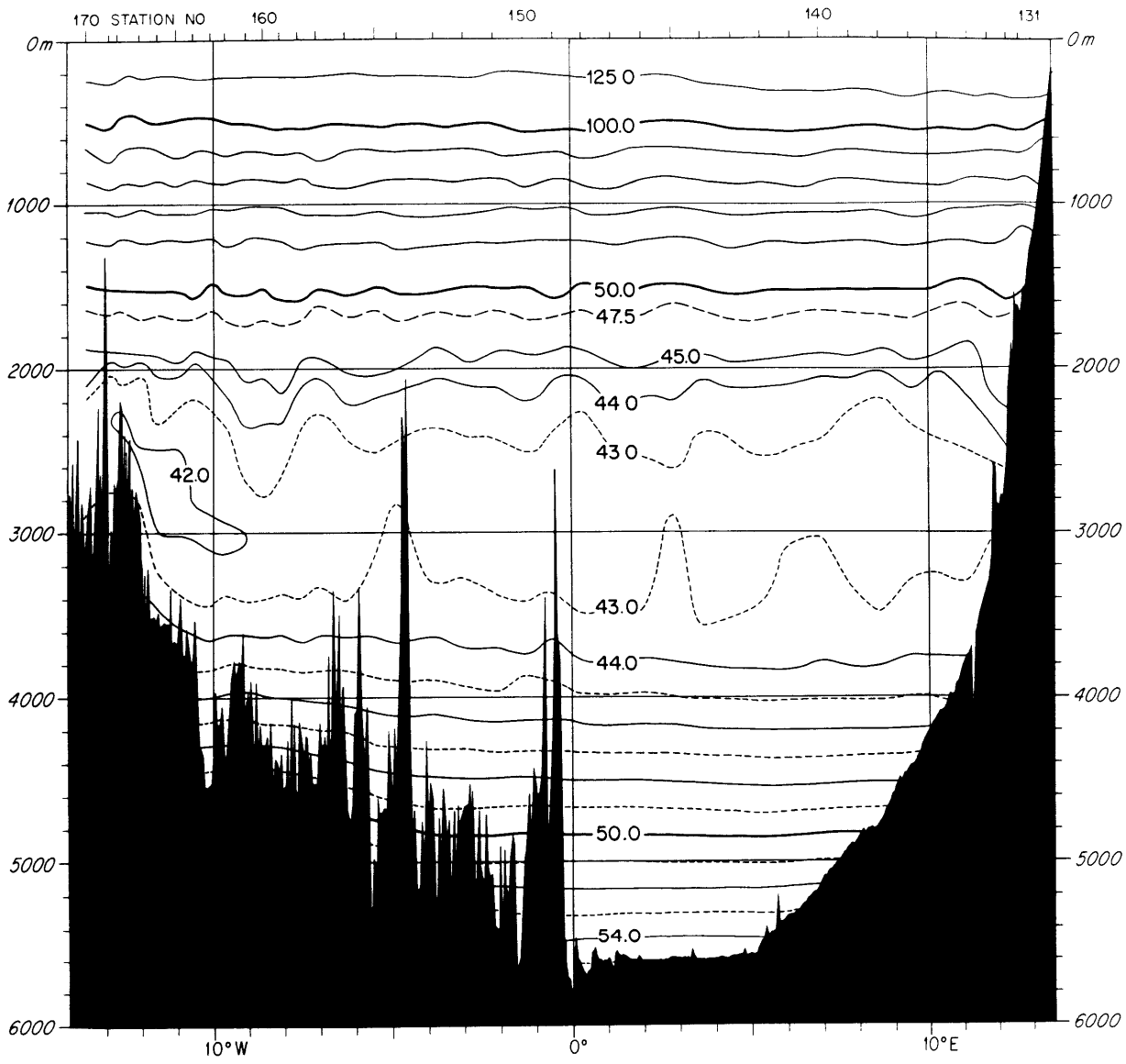
170 STATION NO
160
150
140
131
0m
1000
2000
3000
4000
5000
6000
125 0
100.0
50.0
47.5
45.0
44 0
43 0
42.0
43.0
44.0
50.0
54.0
10°W
0°
10°E

Figure 9

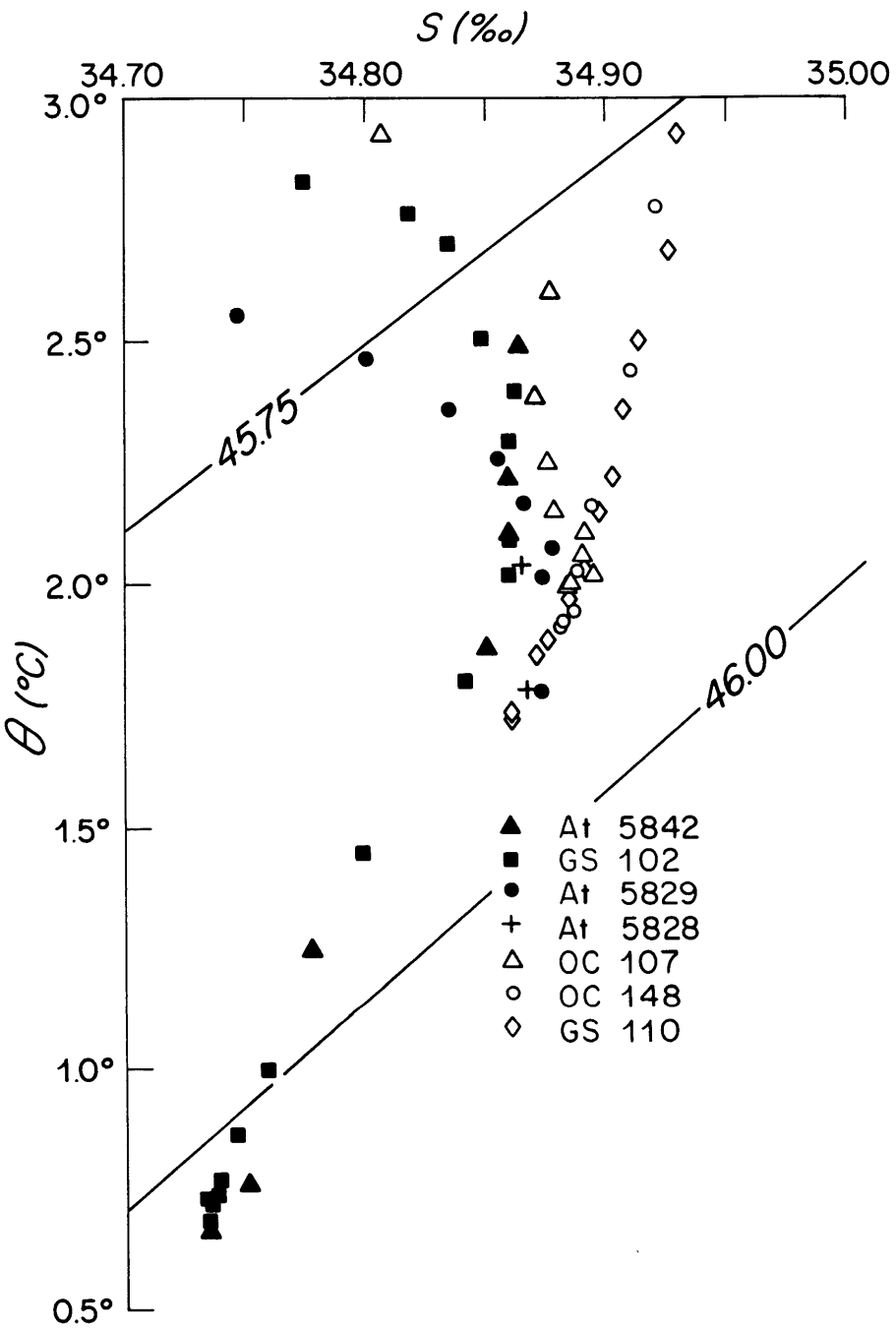
S (‰)
34.70
34.80
34.90
35.00
3.0°
2.5°
2.0°
1.5°
1.0°
0.5°
θ (°C)
45.75
46.00
At 5842
GS 102
At 5829
At 5828
OC 107
OC 148
GS 110

Figure 10

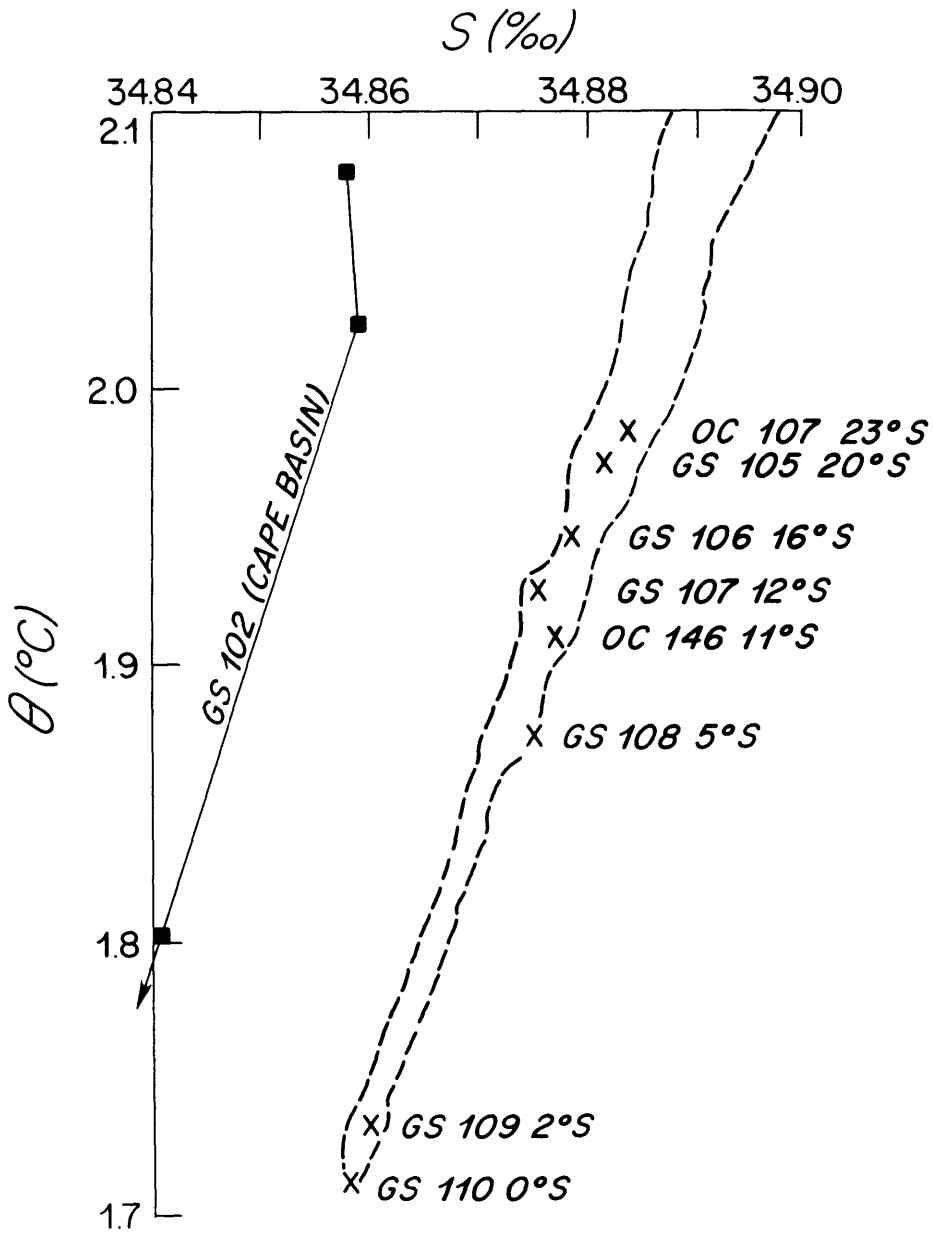
S (‰)
34.84
34.86
34.88
34.90
2.1
2.0
1.9
1.8
1.7
θ (°C)
GS 102 (CAPE BASIN)
OC 107 23°S
GS 105 20°S
GS 106 16°S
GS 107 12°S
OC 146 11°S
GS 108 5°S
GS 109 2°S
GS 110 0°S

Figure 11

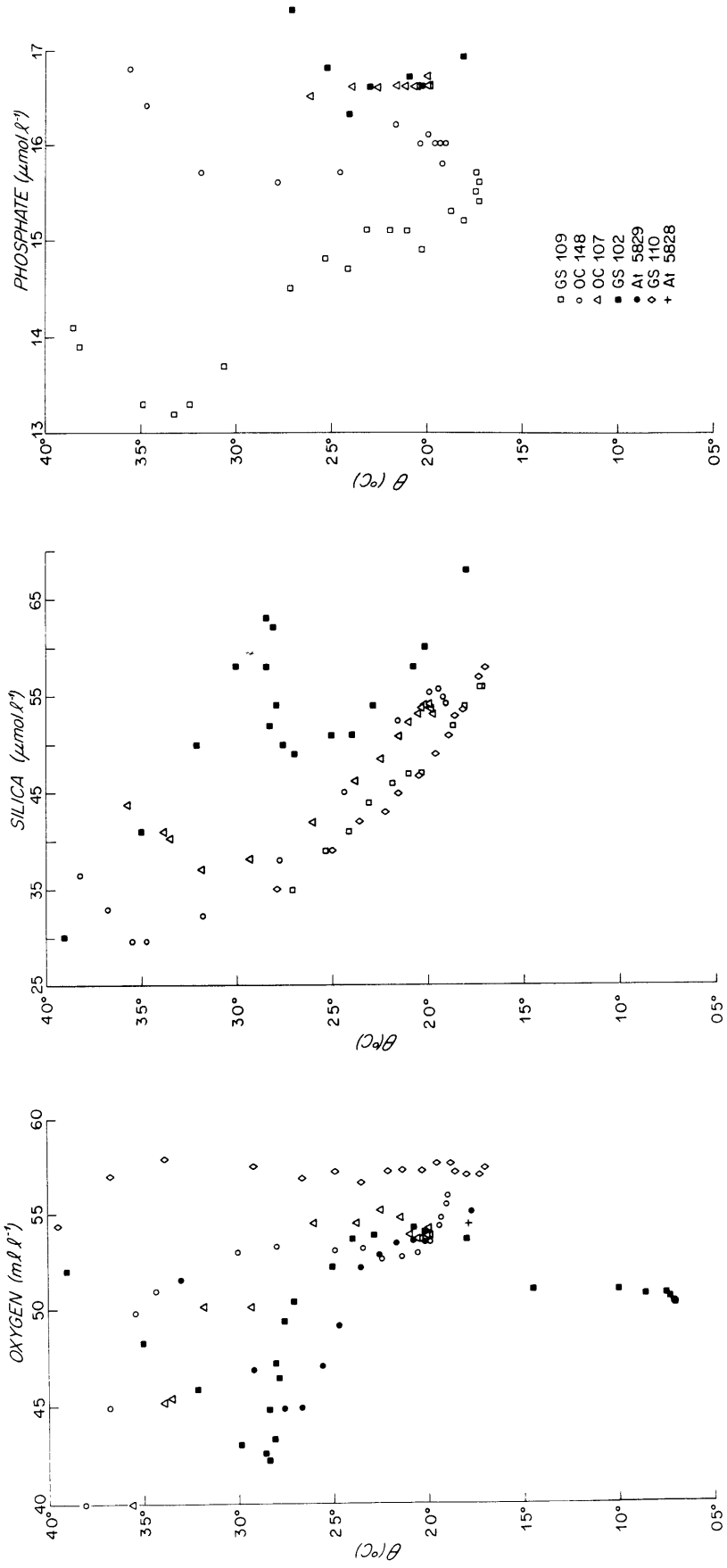
PHOSPHATE (µmol ℓ⁻¹)
SILICA (µmol ℓ⁻¹)
OXYGEN (ml ℓ⁻¹)
θ (°C)
GS 109
OC 148
OC 107
GS 102
At 5829
GS 110
At 5828

Figure 12a

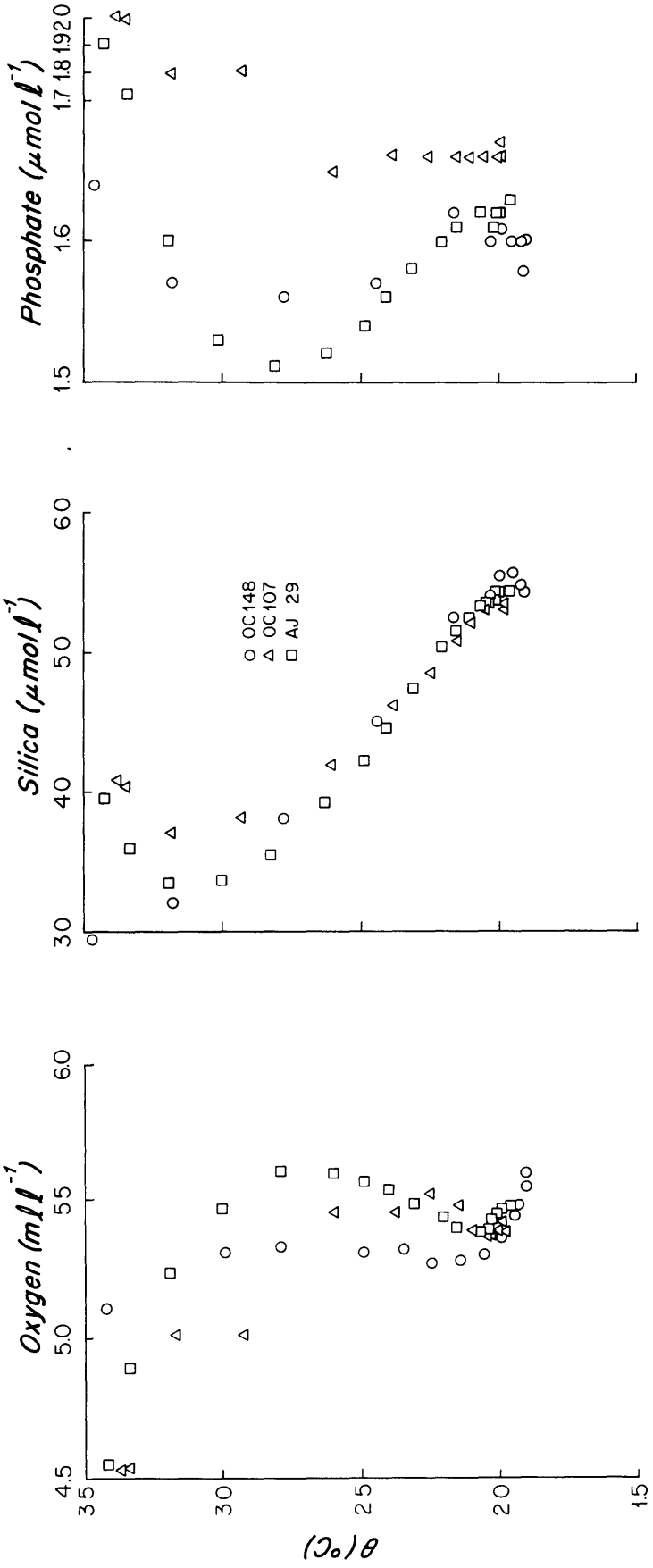
Phosphate (μmol l⁻¹)
1.5
1.6
1.7
1.8
1.9
2.0
Silica (μmol l⁻¹)
30
40
50
60
OC148
OC107
AJ 29
Oxygen (ml l⁻¹)
4.5
5.0
5.5
6.0
35
30
25
20
15
θ (°C)

Figure 12b

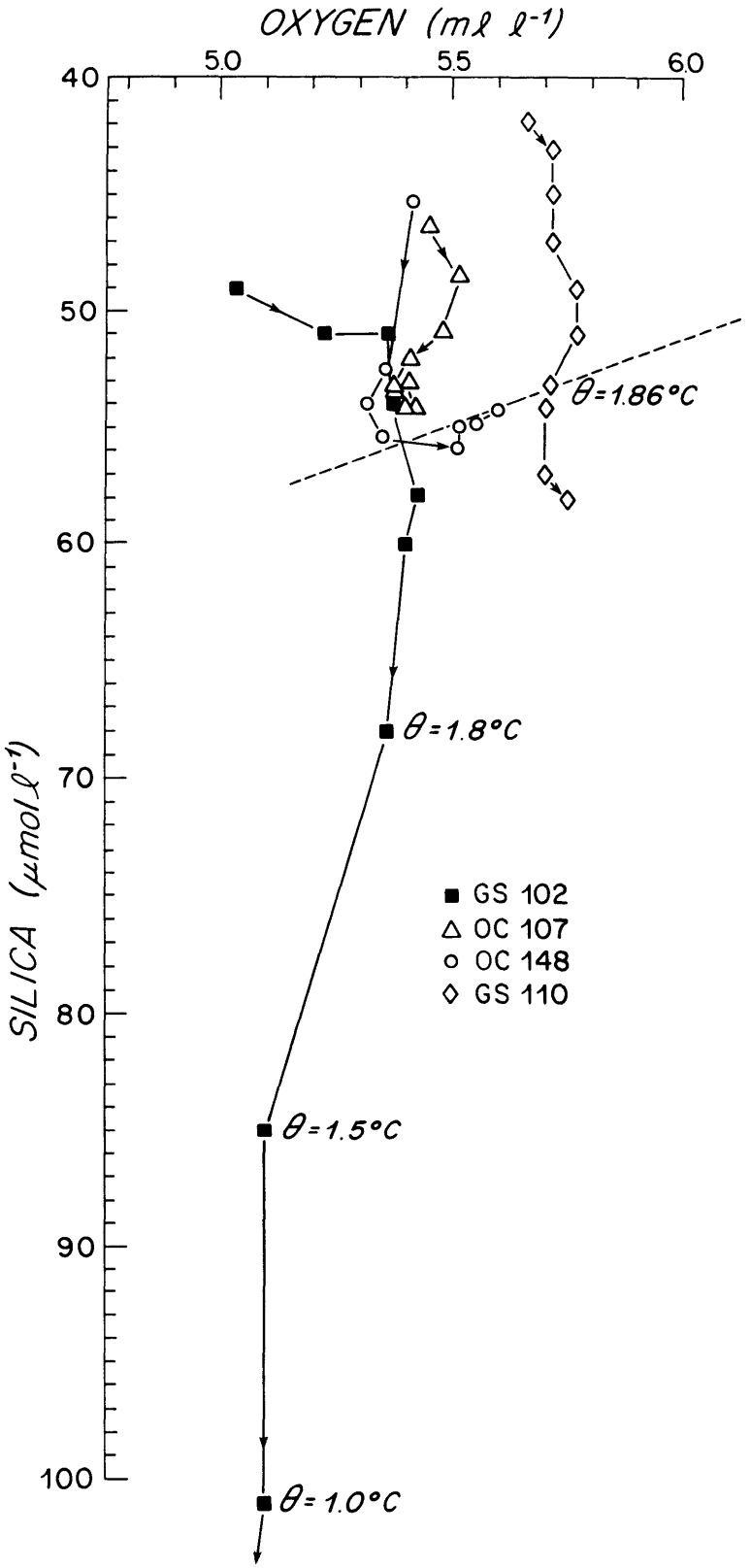
OXYGEN (ml l-1)
5.0
5.5
6.0
40
50
60
70
80
90
100
SILICA (μmol l-1)
θ=1.86°C
θ=1.8°C
θ=1.5°C
θ=1.0°C
GS 102
OC 107
OC 148
GS 110

Figure 13

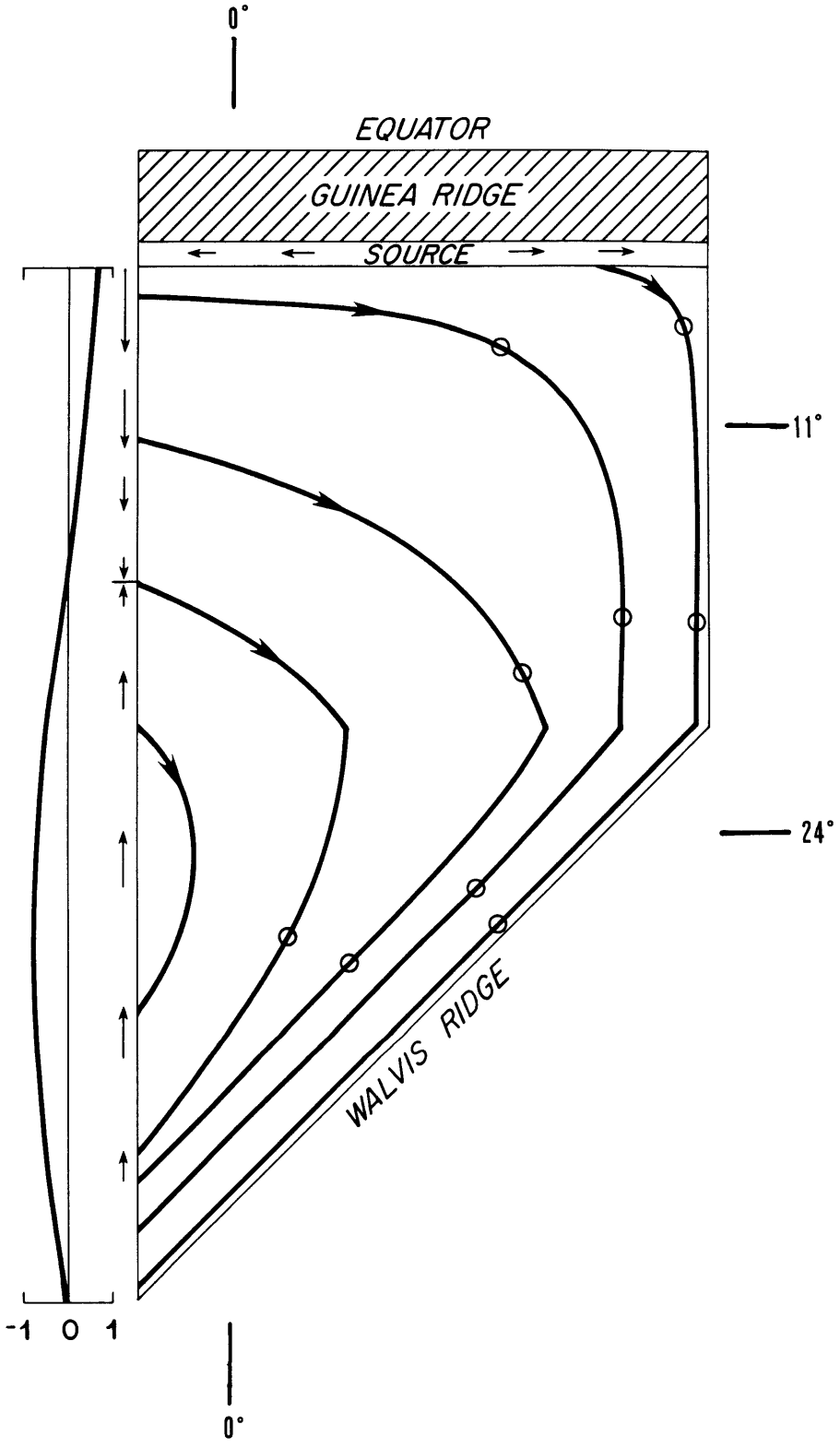

Figure 14

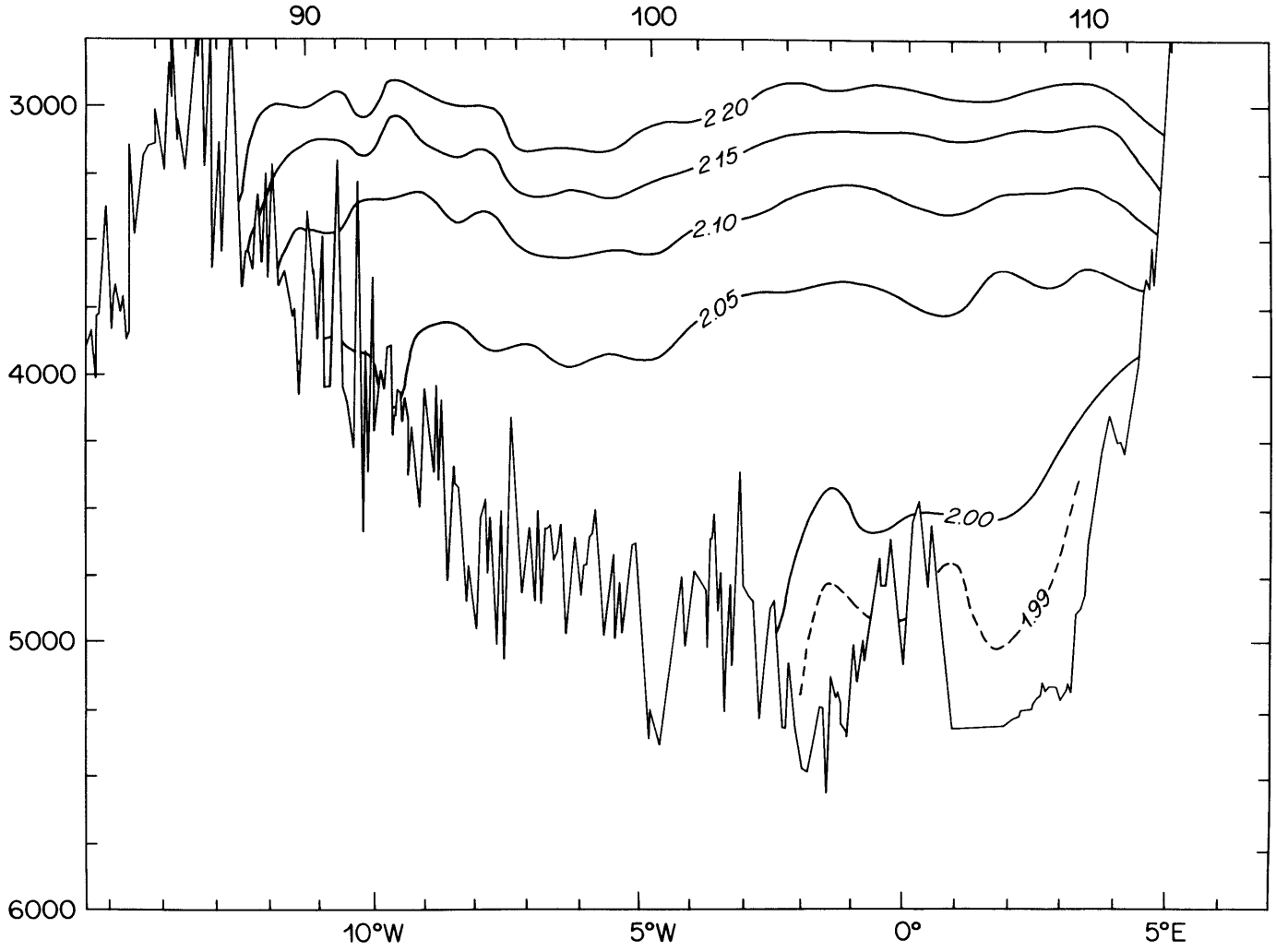
90
100
110
3000
4000
5000
6000
2.20
2.15
2.10
2.05
2.00
1.99
10°W
5°W
0°
5°E

Figure 15

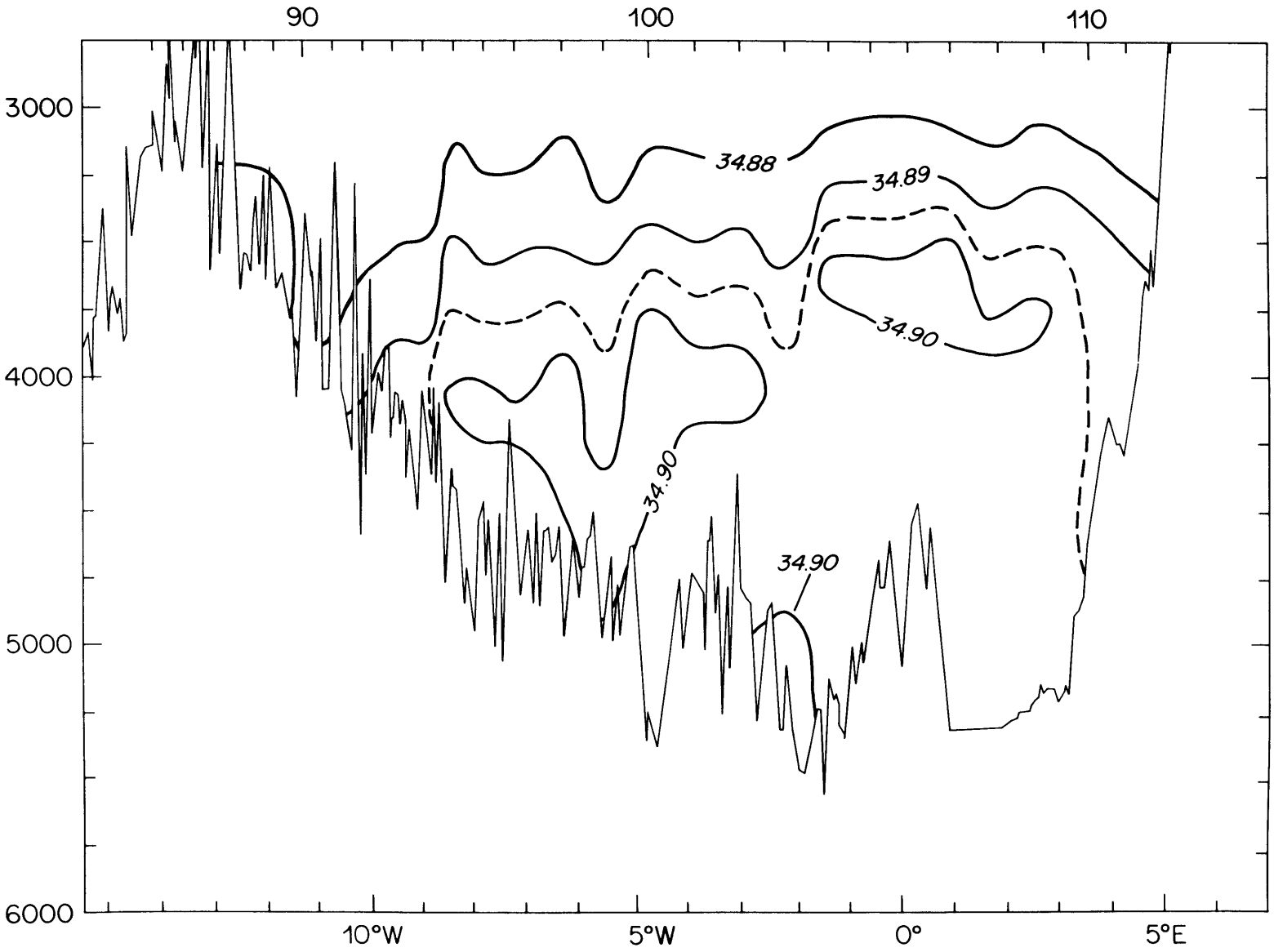
90
100
110
3000
4000
5000
6000
34.88
34.89
34.90
34.90
34.90
10°W
5°W
0°
5°E

Figure 16

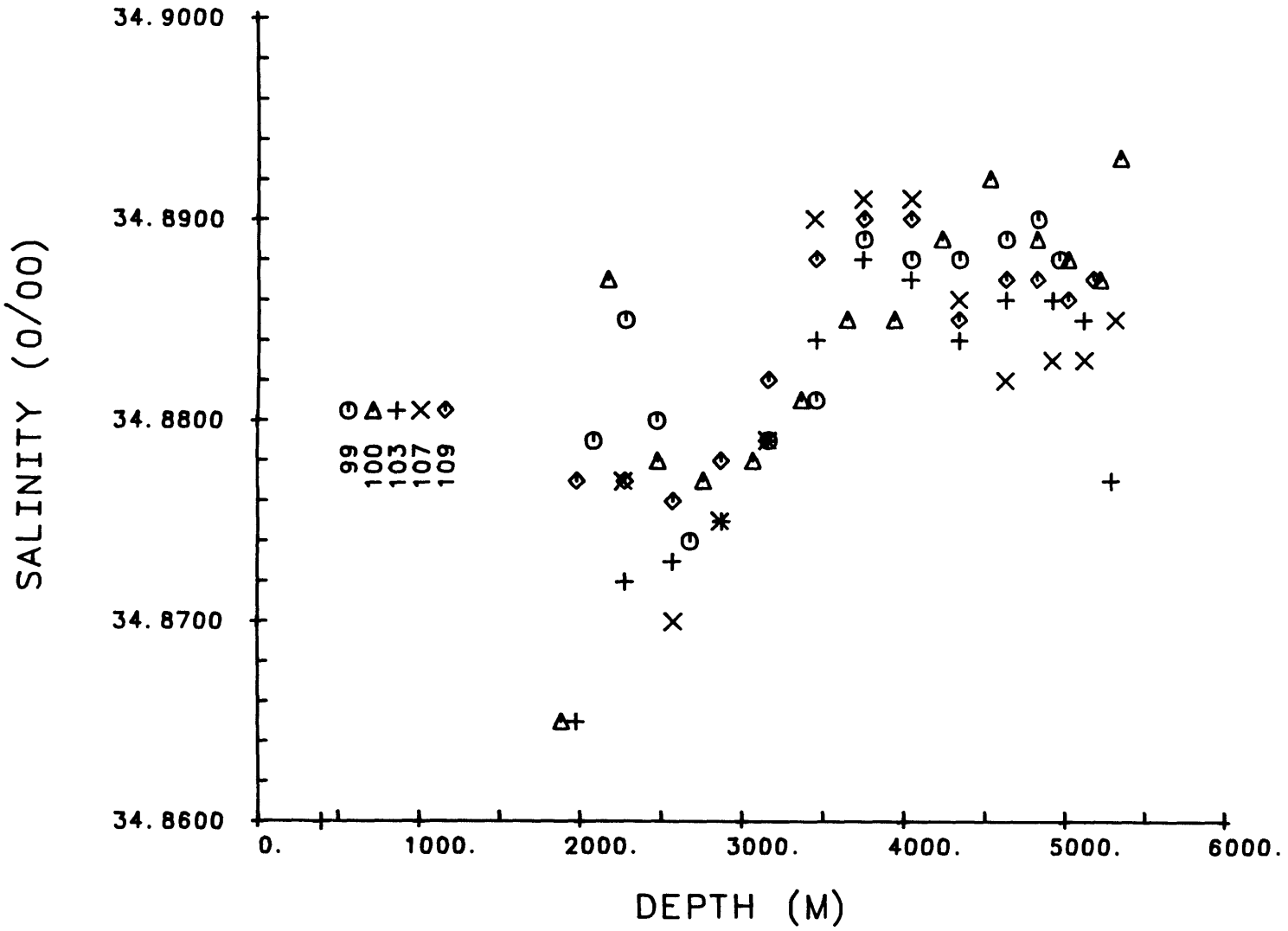
34.9000
34.8900
34.8800
34.8700
34.8600
SALINITY (O/OO)
99
100
103
107
109
0.
1000.
2000.
3000.
4000.
5000.
6000.
DEPTH (M)

Figure 16b

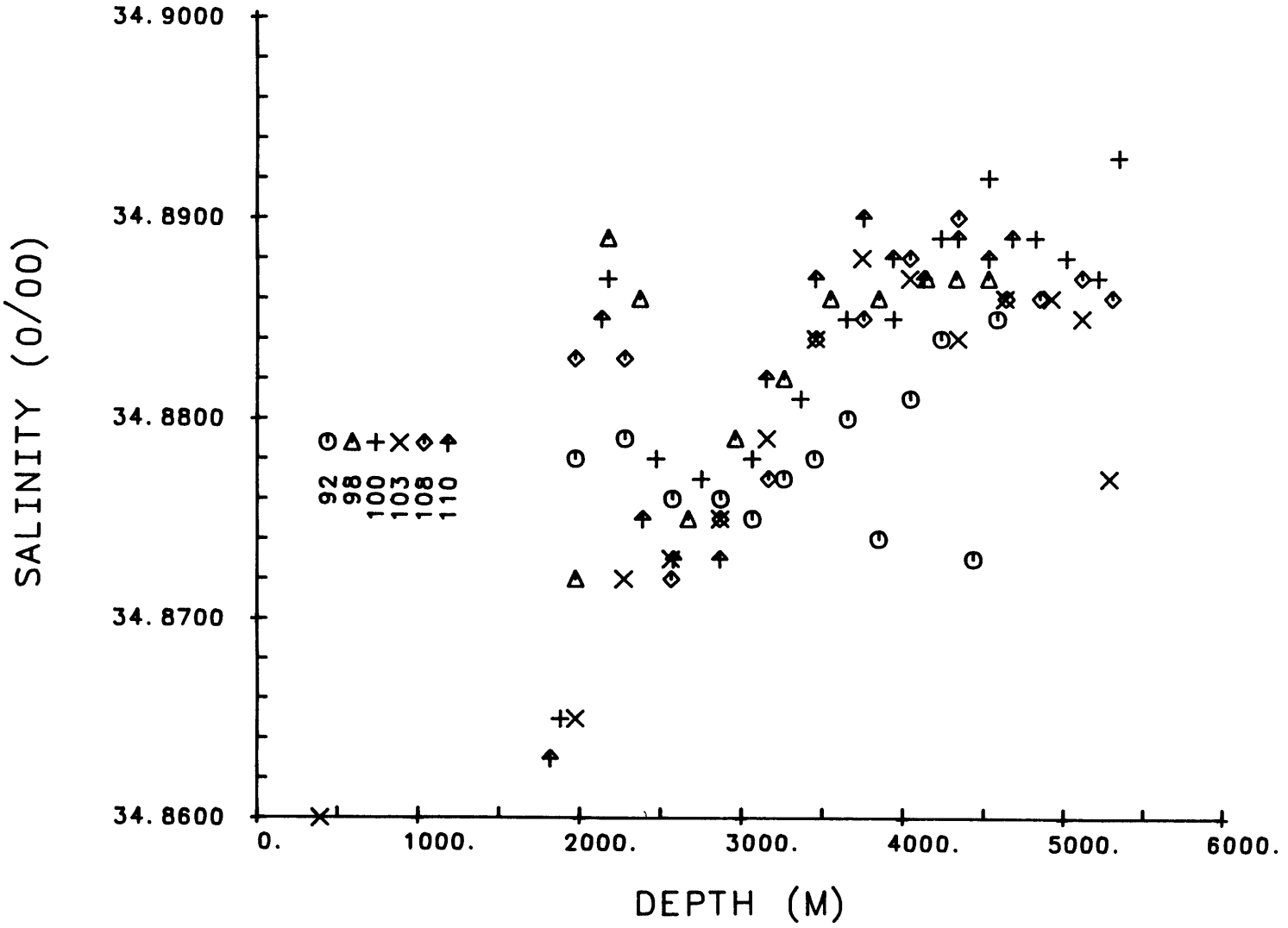
34.9000
34.8900
34.8800
34.8700
34.8600
SALINITY (O/OO)
92
98
100
103
108
110
0.
1000.
2000.
3000.
4000.
5000.
6000.
DEPTH (M)

Figure 16c

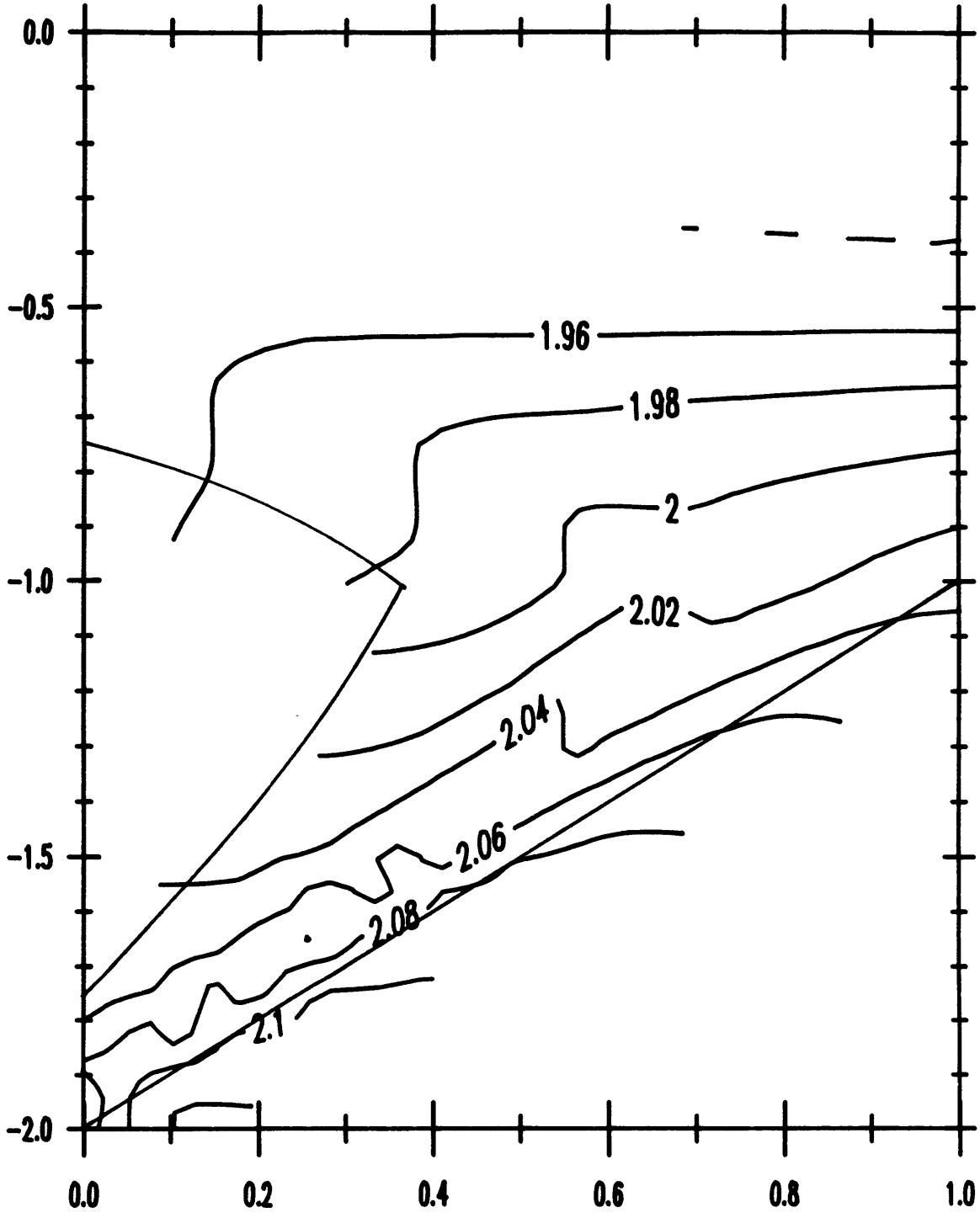

a

Figure 17

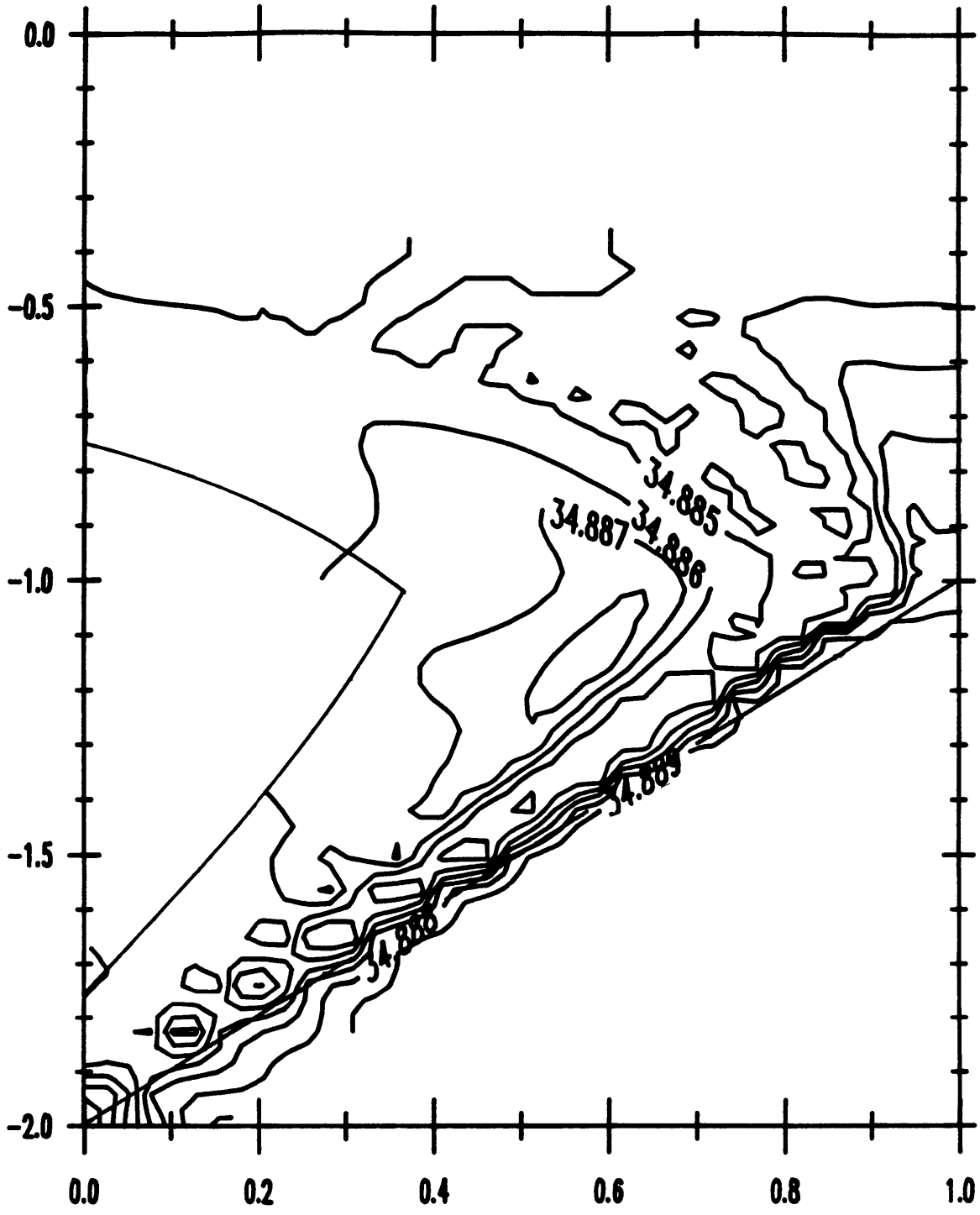

b

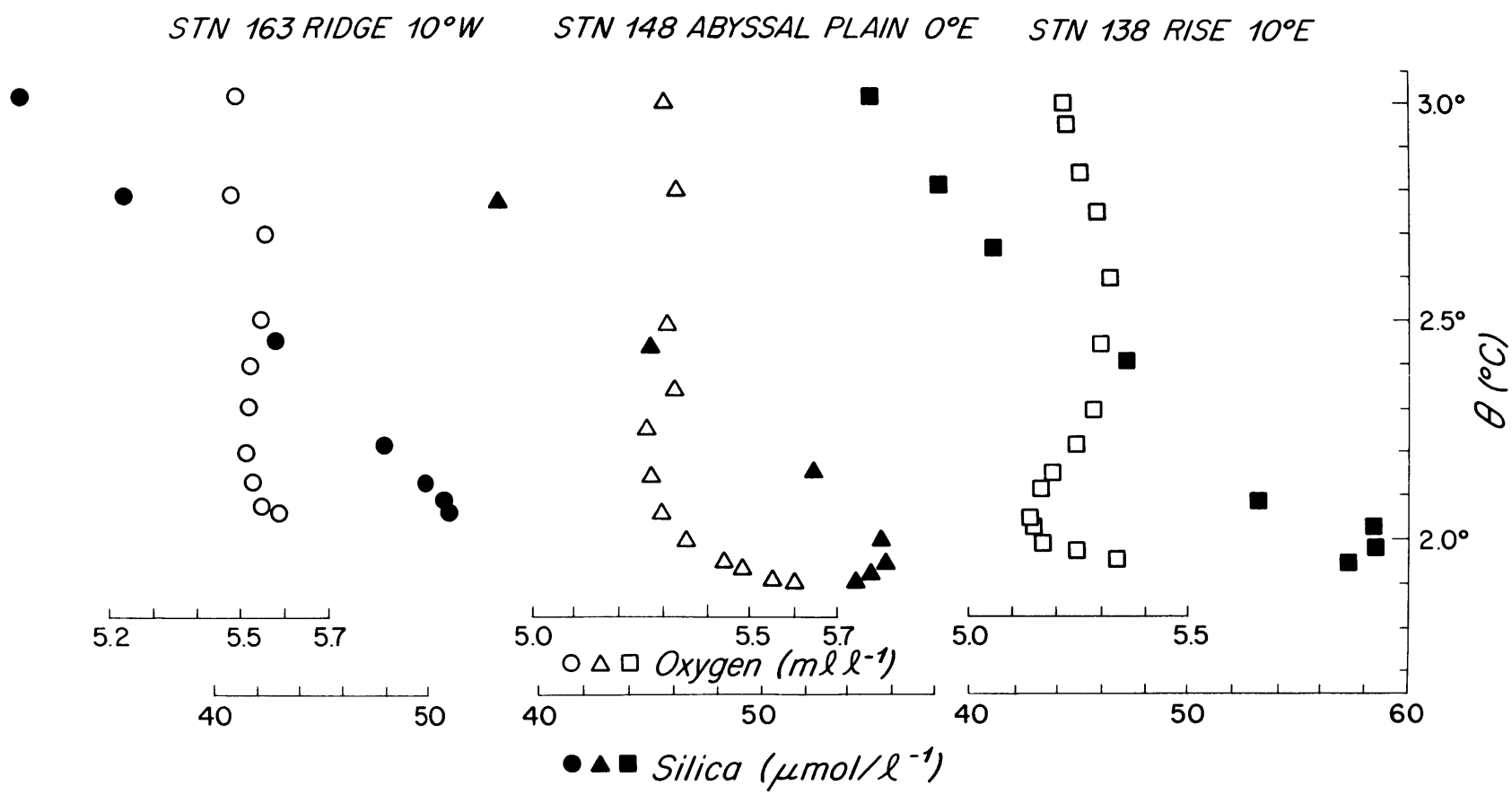
STN 163 RIDGE 10°W
STN 148 ABYSSAL PLAIN 0°E
STN 138 RISE 10°E
3.0°
2.5°
2.0°
θ (°C)
5.2
5.5
5.7
5.0
5.5
5.7
5.0
5.5
○ △ □ Oxygen (mℓ ℓ⁻¹)
40
50
40
50
40
50
60
● ▲ ■ Silica (μmol/ℓ⁻¹)

Figure 18

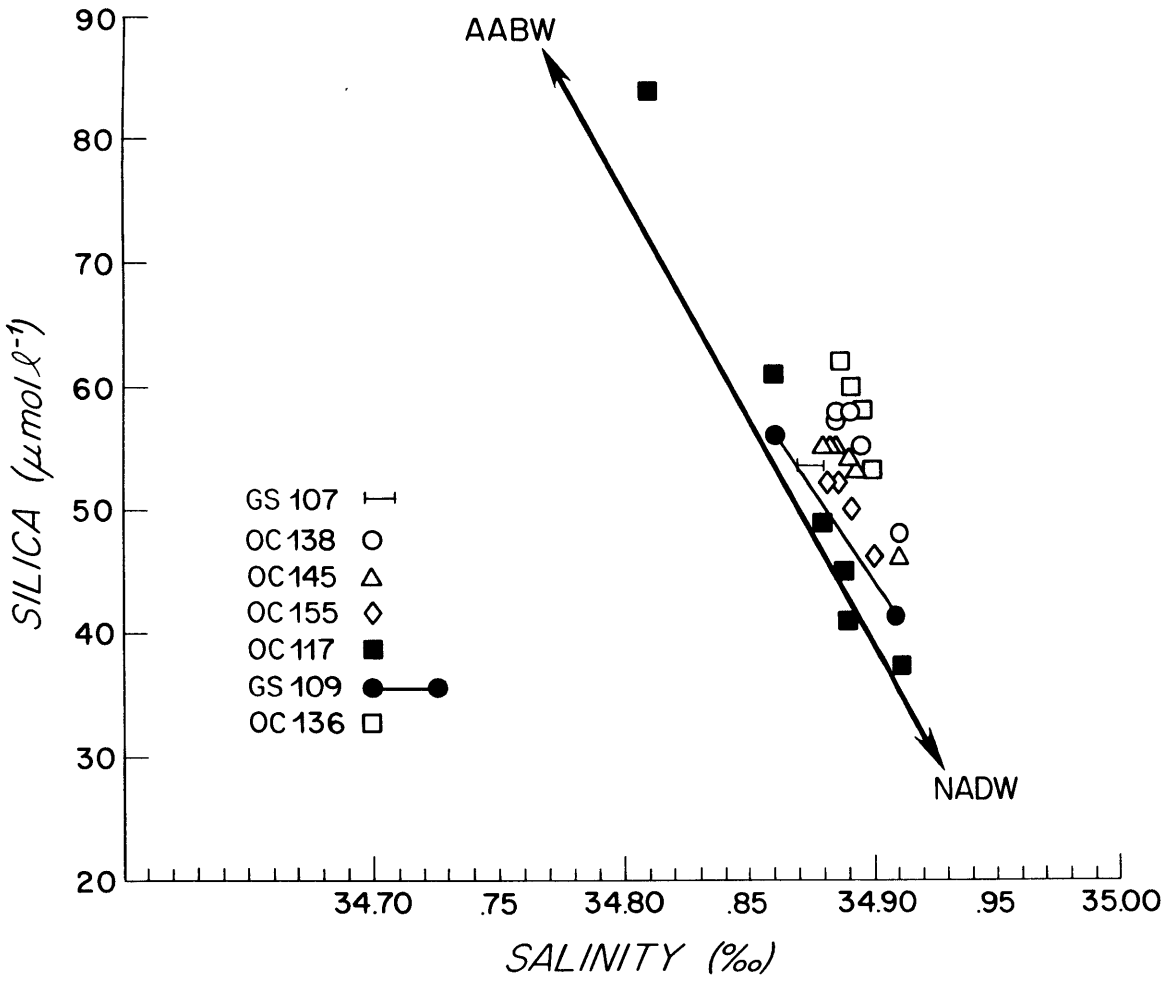
AABW
NADW
GS 107
OC 138
OC 145
OC 155
OC 117
GS 109
OC 136
SILICA (μmol ℓ-1)
SALINITY (‰)
90
80
70
60
50
40
30
20
34.70
.75
34.80
.85
34.90
.95
35.00

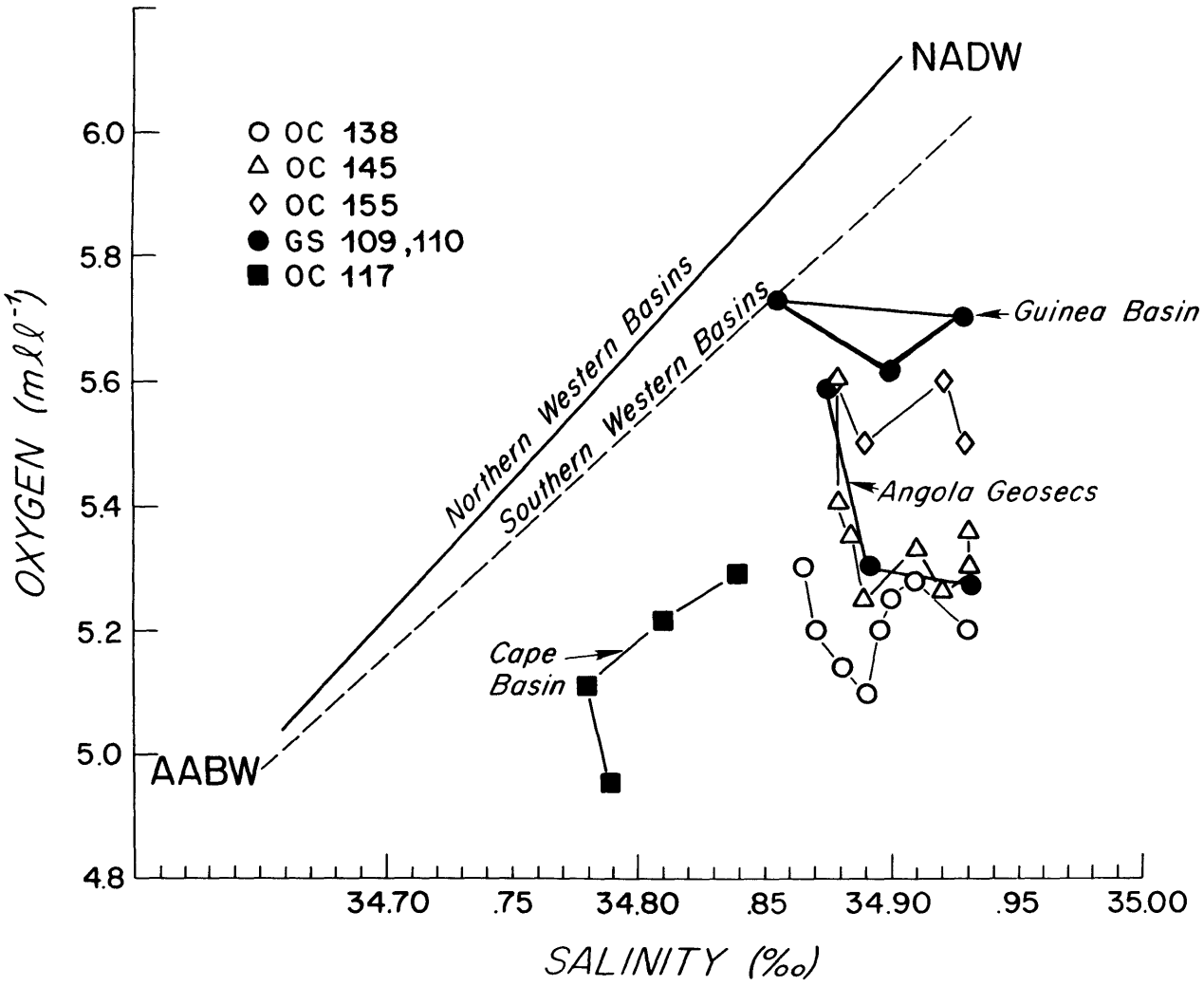
NADW
AABW
Northern Western Basins
Southern Western Basins
Guinea Basin
Angola Geosecs
Cape Basin
OC 138
OC 145
OC 155
GS 109,110
OC 117
OXYGEN (mℓℓ⁻¹)
6.0
5.8
5.6
5.4
5.2
5.0
4.8
34.70
.75
34.80
.85
34.90
.95
35.00
SALINITY (‰)

Figure 20

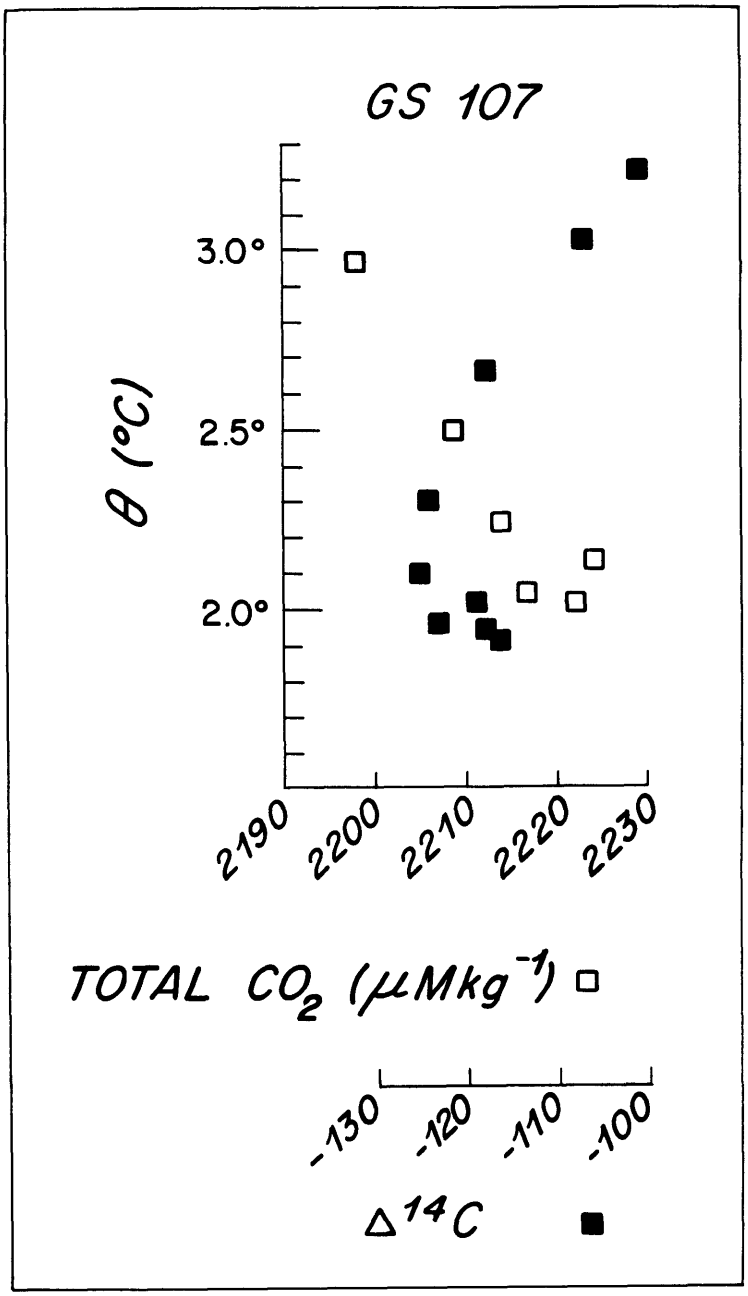
GS 107
θ (°C)
3.0°
2.5°
2.0°
2190
2200
2210
2220
2230
TOTAL CO2 (μMkg-1)
-130
-120
-110
-100
Δ14C

Figure 21

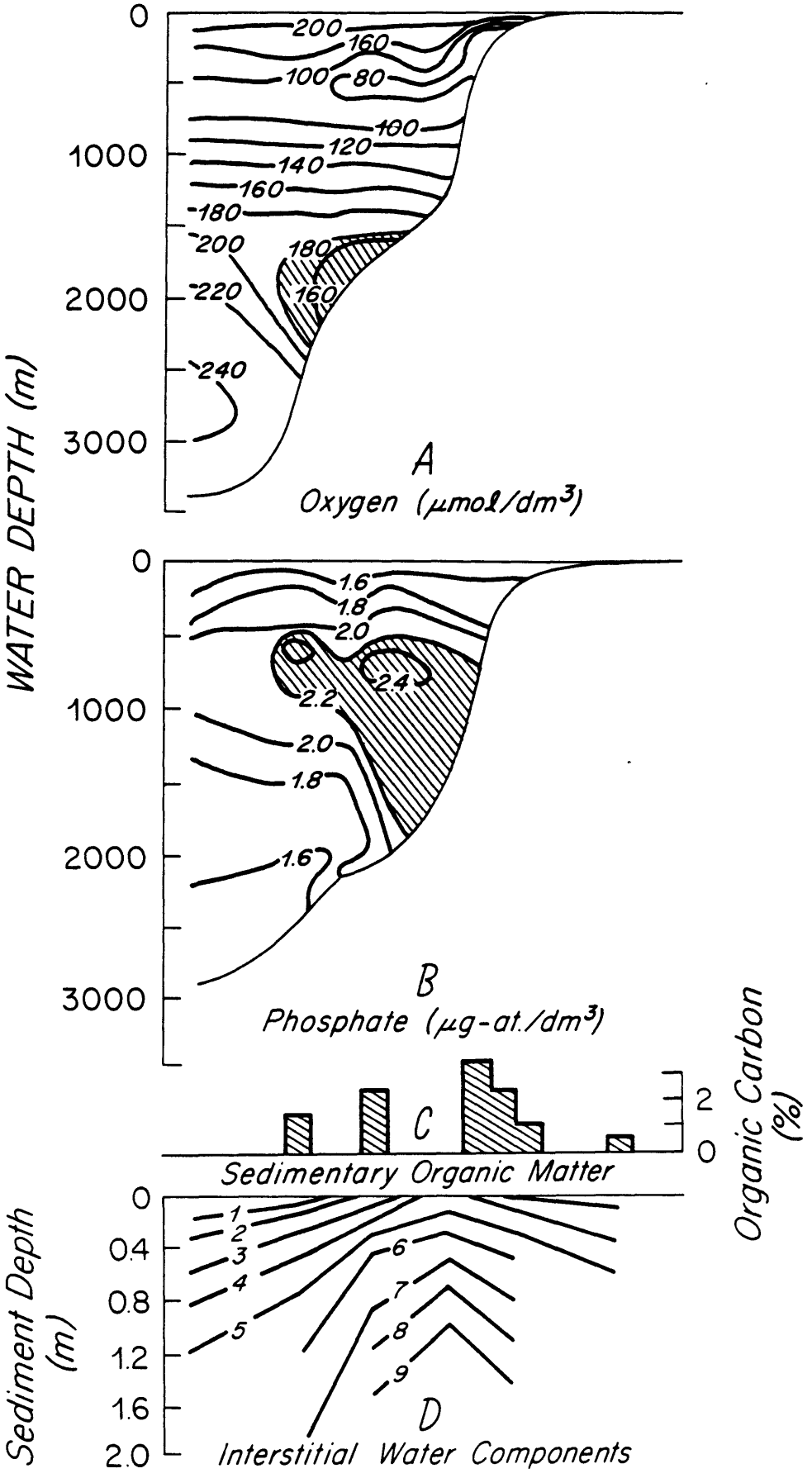
WATER DEPTH (m)
0
1000
2000
3000
200
160
100
80
100
120
140
160
180
200
180
160
220
240
A
Oxygen (μmol/dm³)
1.6
1.8
2.0
2.4
2.2
2.0
1.8
1.6
B
Phosphate (μg-at./dm³)
C
Sedimentary Organic Matter
2
0
Organic Carbon (%)
Sediment Depth (m)
0
0.4
0.8
1.2
1.6
2.0
1
2
3
4
5
6
7
8
9
D
Interstitial Water Components

Figure 22

FLAT BOTTOM SA MODEL

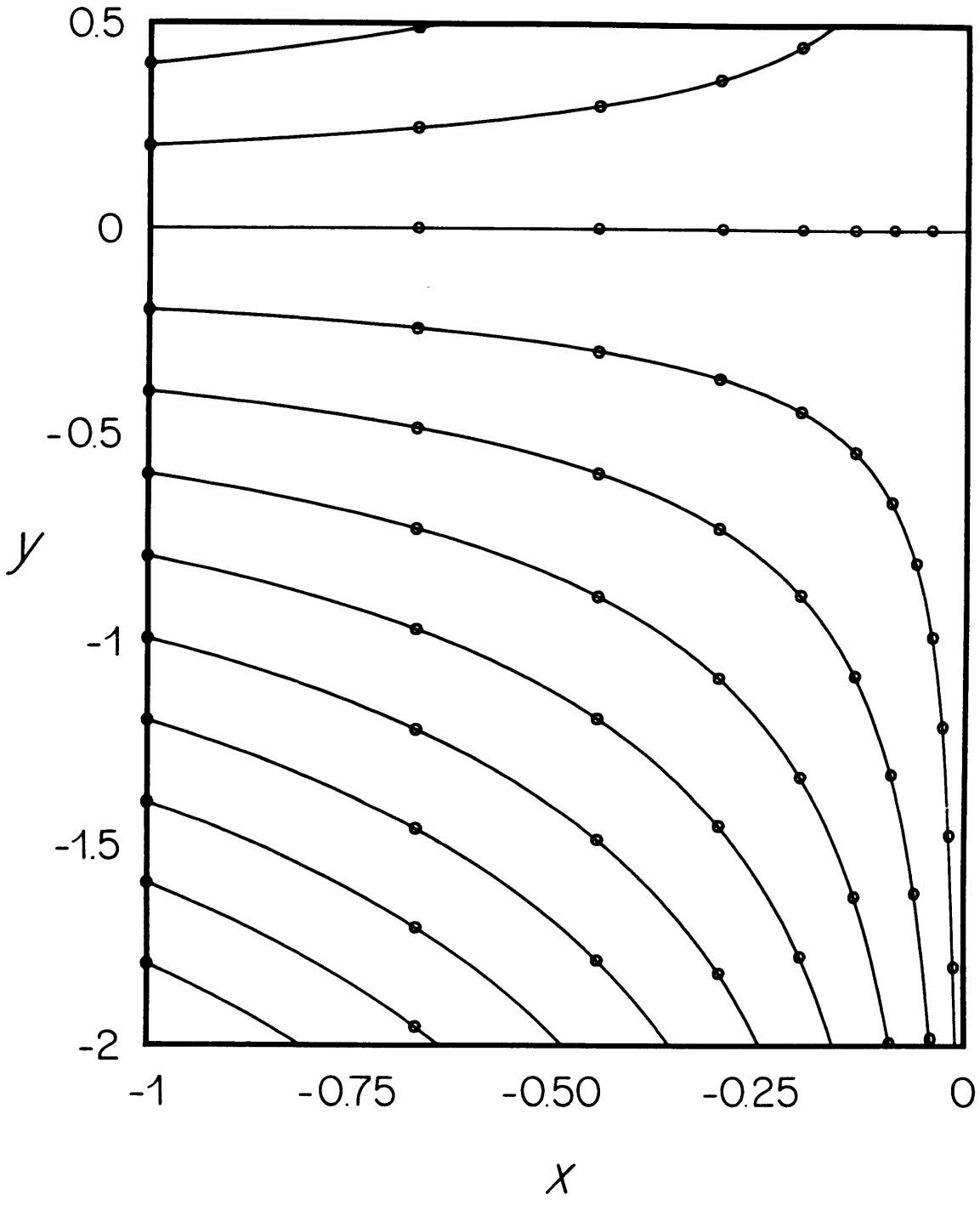

Figure 23

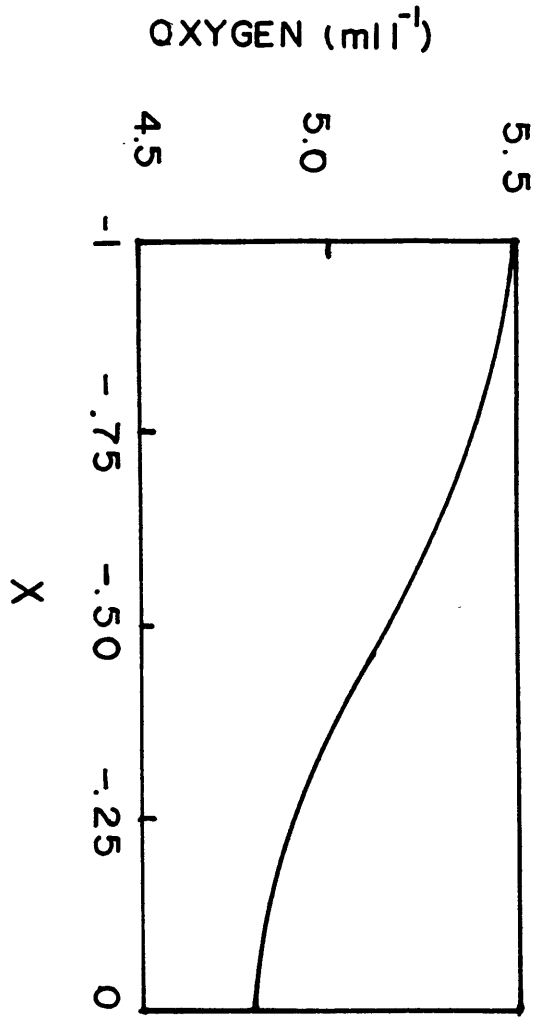

Figure 24

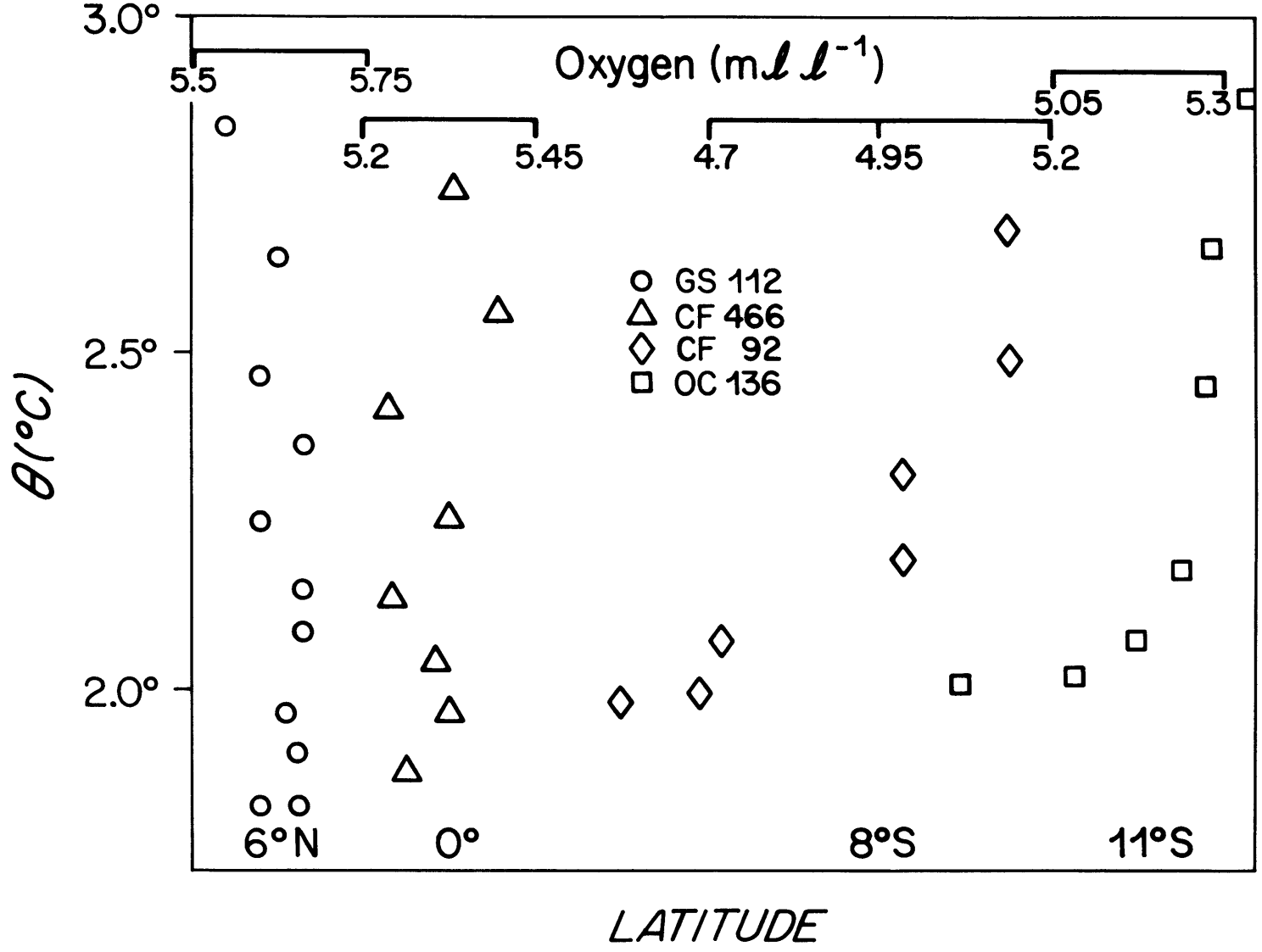
3.0°
2.5°
2.0°
θ(°C)
Oxygen (mℓ ℓ⁻¹)
5.5
5.75
5.2
5.45
4.7
4.95
5.2
5.05
5.3
GS 112
CF 466
CF 92
OC 136
6°N
0°
8°S
11°S
LATITUDE

Figure 25

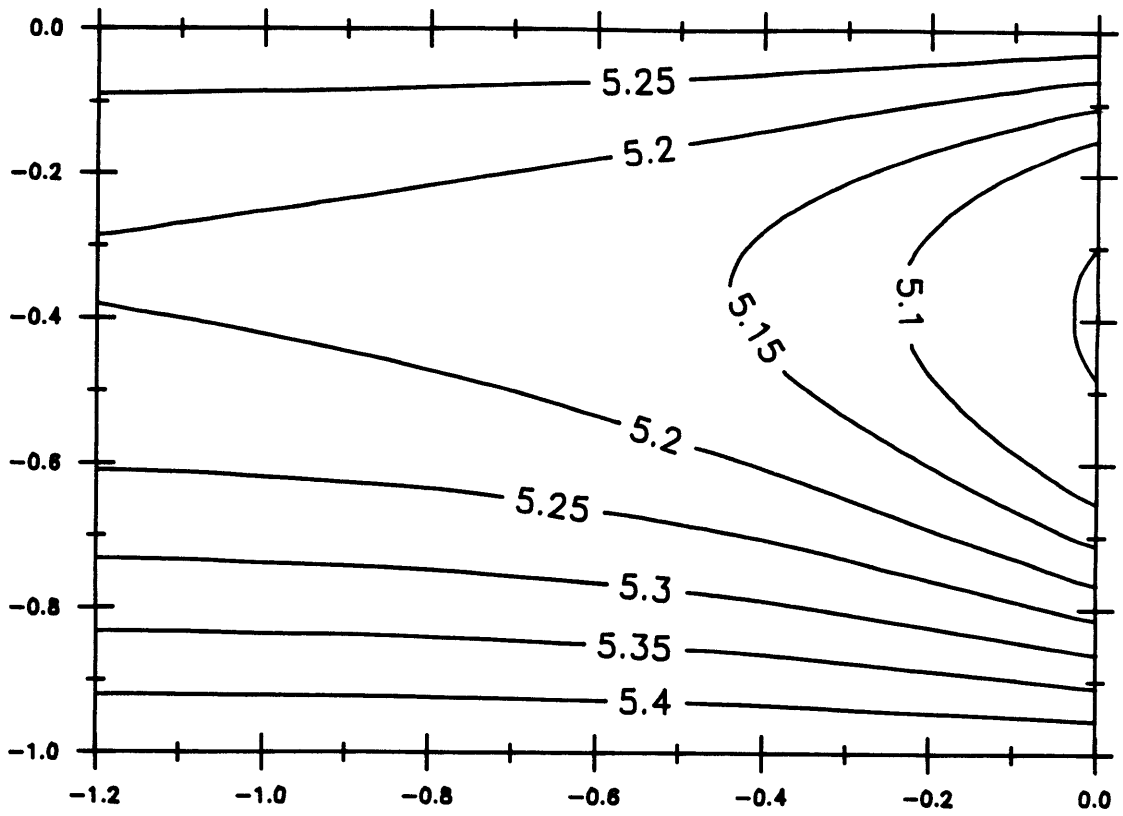
0.0
-0.2
-0.4
-0.6
-0.8
-1.0
-1.2
-1.0
-0.8
-0.6
-0.4
-0.2
0.0
5.25
5.2
5.15
5.1
5.2
5.25
5.3
5.35
5.4

b

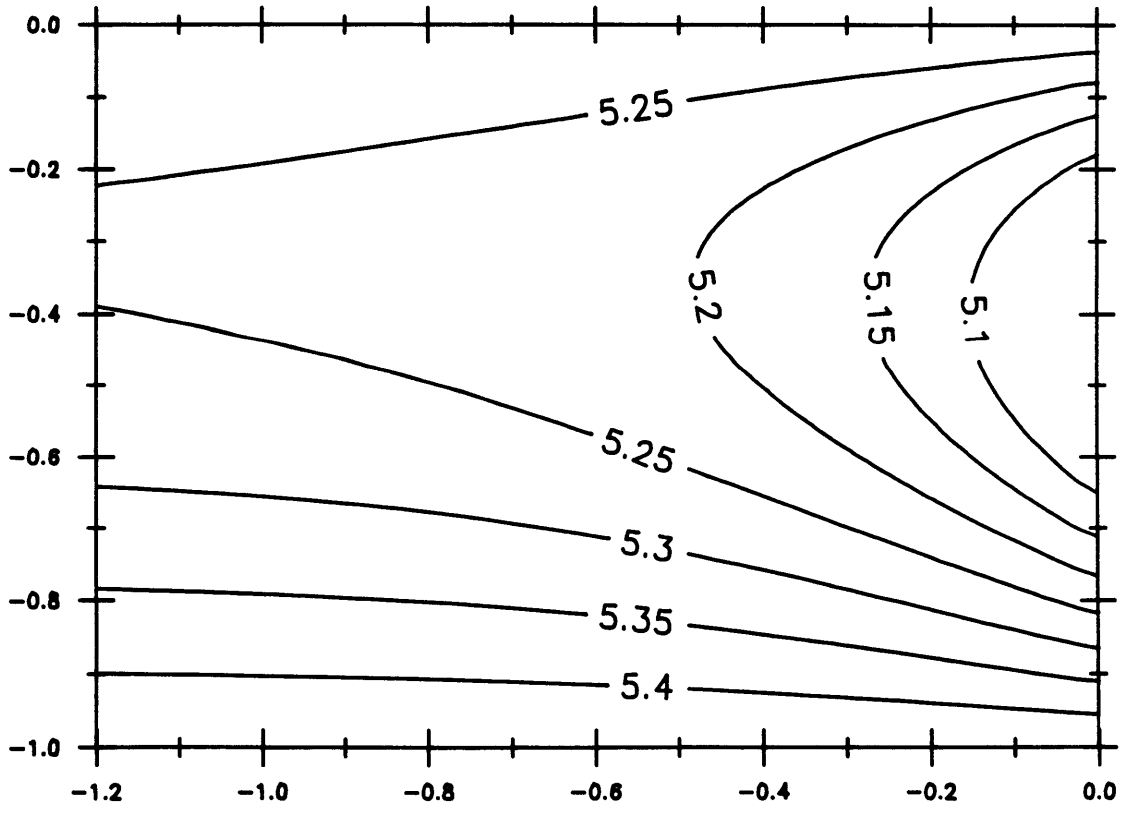
0.0
-0.2
-0.4
-0.6
-0.8
-1.0
-1.2
-1.0
-0.8
-0.6
-0.4
-0.2
0.0
5.25
5.2
5.15
5.1
5.25
5.3
5.35
5.4

a

Figure 26

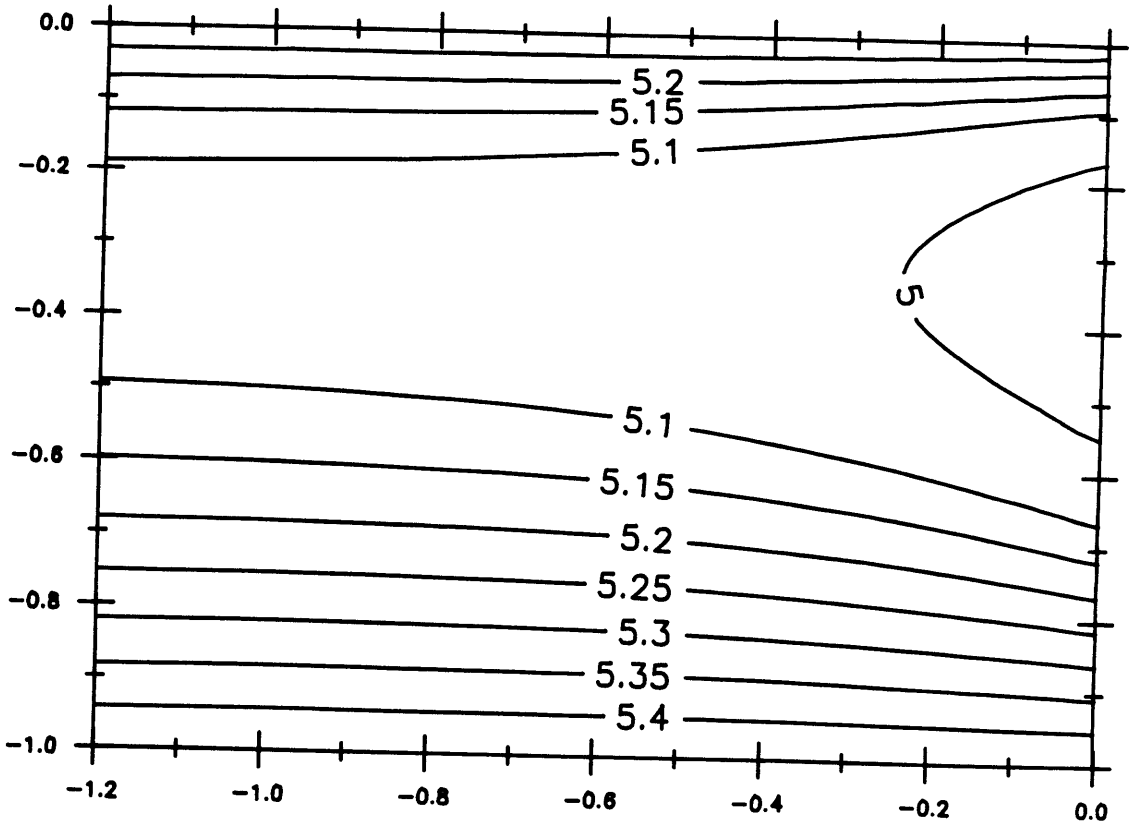
0.0
-0.2
-0.4
-0.6
-0.8
-1.0
-1.2
-1.0
-0.8
-0.6
-0.4
-0.2
0.0
5.2
5.15
5.1
5
5.1
5.15
5.2
5.25
5.3
5.35
5.4

d

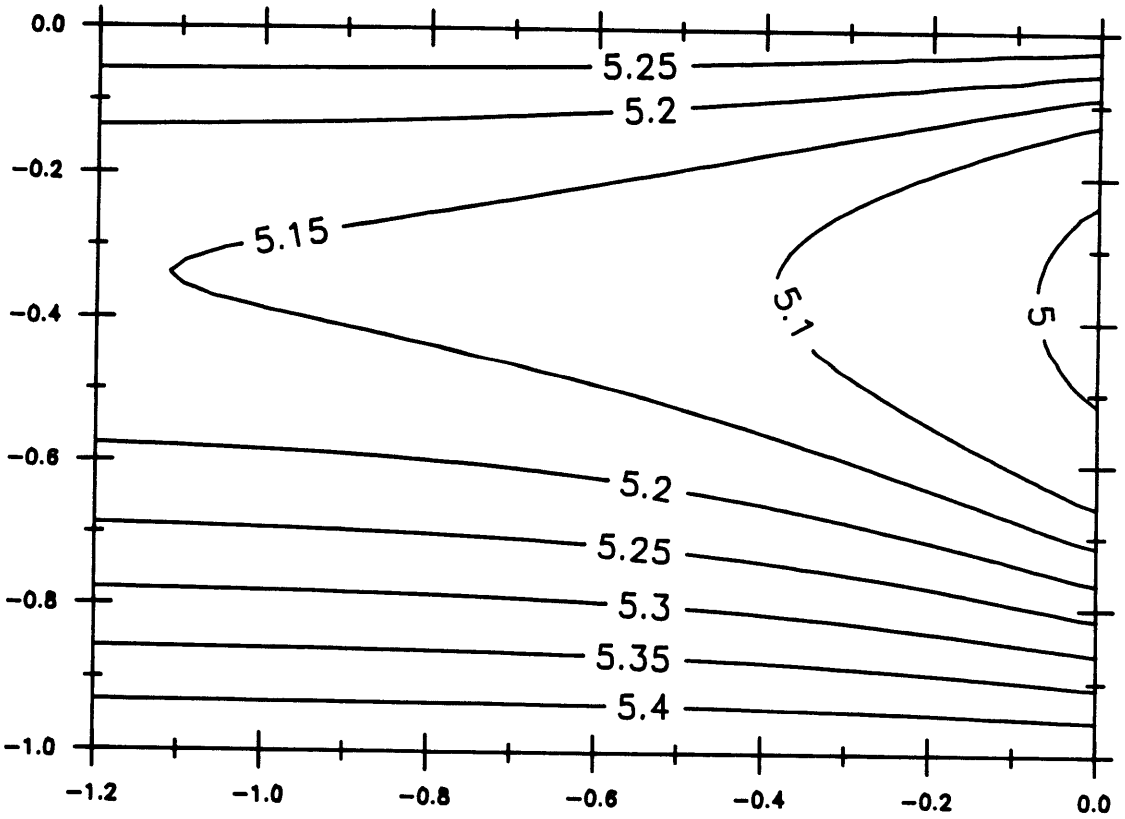
0.0
-0.2
-0.4
-0.6
-0.8
-1.0
-1.2
-1.0
-0.8
-0.6
-0.4
-0.2
0.0
5.25
5.2
5.15
5.1
5
5.2
5.25
5.3
5.35
5.4

c

Biographical Note

Kevin Speer attended the University of California at Santa Barbara from 9/79 to 6/82, graduating with a B.S. in physics with honors and a B.S. in math with honors. In June of 1982 he entered the W.H.O.I.-M.I.T. Joint Program in physical oceanography.